© J. Guthridge

Oceanic

lead author

Sonia Batten

Sir Alister Hardy Foundation for Ocean Science
Nanaimo, B.C., Canada

Citation:
Batten, S., Chen, X., Flint, E.N., Freeland, H.J., Holmes, J., Howell, E., Ichii, T., Kaeriyama, M., Landry, M., Lunsford, C., Mackas, D.L., Mate, B., Matsuda, K., McKinnell, S.M., Miller, L., Morgan, K., Peña, A., Polovina, J.J., Robert, M., Seki, M.P., Sydeman, W.J., Thompson, S.A., Whitney, F.A., Woodworth, P., Yamaguchi, A. 2010. Status and trends of the North Pacific oceanic region, 2003-2008, pp. 56-105 In S.M. McKinnell and M.J. Dagg. [Eds.] Marine Ecosystems of the North Pacific Ocean, 2003-2008. PICES Special Publication 4, 393 p.

NOAA Photo Library

highlights

- The focus period includes a span of years when the atmosphere and ocean were highly variable, particularly in the eastern North Pacific; sea surface temperature anomalies were generally positive (warmer) in the western North Pacific throughout the focus period, positive until 2006-2007 in the eastern North Pacific and then sharply negative in 2008.

- The North Pacific subtropical low chlorophyll region expanded during the focus period because of increased vertical stratification and warmer temperatures.

- The eastern North Pacific was fresher and oxygen levels (>250 m) were lower than the long term average. Surface chlorophyll$_a$ values there were higher than average in winter, and similar to average in the spring and summer. There was a noticeable high chlorophyll event in the summer of 2008 that extended across the central and Northeast Pacific but the cause has yet to be determined. It was accompanied by elevated mesozooplankton biomass in August and September.

- Zooplankton biomass in the western North Pacific increased at the Subarctic Front. The increase could be due to faster development by zooplankton in warmer temperatures or more northerly movement of the Transition Zone communities. To the north, biomass was higher generally in the second half of the focus period but this could also be a seasonal or latitudinal shift rather than an increase in absolute biomass.

- Zooplankton communities in the eastern North Pacific responded to the highly variable ocean climate. In the warmer years of 2003-2005, the seasonal development of biomass peaked early and had a narrow peak while the converse (later with a broad peak) was true in the cooler years and very evident in 2008. Abundances of Subarctic copepods and cool-water chaetognaths increased with upper-ocean cooling and with increases in the strength of the North Pacific Current. The suite of southern “California Current species” that occurs offshore was high in 2003-2006 and low in 2008.

- Data on fish and squid stocks are neither abundant nor comprehensive for the open ocean. Catches of neon flying squid in the western Pacific were relatively high in the focus period. The most abundant species of Pacific salmon (sockeye, pink, chum) rear in the Subarctic region. Total catches of sockeye salmon were average or above average, chum catches were average and pink salmon catches were above average in the western North Pacific and below average in the eastern North Pacific. Some western stocks of chum salmon appeared to be decreasing in size. North Pacific albacore tuna stocks were relatively high during the focus period, but predictions are for them to decline by 2015 if fishing pressure is not reduced. Most data for the central North Pacific fisheries (tuna/billfish) showed declining catches during the focus period when compared with previous data.

- Seabird diversity and abundance increased in the eastern North Pacific, at least up to 2006 but this could reflect a change in distribution. Changes in seabird community structure and relative abundance on Line P may be related to changes in the underlying mesozooplankton community. The reproductive success of Laysan and black-footed albatrosses that rear their young in the Hawaiian archipelago in the central North Pacific was stable and relatively high in the early part of the focus period. Seabirds are considerably more abundant in the western than the eastern North Pacific but trend data there were not available.

Introduction

The Oceanic Region of the North Pacific Ocean is defined to include the area of deep waters located beyond the continental margins and major coastal boundary currents. It is characterized by strong latitudinal gradients in surface temperature and salinity (high in the south and low in the north), multiple water masses, major oceanic gyres, large (~200 km) mesoscale eddies, and a complex bathymetry of deep trenches and remote sea mounts. Natural variability in the Oceanic Region is intimately linked to variability in the global climate system. Biological production in this region is responsible for major commercial fisheries for tunas and Pacific salmon.

Sub-regions in the Oceanic Region are treated separately in this chapter where the availability of data warrants it. The Aleutian Island chain constricts the main gyre and causes a re-circulation as two sub-gyres; the Western Subarctic and Alaskan Gyres. These gyres have distinct characteristics, often supporting different species and patterns of production. The North Pacific Transition Zone to the south represents a physical and biological transition between the subtropical and Subarctic gyres. It is a physically complex region bounded to the north by the Subarctic Frontal Zone which stretches east to west across the central North Pacific, and to the south by the Subtropical Frontal Zone. The latter is the southern limit of the Oceanic Region described in this chapter. It is characterized by zonal gradients (fronts) in temperature and salinity. Some of its more abundant species [e.g., flying squid (*Ommastrephes bartrami*), Pacific pomfret (*Brama japonica*), blue shark (*Prionace glauca*), Pacific saury (*Cololabis saira*)] undergo extensive seasonal migrations between summer feeding grounds at the Subarctic fronts (or within the Subarctic) to winter spawning grounds in the subtropics. The North Pacific subtropical gyre supports a diverse assemblage of apex predators including tunas, billfishes, sharks, marine mammals and seabirds. This chapter contains a review of the status and trends of the Oceanic Region from 2003-2008, hereafter the *focus period*.

2.0 Large-scale Indices *(McKinnell)*

Many of the large-scale monthly and seasonal atmospheric climate indices in the North Pacific are highly correlated, particularly in winter because each reflects similar aspects of a common dominant climate pattern. To recognize the pioneers in this field and to reduce redundancy, priority for selecting indices to report is given to those that were first established for that purpose.

2.1 Atmospheric

2.1.1 Pacific North American pattern

The PNA index (Fig. OC-1) is calculated from the 500 hPa height anomalies and its value provides an indication of the state of a dominant mode of low frequency climate variability in the North Pacific (Wallace and Gutzler 1981). Its positive phase tends to produce above-average air temperatures over western North America, Alaska, and to a lesser extent from the Hawaiian latitudes and southward (Fig. OC-1b) and below-average temperatures in the western Pacific, especially across Korea and Japan at latitudes in the range 35-45°N; strongest near the date line. The PNA-surface air temperature correlation pattern bears a strong resemblance to the Pacific Decadal Oscillation spatial pattern (based on ocean surface temperature) indicating a strong atmosphere/ocean interconnection in the Pacific.

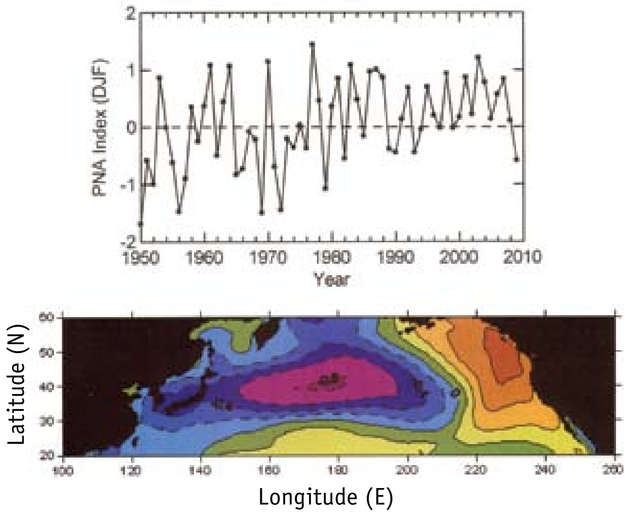

[Figure OC-1] Average December to February Pacific-North American (PNA) index variation from 1950-2009 (upper panel) and spatial correlation pattern of PNA with mean air temperature (lower panel).

During the focus period, the average winter PNA index was persistently >0 but it declined to its lowest value in 30 years during the winter of 2008-2009.

2.1.2 North Pacific index

The NP index is the area-weighted monthly average sea level pressure (minus 1000 hPa) in the region 160°E-140°W, 20°-65°N (Trenberth and Hurrell 1994). Low values of the index represent lower than average sea level pressures and generally stormier months (the inverse of the PNA index). NP index values were converted to monthly anomalies using the 1950-2009 mean, then standardized. Average winter sea level pressures in the North Pacific increased during the focus period reflecting a trend toward declining storminess (Fig. OC-2). The winter of 2008-2009 had the highest average value of the index in the record. Some extreme monthly values occurred during the focus period: the two lowest values since 1950 in July occurred during 2004 and 2007, and the highest value observed in any December during that period occurred in 2008. There was no significant linear trend in the NP index in any month except July and that was due to the influence of the two extremes at the end of the timeseries.

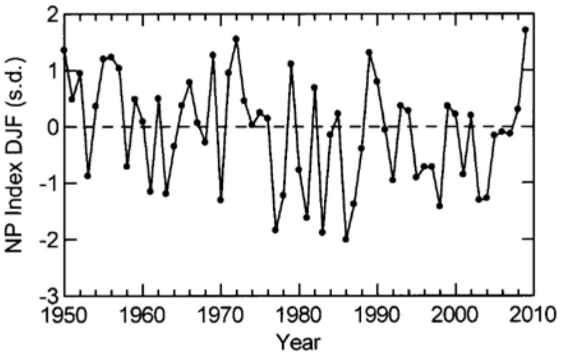

[Figure OC-2] Standardized winter (DJF) NP index anomalies from 1950-2009.

2.1.3 Southern Oscillation index

The SO index is the difference of the sea level pressure anomalies at Tahiti and Darwin, Australia divided by the standard deviation of their difference (Troup 1965). It reflects the strength of a zonal atmospheric circulation cell in the tropical Pacific known as Walker Circulation. Since the 2002-2003 El Niño, the SOI has varied between brief periods of El Niño and La Niña conditions, including an El Niño in the winter of 2006-2007 (Fig. OC-3). This El Niño has received scant attention in the North Pacific because it appears to have had very little extra-tropical boreal influence. In the fall of 2007, the SOI shifted abruptly to a strong La Niña and that state persisted through the end of 2008.

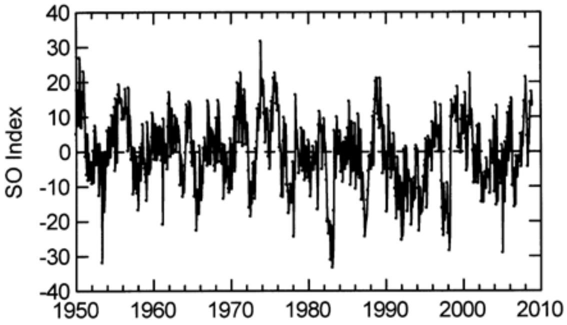

[Figure OC-3] Monthly Southern Oscillation Index variation from 1950-2008.

2.1.4 Arctic Oscillation index

The AO index is defined as the dominant eigenvector of the covariance matrix of the area-weighted monthly non-seasonal sea level air pressure anomalies northward of 20°N (Thompson and Wallace 1998). It is characterized by negative covariation in sea level pressures over the Arctic and over temperate latitudes of the Atlantic and Pacific oceans. Variation in the AO is seasonal with stronger expression in winter. There is a weak autocorrelation at lag= 1 month (r= 0.29). The mean winter (DJF) values tended to be negative during the first few years and positive for the last two winters and the start of the winter of 2008/09 (based on Dec. 2008 value only) (Fig. OC-4). Positive AO anomalies are correlated with higher than average SLP over the temperate latitudes of the North Pacific. The AO value for October 2008 was the highest observed in any October in the time series. The AO value for December 2009 was the lowest observed in any December since 1950.

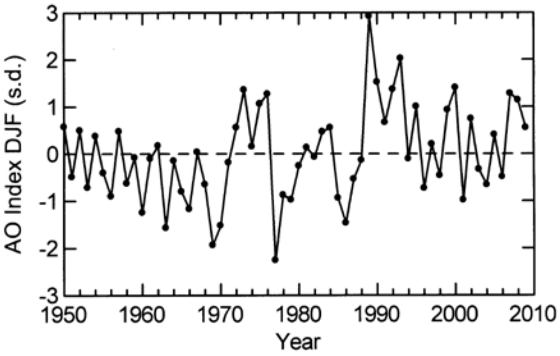

[Figure OC-4] Winter (DJF) average Arctic Oscillation index from 1950-2009.

2.2 Oceanic

2.2.1 Pacific Decadal Oscillation index

The PDO index (Fig. OC-5) is derived from the dominant eigenvector of the covariance matrix of area-weighted monthly anomalies of sea surface temperatures (SST) from 20°-65°N in the Pacific (Mantua et al. 1997). In winter, it is highly correlated with North Pacific atmospheric indices (NPI, PNA). During the last three decades, the PDO index has varied between positive and negative phases with greater frequency than was observed at the time of its first description. Average SST anomalies within these ~5-year stanzas (Fig. OC-6) varied in typical PDO fashion until the 2002-2003 El Niño. Positive PDO values (warm in the eastern Pacific, cool in the central and western Pacific) at the beginning of the focus period diminished after about 6 months and remained near neutral or slightly positive. A broad pattern of weak to strong positive SST anomalies throughout most of the basin persisted until September 2007 when the PDO index shifted abruptly to negative. The negative PDO pattern (cold along the North American continent and Gulf of Alaska and warm in the central and western Pacific) persisted through most of 2009 in spite of El Niño-like conditions at the Equator.

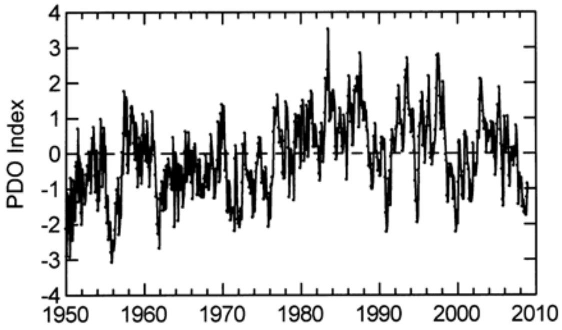

[Figure OC-5] Monthly variation in the Pacific Decadal Oscillation index from 1950-2008.

2.2.2 Basin-scale average SST anomalies

Since the advent, in the early 1980s, of blended SST measurements that are primarily determined by satellite remote sensing, the North Pacific Ocean has been oscillating more frequently (~10-11 y) between warm and cool phases of the PDO than the multi-decadal period that is normally associated with the PDO. Based on an EOF analysis of these SST data to determine phase shifts, the corresponding average SST anomalies within stanzas are: Jan/82-Jun/82, Jul/82-Dec/87, Jan/88-Sep/91, Oct/91-Apr/98, May/98-Aug/02, Sep/02-Sep/07, and Oct/07-Dec/08 (Fig. OC-6a-g). Average anomalies within each phase feature a PDO-like pattern except for the period from September 2002 - September 2007 (Fig. OC-6f) when the PDO pattern in SST anomalies was largely absent for a period of about 5 years. After September 2007, the negative phase of the PDO re-appeared and was sustained through the focus period to 2009 (Fig. OC-6g).

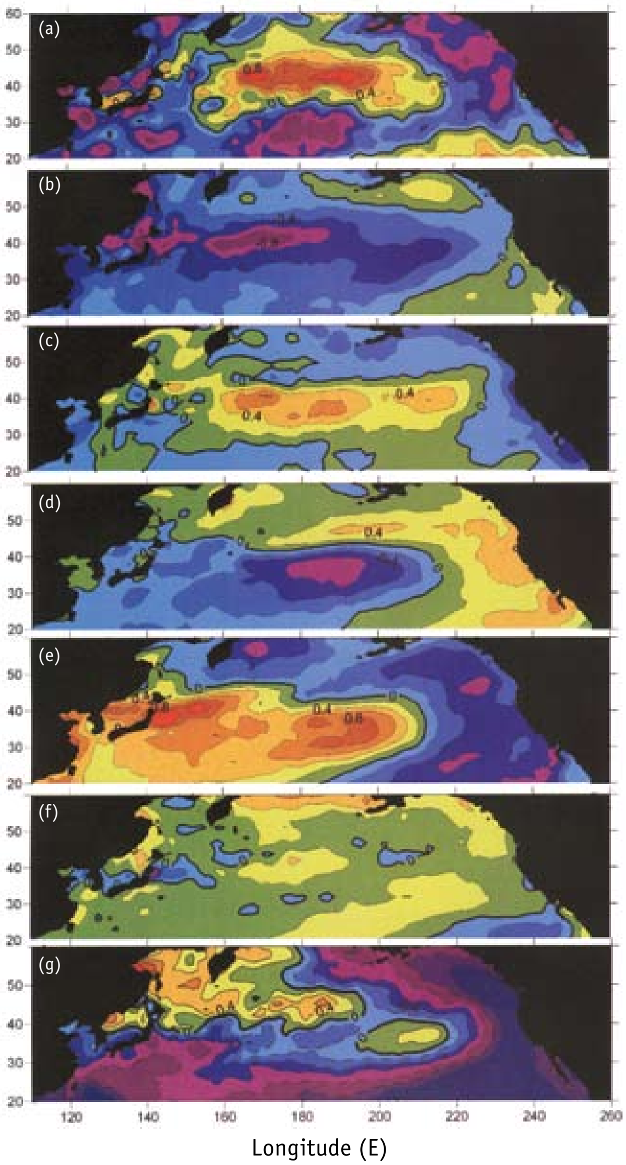

[Figure OC-6] Average SST anomalies: (a) Jan/82-Jun/82, (b) Jul/82-Dec/87, (c) Jan/88-Sep/91, (d) Oct/91-Apr/98, (e) May/98-Aug/02, (f) Sep/02-Sep/07, and (g) Oct/07-Dec/08 (Data from Reynolds et al. 2002).

2.2.3 Gulf of Alaska annual SST

Area-weighted annual average surface temperatures in the Gulf of Alaska from 1900-present (Fig. OC-7) reveal a pattern of high variability during the focus period. Three years of higher than average temperatures from 2003-2005 were followed by an abrupt shift to cool in 2006 to cold in 2007 and even colder in 2008. The surface of the Gulf of Alaska has not been as cold since 1972.

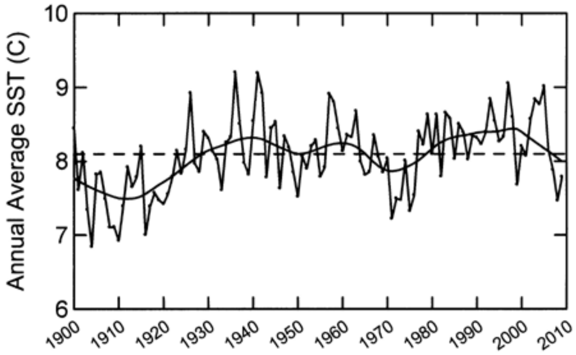

[Figure OC-7] Area-weighted annual average SST in the NE Pacific (50-60°N, 160°W to coast) from 1900-2009 (Data from: Smith et al. 2008) with loess smoother indicating trend. Horizontal dashed line is the mean of the time series (8.1°C).

2.2.4 Western Subarctic Gyre annual SST

Area-weighted annual average of monthly SST in the core of the Western Subarctic Gyre suggests 3 periods: below average years before 1914, followed by an untrended period near the long-term average until 2002, followed by a recent period where negative annual anomalies are rare (Fig. OC-8). All months except August-October show significant positive linear trends since 1950. During the focus period, monthly anomalies were positive in all years; the positive anomaly in 2008 was the fourth largest since 1900.

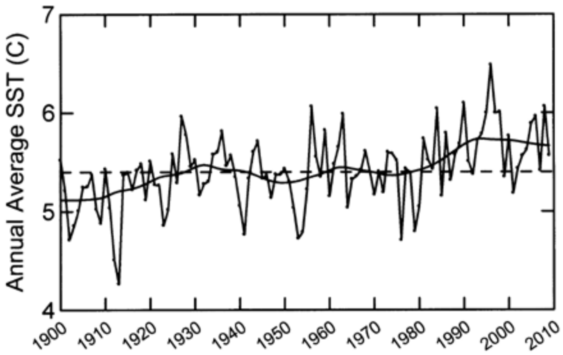

[Figure OC-8] Area-weighted annual average SST in the Western Subarctic Gyre from 1900-2009 (Data from: Smith et al. 2008) with loess smoother indicating trend. Horizontal dashed line is the mean of the time series (5.4°C).

2.2.5 Spring timing estimated from water column stability

Gargett et al. (2001) defined an index of water column stability based on average density differences between 0-20 m and 60-80 m for individual CTD casts. This index was computed for each of about 75,000 Argo profiles in the North Pacific. The index values were grouped by year, by week, and by block (5° latitude × 10° longitude). Within each block, for each year, a loess smoother of stability index versus week was used to generate a seasonal timing curve of increasing stability from winter through spring/summer. Within each block-year, the week when water column stability reached 40% of its maximum was noted.

During the focus period, water column stability developed earliest along the North American coast and in the subtropical region where surface warming occurs earlier (Fig. OC-9). A zonally oriented region centred on about 40° N tended to stabilize later in the year, with a tendency for the northwestern Pacific to be later than the northeastern Pacific (indicated by size of region >20 week contour). In the Gulf of Alaska, stability arrived latest in 2008. In general, there appear to be later springs (more blue) from 2006-2008 than in 2003-2005.

2.2.6 Western Subarctic Gyre mixed layer depth

Mixed layer depths (defined as the distance from the surface to a depth required to observe a $\Delta\sigma_\theta$ = 0.0125) were deepest in the core of the Western Subarctic Gyre in early spring (MAM). During the focus period, the month of June had the greatest variability (some areas deeply mixed and others very stable). By July of each year from 2003-2008, a stable water column had developed fully that lasted for several months. Only 2005 differed from this pattern with water column stability developing in May in some locations rather than June (Fig. OC-10).

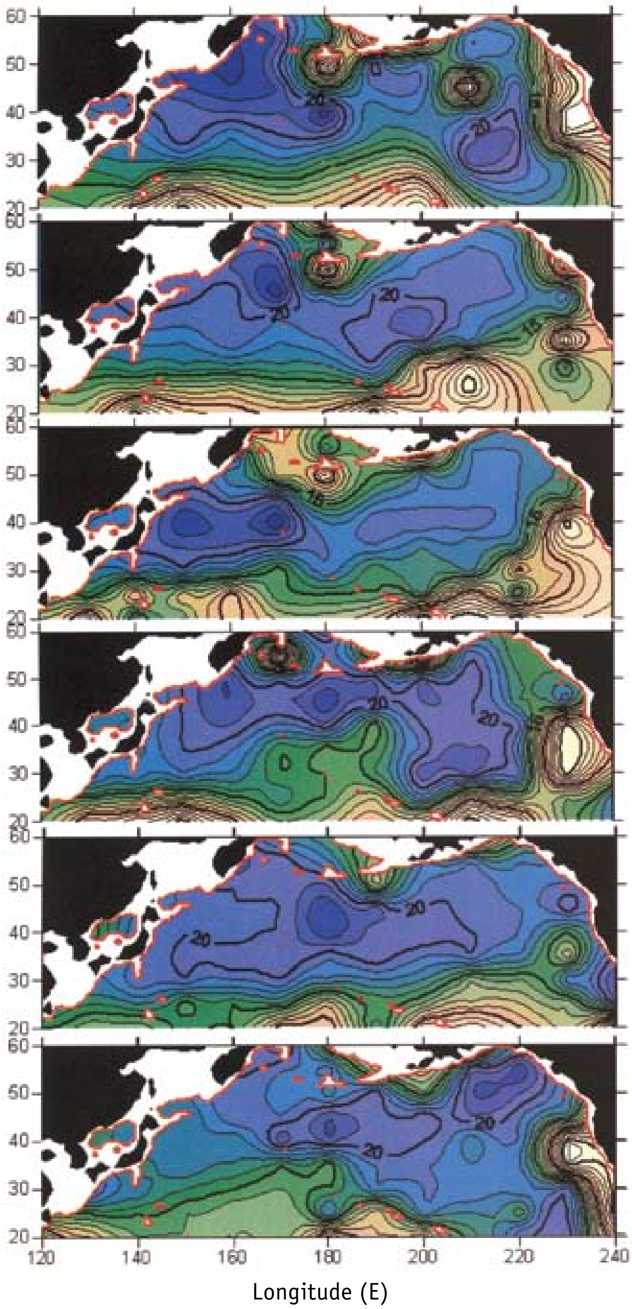

[Figure OC-9] Contours indicate week of year when the water column reached 40% of its maximum stability. Years appear sequentially; the top panel is 2003 and the bottom panel is 2008. Colours are chosen such that blue is later, green is intermediate, tan is earlier. Week 20 is approximately mid-May. The red lines indicate the 2000 m contour (few floats here). Remember that fewer profiles occurred in the earlier years as Argo met its target number of floats about 2007 so comparisons with years before 2003 were not made. Argo profiles were acquired from the US Global Argo Data Server.

2.2.7 Northeast Pacific mixed layer depth *(Whitney)*

Deeper mixing at Station Papa (50°N 145°W) in 2008 coincided with SSTs <5° C for most of January through May and a persistent outcropping of the 25.8 isopycnal. In the Alaska Gyre, the 26.2 isopycnal surfaced which would have resulted in oxygen influxes and carbon dioxide outgassing from waters that do not frequently come in contact with the atmosphere in the eastern subarctic Pacific. Mixed layer depths from 2002 onwards were calculated from Argo data. Mean values after 1976 were shallower than the earlier part of the time series (108 ±12 m vs 125 ±9 m), with the shallowest mixed layer depth of the entire time series occurring during the focus period in 2003 (Fig. OC-11). Through the rest of the focus period, mixed layer depth has steadily increased although still remaining shallower than the earlier part of the time series.

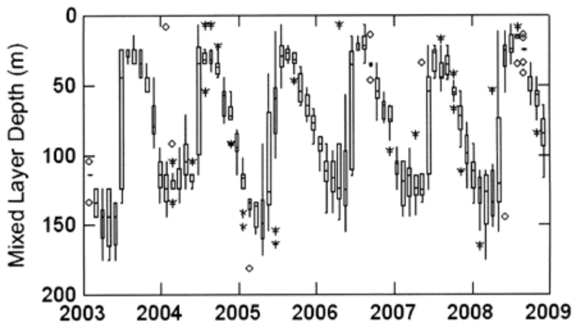

[Figure OC-10] Box and whisker plots indicating variability of monthly mixed layer depth across the North Pacific during the focus period. The greatest range of values occurred in spring when some areas stabilized and others were still mixing deeply. Argo data used to calculate mixed layer depths were acquired from the US Global Argo Data Server.

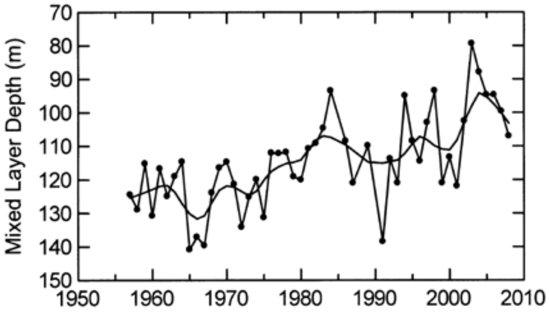

[Figure OC-11] Mixed layer depth at Station Papa, updated from Freeland et al. (1997). Depth profiles were obtained at least weekly before 1982 by hydrocast. After 2001, they were estimated from Argo profile data extrapolated to Station Papa. From 1982 to 2001 annual winter mixed layer depths were determined from hydrocasts deployed during single winter cruises to Station Papa. A loess trend line is indicated.

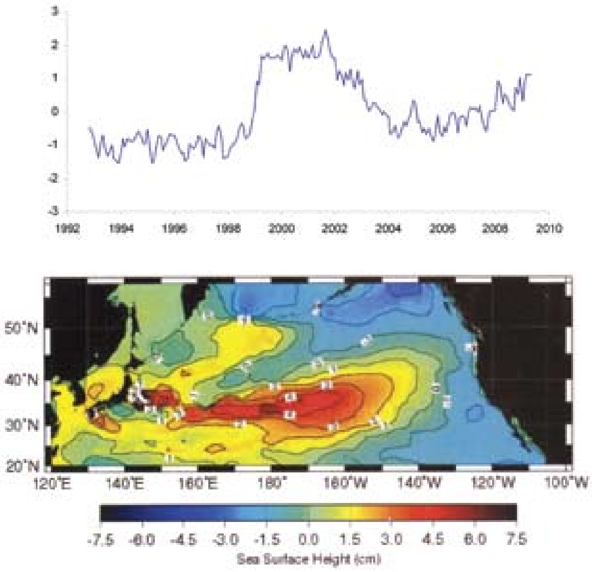

[Figure OC-12] Time series of the detrended variation of the first mode of the EOF analysis of sea surface height (upper panel) and the spatial pattern of the first mode of the sea surface height EOF (lower panel).

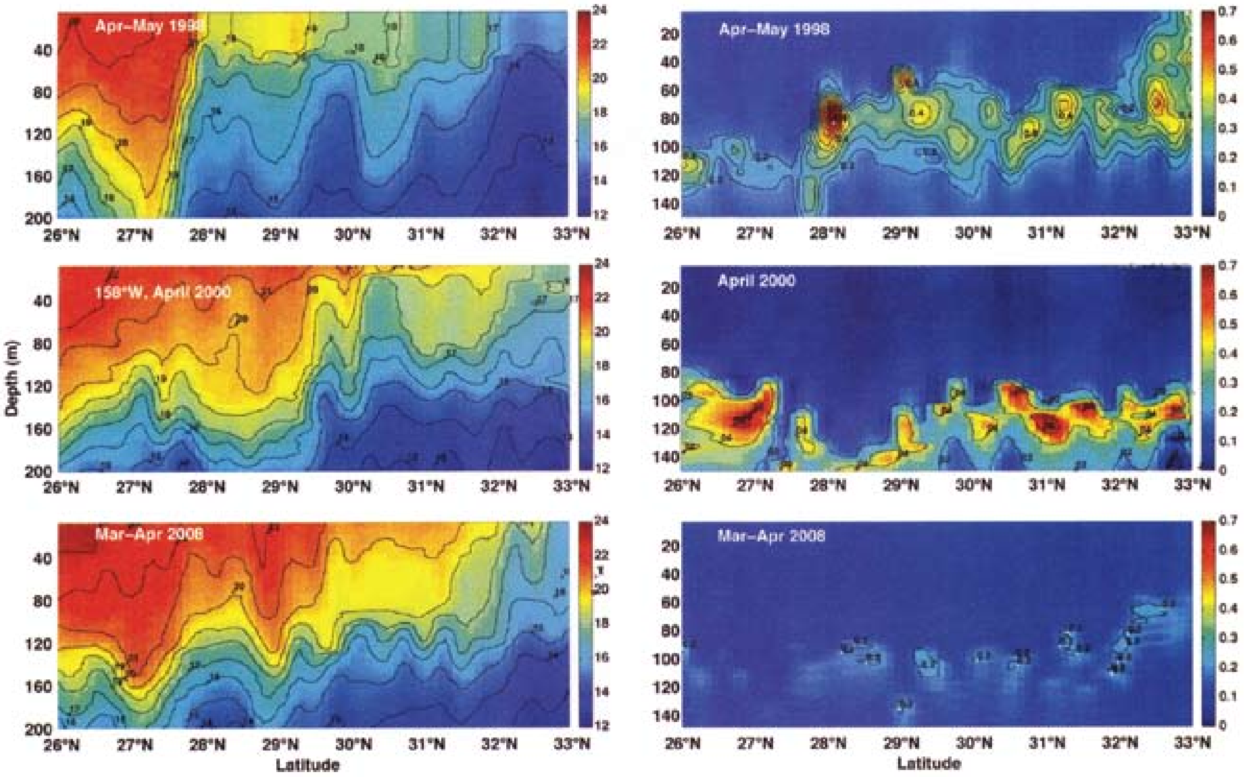

[Figure OC-13] Comparative vertical sections of temperature (°C) (left) and chlorophyll (mg·m⁻³) (right) from annual surveys April-May 1998, April 2000, and March-April 2008 along 158°W longitude.

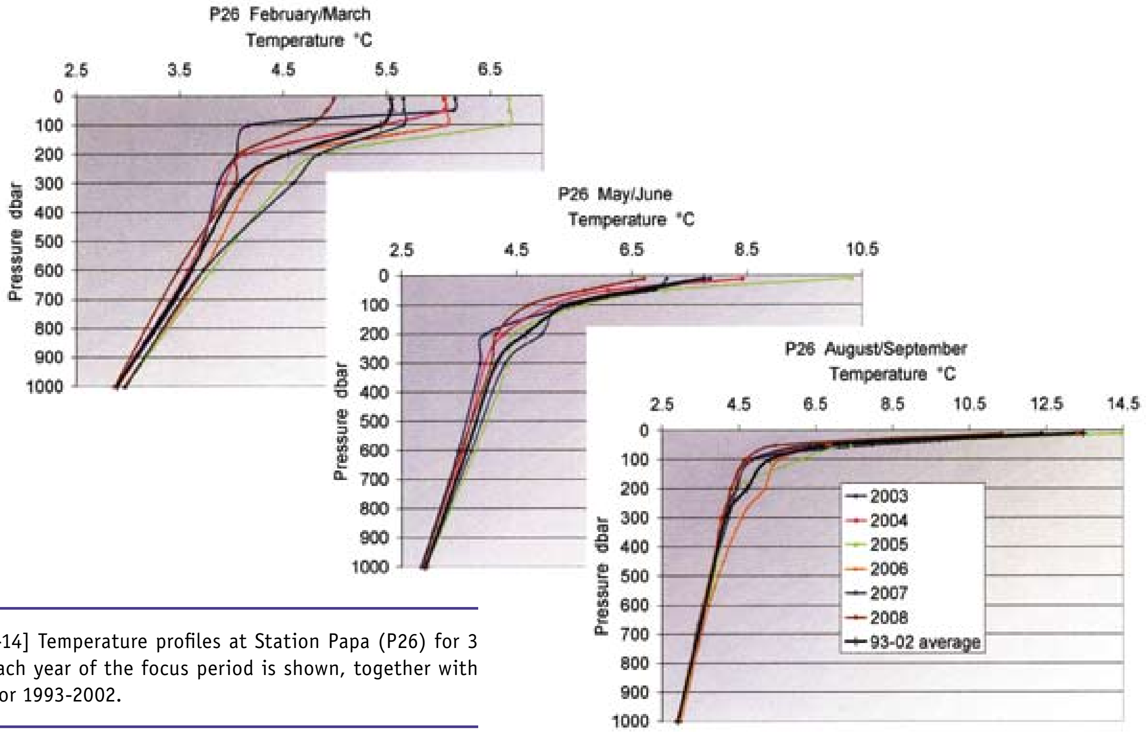

[Figure OC-14] Temperature profiles at Station Papa (P26) for 3 seasons. Each year of the focus period is shown, together with the mean for 1993-2002.

3.0 Oceanography

3.1 Subarctic North Pacific

3.2 Central North Pacific *(Polovina)*

The first EOF of sea surface height (SSH) shows that the central Pacific and Transition Zone region exhibits a pattern of low frequency variation characterized as a horseshoe-like spatial pattern with the central Transition Zone out of phase with areas to the south, east and north (Fig. OC-12). During the period 1992-1998 SSH was low in the central Transition Zone and high in the surrounding areas. Between 1999-2003 SSH rose abruptly in the central Transition Zone and dropped in the surrounding regions. Between 2003-2007 the SSH pattern returned to the pattern observed in the 1992-1998 period, and then in 2008 and 2009 the SSH pattern reverted to more closely resemble the 1999-2003 pattern (Fig. OC-12). Changes in SSH reflect changes in the vertical structure of the ocean with a rise (drop) in SSH reflecting increased (decreased) vertical stratification. The period 1999-2003 was a strong La Niña period while 2008 and early 2009 was a moderate La Niña event and the observed SSH rise in the central Transition Zone appears to represent a mid-latitude La Niña response. Three longitudinal sections of temperature-depth and chlorophyll-depth taken along 158°W longitude during spring 1998, 2000, and 2008 show a northward shift over time in the vertically stratified warm water and low surface chlorophyll waters (Fig. OC-13). This pattern is consistent with the mid-latitude rise in SSH, representing an increase in vertical stratification, observed in 2000 and 2008 relative to 1998 (Figs. OC-12, OC-13).

3.3 Water properties along Line P *(Robert)*

The Line P program began in 1959 when hydrographic casts were made at a series of stations along a transect leading to Station Papa (Freeland 2007). This is one of the world's longest deep-ocean time series in existence and is now sampled 2-5 times per year, usually in late winter (February/March), spring (May/June) and summer (August/September). Data shown here are mainly from Station Papa (station P26) but data from landward stations P16 (49° 17'N, 134° 40'W, water depth 3550 m) and P12 (48° 58.2'N, 130° 10'W, water depth 3300 m) are also included.

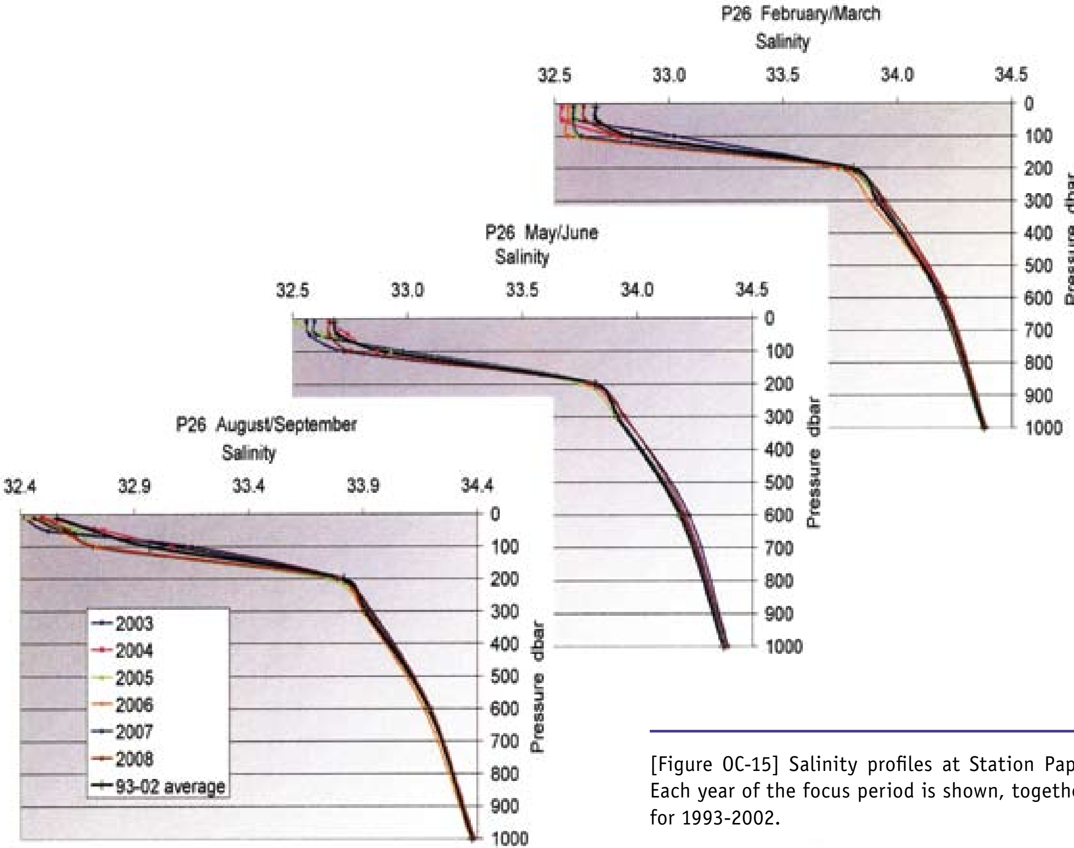

[Figure OC-15] Salinity profiles at Station Papa for 3 seasons. Each year of the focus period is shown, together with the mean for 1993-2002.

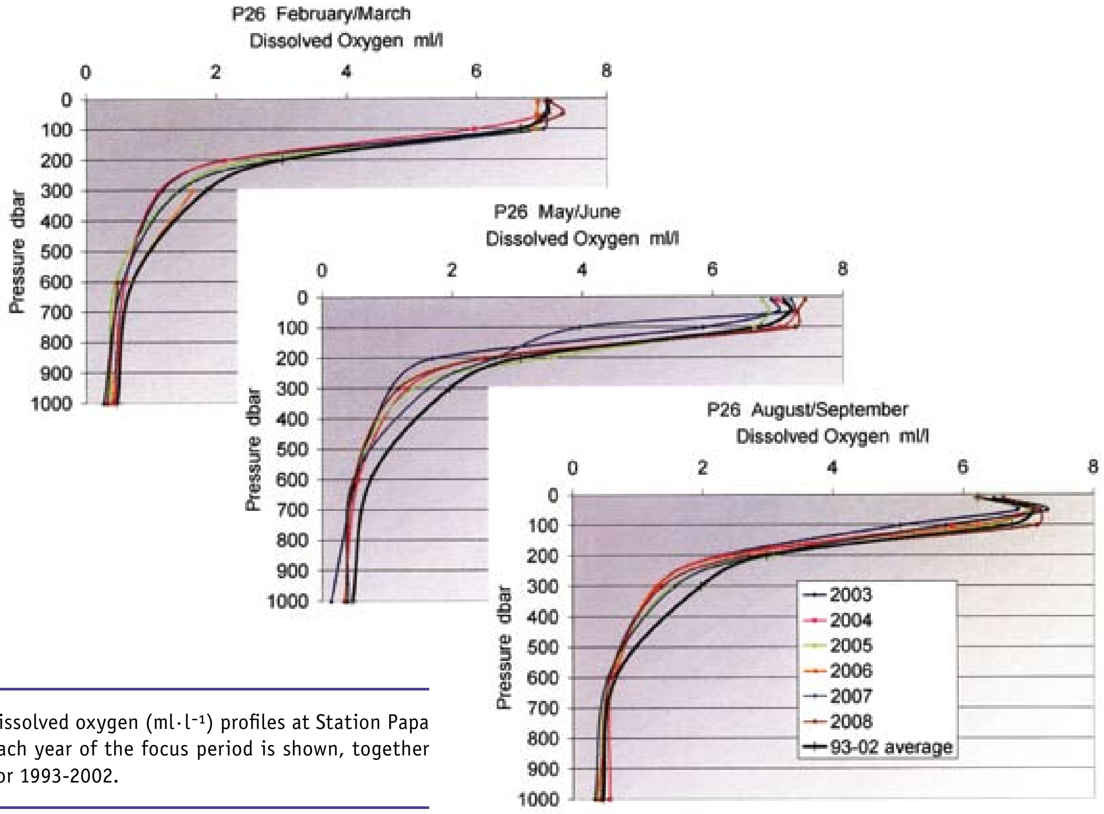

[Figure OC-16] Dissolved oxygen (ml·l⁻¹) profiles at Station Papa for 3 seasons. Each year of the focus period is shown, together with the mean for 1993-2002.

3.3.1 Temperature

Profiles for each season and each year at Station Papa are plotted in Figure OC-14 together with the mean for 1993 to 2002. In late winter (February/March) all years of the focus period, except 2008, were warmer than the 1993-2002 average at the surface (to ~50 m). 2005 was exceptionally warm through the upper 200 m at Station Papa and was the warmest or second warmest year at P16 and P12 in all seasons (2003 and 2004 were other warm years). However, surface waters were coldest in 2008 at all stations and in all seasons, in agreement with the basin scale anomaly (Fig. OC-7).

3.3.2 Salinity

The surface waters were fresher in all seasons and all years of the focus period (Fig. OC-15) than the average for 1993-2002 (to ~70 m in February/March, to ~30 m in May/June, to ~40 m in August/September). Mean salinity over the surface 1000 m was also less in all seasons and all years than the average for 1993 to 2002 (except for summer 2004) suggesting that the quantity of salt in the water column has decreased. Surface waters were also fresher than the long-term mean at P16 and at P12 in winter and spring of each year, though summer surface waters were slightly more saline than the mean in 2004, 2006 and 2008 at P12.

3.3.3 Density

Warmer temperatures and fresher water resulted in least dense surface waters in 2005. Conversely, the cold conditions and slightly higher salinities in 2008 caused the most dense surface water during the focus period. Only 2008 had denser surface waters in winter than the average for 1993-2002 and this was the case at all 3 stations.

3.3.4 Dissolved Oxygen

Declining oxygen levels in sub-surface waters of the Subarctic Pacific are occurring (Whitney et al. 2007) and are evident in the Line P dataset (Fig. OC-16). With the exception of summer 2004, all years and all seasons had lower dissolved oxygen below about 250 m at Station Papa than the average for 1993-2002. The warm temperatures of 2005 led to the lowest surface oxygen levels of the focus period, while cold conditions in 2008 led to generally the highest surface oxygen levels.

© R. Hopcroft

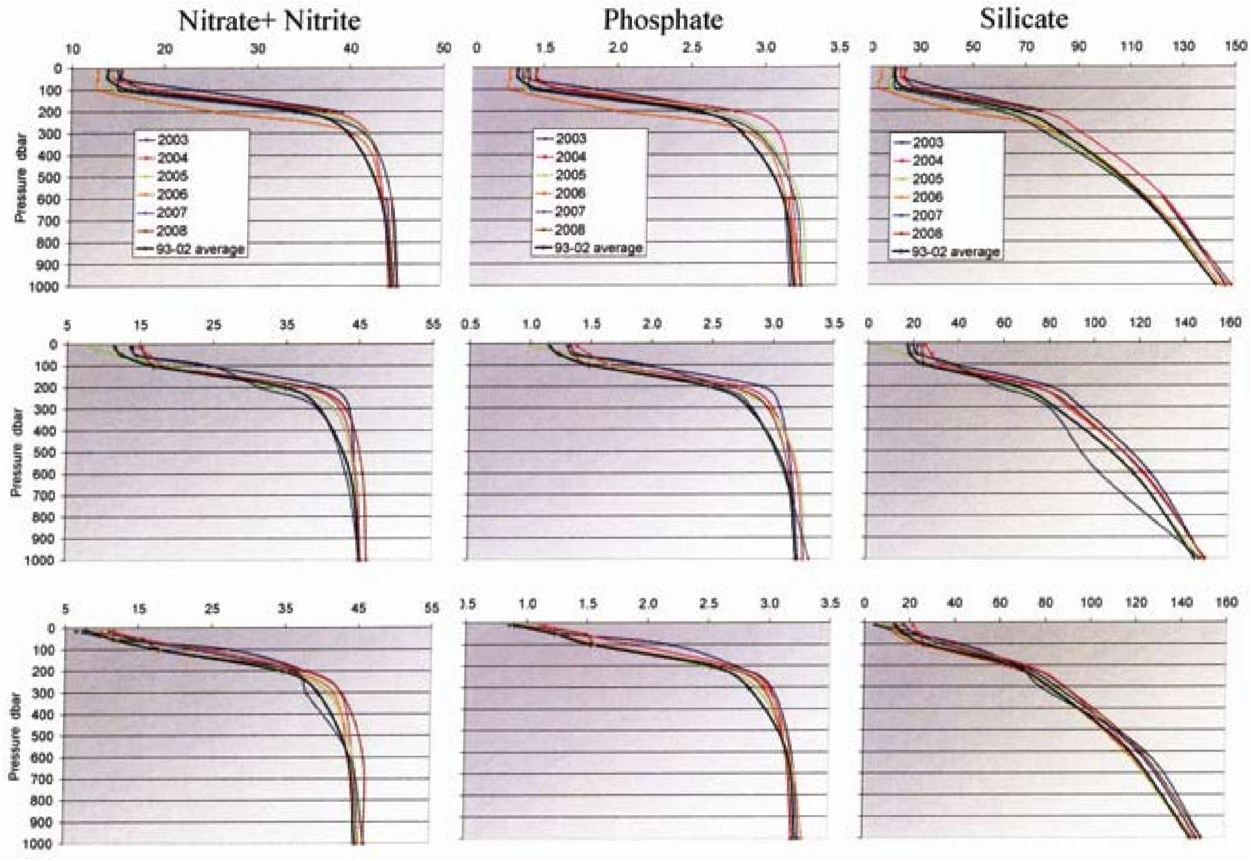

[Figure OC-17] Nutrient profiles (µmol·l⁻¹) at Station Papa. Top row = winter, centre row = spring, bottom row = summer.

3.3.5 Nutrients

As a general rule the level of nitrate (plus nitrite) was higher during the focus period than the 1993-2002 average for most years and most seasons (Fig. OC-17). The 2008 concentrations of nitrate were particularly high at depth, especially in spring and summer. The 2006 concentrations were particularly low, especially in winter, but also at the lower end in summer (no cruise in spring 2006). Most phosphate concentrations during the focus period were higher than the 1992-2003 mean although the concentrations in 2006 were quite low in winter. Similarly high levels of silicate occurred, except in spring 2007 below 150 m, and in 2005 when concentrations were similar to the long-term mean. Note that spring 2005 was the only spring with lower values of nitrate, phosphate, and silicate than the 1993-2002 average, and it had the lowest dissolved oxygen during the focus period.

3.3.6 pH *(Miller)*

The time period between 2003 and 2008 is too short to confidently identify a pH decrease in the oceans due to anthropogenic carbon dioxide emissions. However, these data will provide a valuable comparison to the historical data, dating back to the summer of 1956, when they have been quality-controlled and released. Average profiles of pH data collected along Line P show that the pH distribution is consistent with depth across the transect. Surface values are around 8.05, with a minimum of about 7.55 at 500-1000 m, rising to above 7.7 in deep waters (Fig. OC-18). This pattern parallels the oxygen profiles and is primarily a result of varying spatial distributions of photosynthesis and respiration. The greatest variability is seen in the surface waters and at the pycnocline. Note that because of the depth distribution of pH, bottom communities nearer the coast live in lower pH waters than those off the coast.

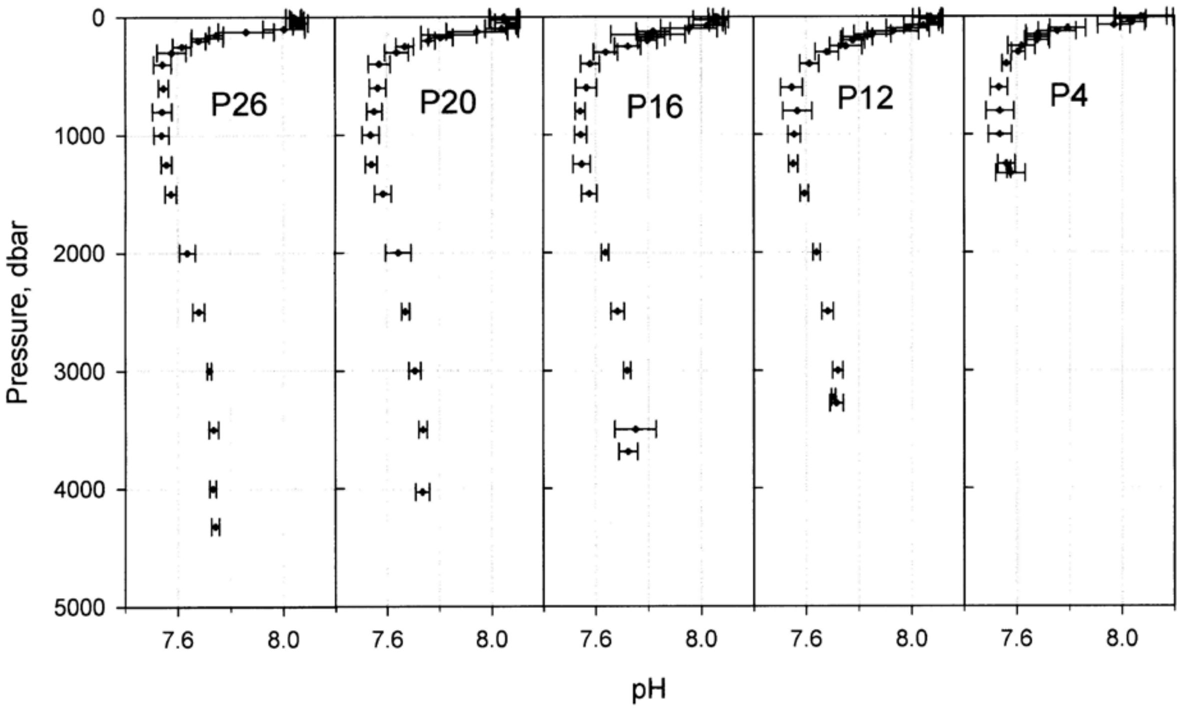

[Figure OC-18] Profiles of *in situ* pH along Line P. Error bars give ±1 standard deviation between seasonal (spring, summer, and fall) cruises, 2004-2008.

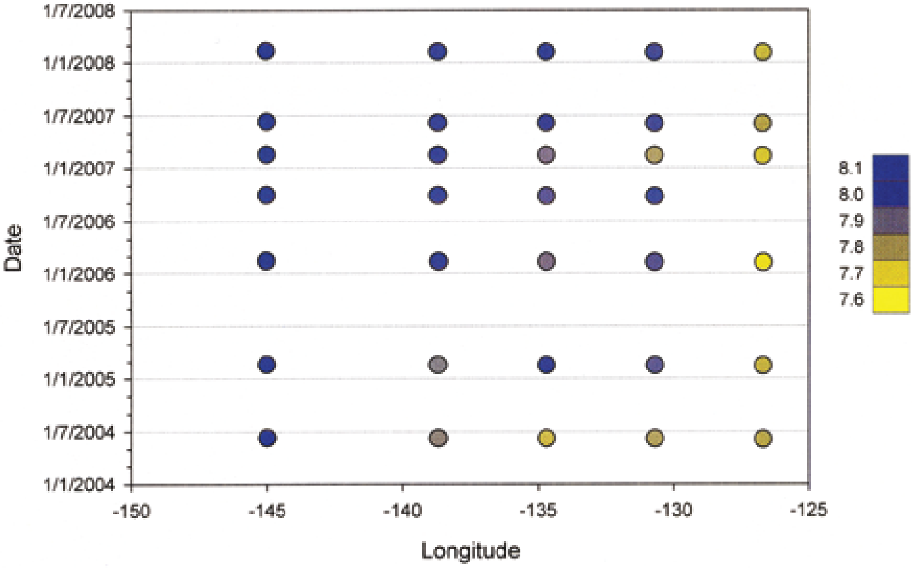

[Figure OC-19] pH on the 26.0 σ_θ surface along Line P over time.

On the 26.0 σ_θ density surface, which is roughly the source of coastal upwelling water and coincident with the permanent pycnocline, pH appears to have increased between 2004 and 2008 (Fig. OC-19), contrary to the long-term global trend. This increase is also contrary to the change in salinity, which was decreasing and would have lowered pH, if acting alone. Interestingly, dissolved oxygen also increased on the 26.0 σ_θ during this period, again contrary to the general trend over the last 50 years. If that increase in oxygen content in the pycnocline between 2004 and 2008 is the result of decreasing respiration rates, this would also explain the increase in pH.

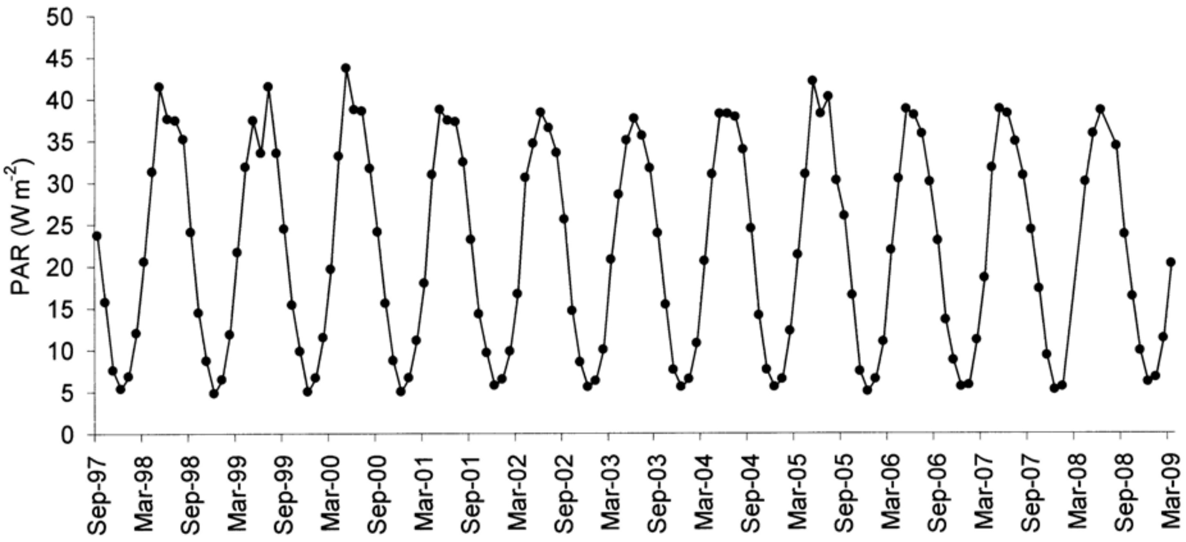

[Figure OC-20] Monthly Photosynthetically Active Radiation from SeaWiFS for a region of the NE Pacific centred on Station Papa produced with the Giovanni online data system, developed and maintained by the NASA Goddard Earth Sciences (GES) Data and Information Services Center (DISC).

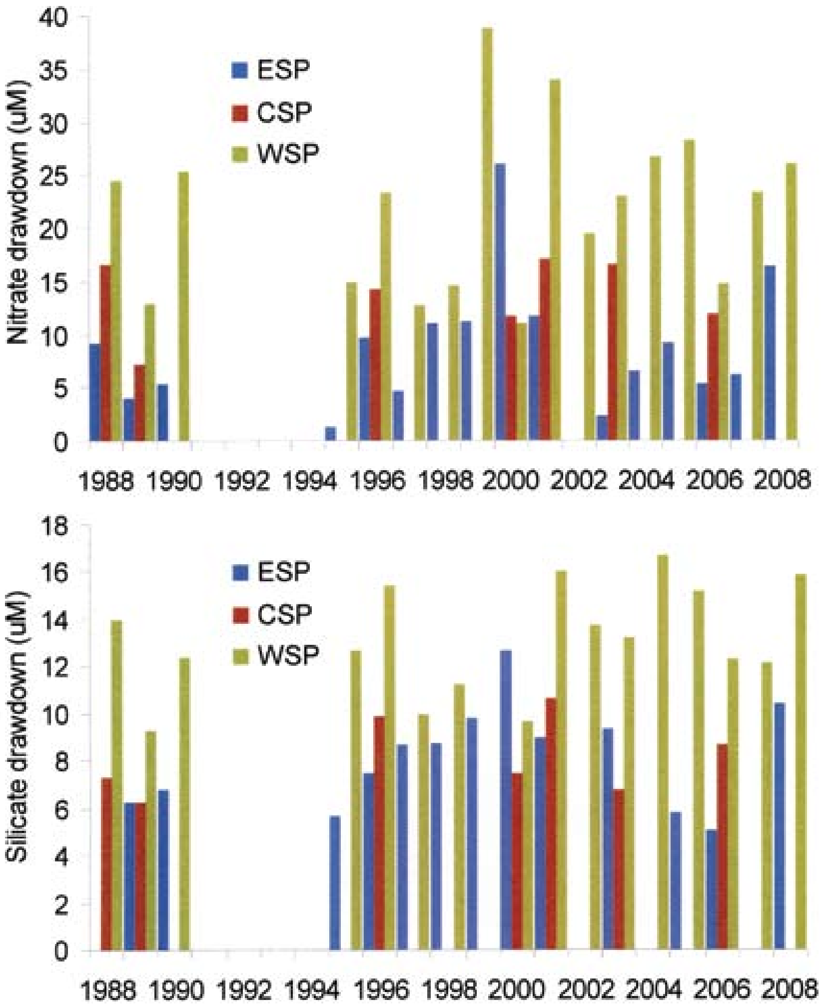

[Figure OC-21] Estimated seasonal nutrient drawdown for 3 regions of the North Pacific. Upper panel – nitrate drawdown, lower panel – silicate drawdown.

3.3.7 Photosynthetically active radiation *(Peña)*

The monthly time series of SeaWiFS Photosynthetically Active Radiation (PAR) shows highest values during May to July and little interannual variability (Fig. OC-20).

3.4 Nutrient data from ships of opportunity *(Whitney)*

Commercial ships crossing the North Pacific were used since 1987 to collect water samples that have been analysed for nutrient drawdown. Data for three geographical domains are included here; the Western Subarctic Pacific (WSP, 155-172°E, 45-53°N), the Eastern Subarctic Pacific (ESP, 140-155°W, 49.5-57°N) and the Central Subarctic Pacific (CSP, 45-51°N 160-180°W). Estimates of annual drawdown of silicate and nitrate were made by averaging all available data in each geographical domain for February and March (January was included if February and March data were scarce) and August/September (Fig. OC-21). Drawdown indicates nutrient use by phytoplankton in regions where winter storms are the dominant cause of mixing the ocean. It is not useful for this purpose in regions where tidal mixing is strong such as near the Aleutian or Kuril Islands.

Nutrient drawdown is stronger in the WSP where winter levels average 24 µM nitrate and 40 µM silicate, compared to the central and eastern domains where 18 µM nitrate and 26 µM silicate are typical winter levels. Transport of iron is stronger in the WSP due to prevalent current and wind directions, allowing 13 µM nitrate (18 µM silicate) to be drawn down seasonally compared to 8 µM nitrate (9 µM silicate) in the ESP. In all regions, strong or weak drawdown events were observed but no evidence of trends was found. The stronger stratification that reduced nutrient supply to surface waters along Line P in the 1990s, compared to the 1970s (Whitney and Freeland 1999) has broken down in recent years. Next to 2000, strongest nutrient drawdown in the ESP was in 2008.

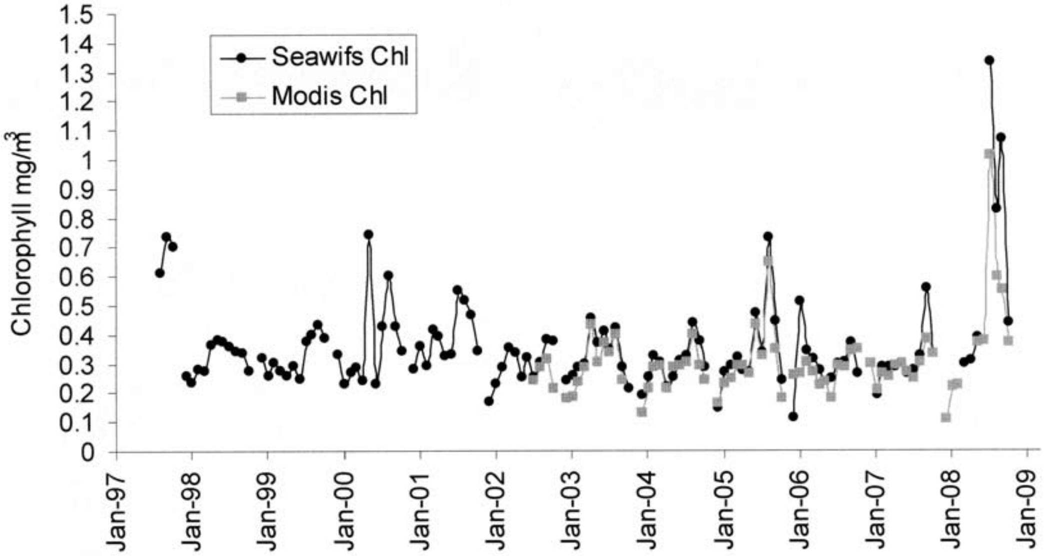

[Figure OC-22] Satellite-derived chlorophyll concentrations for a region of the NE Pacific centred on Station Papa from the MODIS and SeaWiFS satellites produced with the Giovanni online data system, developed and maintained by the NASA Goddard Earth Sciences (GES) Data and Information Services Center (DISC).

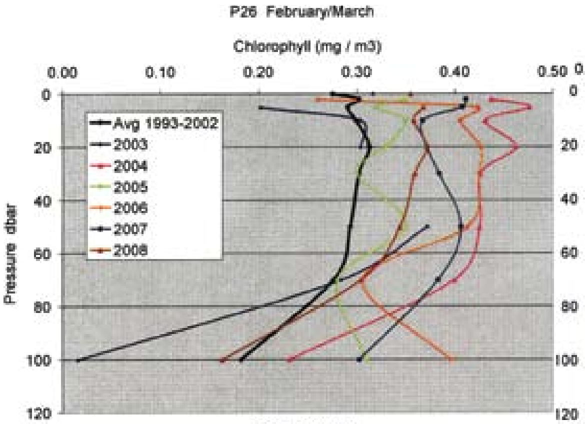

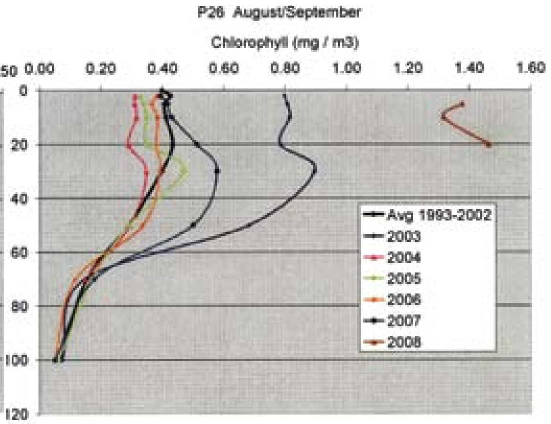

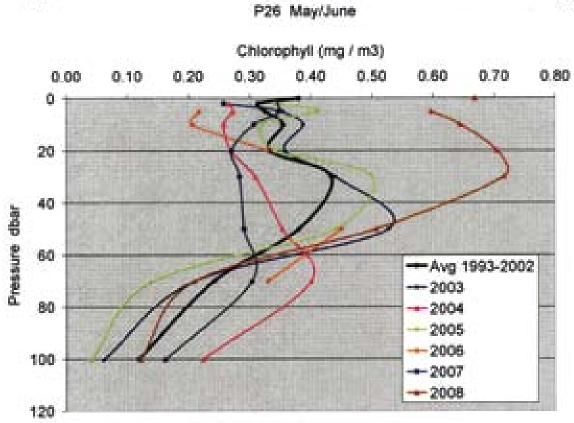

[Figure OC-23] Profiles of chlorophyll concentration at Station Papa in each year in each season, together with the long term mean (1993-2002).

4.0 Phytoplankton

4.1 Chlorophyll at Station Papa *(Peña)*

Chlorophyll concentrations are usually low (<0.5 mg·m^{-3}) and show little seasonal variability in the eastern Subarctic Pacific (Fig. OC-22) and Station Papa field data (Fig. OC-23). Satellite data show four peaks in chlorophyll concentration: fall 1997, spring 2000, fall 2005 and summer 2008. The origins of the anomalous peak in 2008 are currently being investigated. Ship-based observations at Station Papa show chlorophyll concentrations in winters of 2004 to 2008 were slightly higher than the average for 1993-2002 (Fig. OC-23). This increase could be related to the shallowing of the winter mixed layer depth that has been previously reported (Freeland et al. 1997). In spring of 2003-2008, chlorophyll values were similar to the average, with the exception of 2008 which was higher. Late summer values were also similar to the long-term average except for 2003 and 2008 which were also higher.

4.2 Community composition at Ocean Station Papa *(Peña)*

Prymnesiophytes dominate phytoplankton biomass during the year (Fig. OC-24). In general, diatoms and cryptophytes are also abundant in spring whereas in summer dinoflagellates are the second most abundant phytoplankton group. Unusually high chlorophyll concentrations were observed by satellite data across the eastern Gulf of Alaska in August and September 2008 compared to these months the previous six years. The high concentrations observed by the satellite in August were confirmed by *in situ* observations (~1.3 mg·m^{-3}; Fig. OC-23). Despite the strong change in phytoplankton biomass in August 2008, the phytoplankton composition at Station Papa looks similar to that of August/September in the previous 2 years (Fig. OC-24). As before, prymnesiophytes and dinoflagellates contributed to most of the chlorophyll concentration (~70%). The main difference in composition compared to previous years was a slight increase (~10%) in diatoms at Station Papa, but not at the other offshore stations along Line P. Similarly, PAR values in August and September 2008 were not different to the values from previous years (Fig. OC-20).

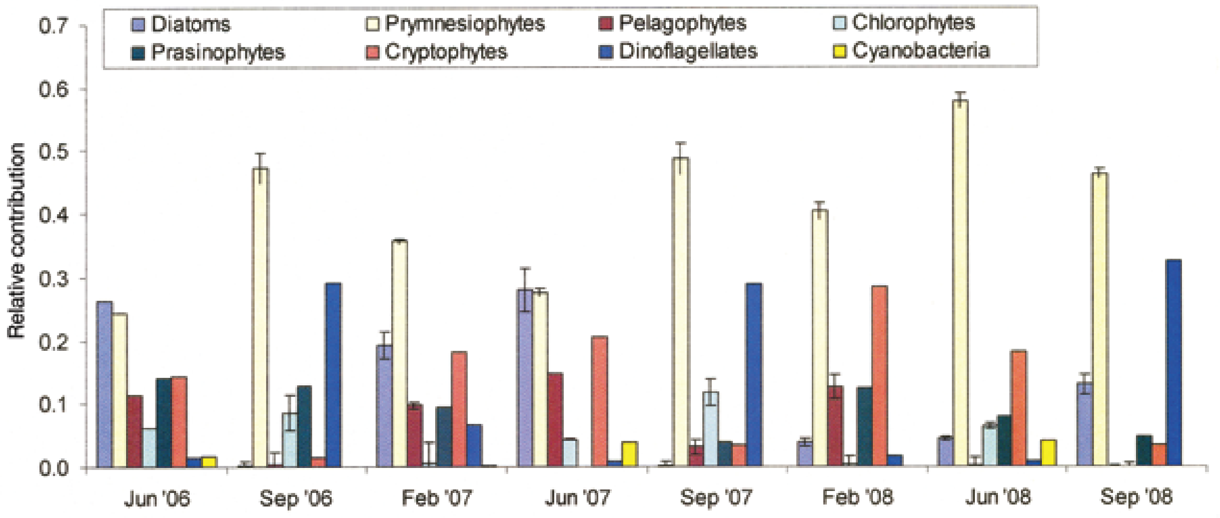

[Figure OC-24] Relative contribution of the main phytoplankton groups in the surface mixed layer at Station Papa obtained by CHEMTAX (Mackey et al. 1996) using pigment data from 5 and 10 m.

4.3 Chlorophyll in the Subtropics

(Polovina, Woodworth)

With limited information available from direct observations, satellite remote sensing of surface chlorophyll$_a$ provides the best insight into the phytoplankton dynamics of the Subtropical region. In the Subtropical central Pacific, surface concentrations are generally <0.15 mg·m^{-3} and closer to the Subarctic they are >0.25 mg·m^{-3}. From the SeaWiFS ocean color sensor there is a time series of surface chlorophyll available from 1998 to the present. An increase was observed in the magnitude of the area of lowest surface chlorophyll waters in the central North Pacific (≤0.07 mg·m^{-3}) from 1998 to 2006 by about 2% per year in both the winter and summer seasons coherent with increases in sea surface temperature (Fig. OC-25) (Polovina et al. 2008). There was an eastward expansion of these low surface chlorophyll waters between the beginning and end of the time series (Fig. OC-26) that tracked similar expansions in the South Pacific, North Atlantic, and the South Atlantic, at rates ranging from 1-4% per year (Polovina et al. 2008). The expansion of low surface chlorophyll waters is consistent with a global warming scenario of increased vertical stratification but the observed rates already exceed long-term model predictions (Polovina et al. 2008).

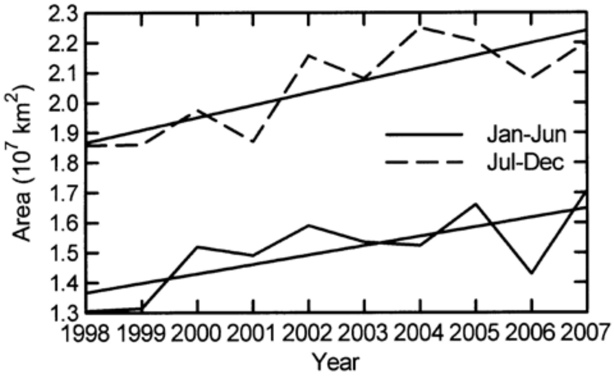

[Figure OC-25] Area for the mean January-to-June and July-to-December seasons with surface chlorophyll ≤0.07 mg·m^{-3} from SeaWiFS ocean colour sensor, 1998-2007. Straight lines indicate linear model fits to the data.

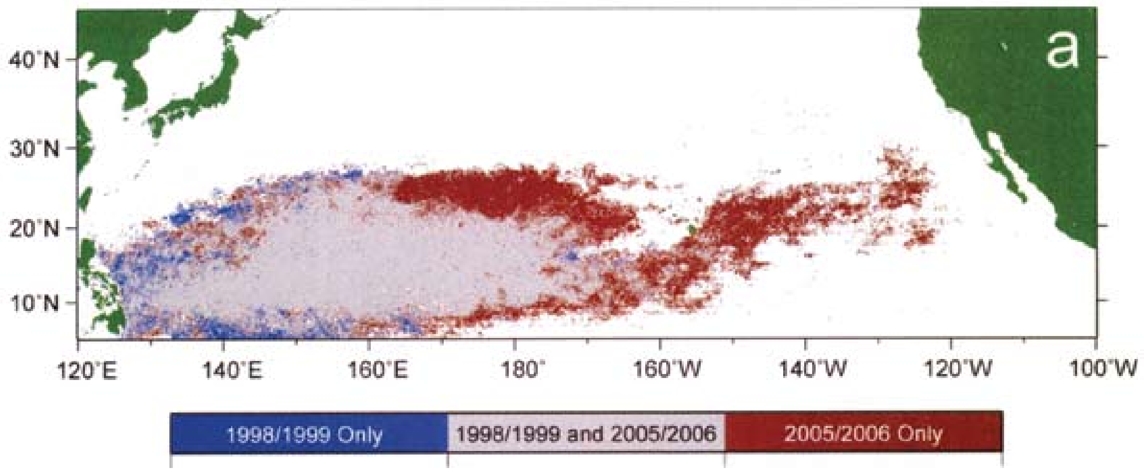

[Figure OC-26] The area ≤0.07 mg·m^{-3} surface chlorophyll in December 1998/1999 and 2005/2006 (grey), present in 1998/1999 but not in 2005/2006 (blue) and present in 2005/2006 but not in 1998/1999 (red).

a) February 1998

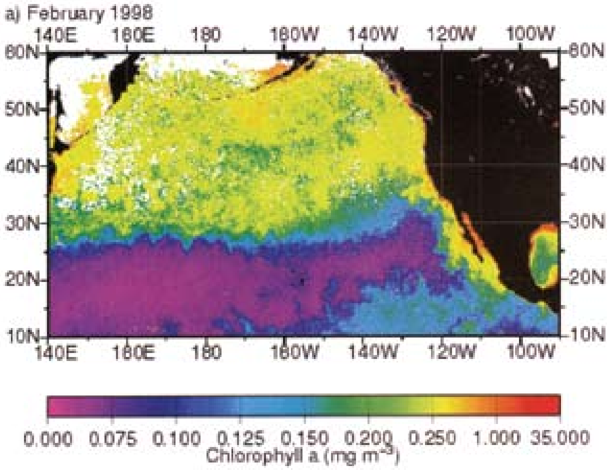

b) The 0.2 mg m^{-3} Ocean Color Contour for January+February

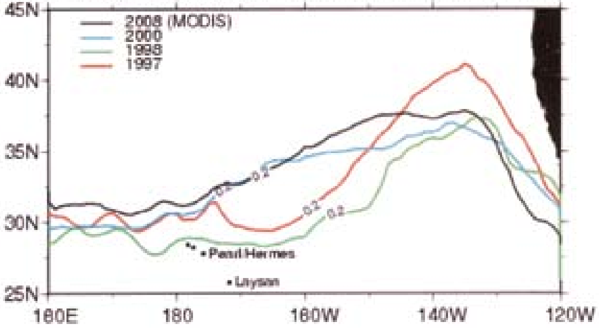

[Figure OC-27] Surface chlorophyll density (mg·m^{-3}) estimated from SeaWiFS ocean colour for (a) February 1998 and (b) the mean position, averaged over January and February, of the Transition Zone Chlorophyll Front defined as the 0.2 mg·m^{-3} contour illustrating the south-shifted position in El Niño years 1997 and 1998, and the north-shifted position in La Niña years 2000 and 2008.

Between these regions of high/low surface chlorophyll lies the sharp basin-wide surface Transition Zone Chlorophyll Front (TZCF) (Polovina et al. 2001). The TZCF oscillates seasonally north to south about 1000 km with a latitudinal minimum in January-February and maximum in July-August (Polovina et al. 2001). The southernmost winter position of this biological front also exhibits considerable interannual variability. During the 1997-1998 El Niño, the southern extreme of the TZCF was south of 30°N, reaching the northwestern part of the Hawaiian Archipelago. During the 2000 and 2008 La Niña periods, however, the southern extreme of the TZCF shifted by as much as 500 km northward (Fig. OC-27). There is coherence between SSH EOF1, vertical temperature and chlorophyll sections, and the southernmost winter position of the TZCF (Figs. OC-12, OC-13, OC-27). The SSH rises (drops) reflecting an increase (decrease) in warm stratified water between 28-32°N latitude, and the TZCF southern minimum shifts northward (southward).

4.4 Chlorophyll in the Subarctic *(Whitney)*

Satellite-derived chlorophyll$_a$ estimates from SeaWiFS and MODIS satellites for the same three geographical domains discussed in Section 3.4 are included here (Fig. OC-28). Areas averaged are entirely oceanic for the Central Subarctic Pacific (CSP) and Eastern Subarctic Pacific (ESP), but cover a small area of coast in the Western Subarctic Pacific (WSP) which may enhance the spring bloom characteristics of this time series. Both concentration and seasonal variability were greatest in

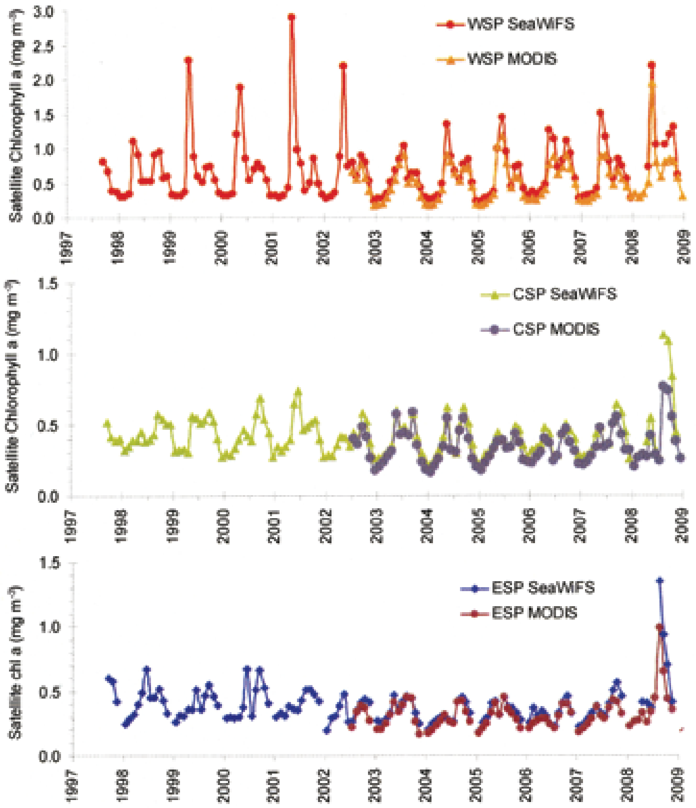

[Figure OC-28] Chlorophyll$_a$ concentration for 3 regions (WSP, 155-172°E, 45-53°N; ESP, 140-155°W, 49.5-57°N; CSP, 45-51°N 160-180°W) estimated from ocean colour sensing satellites.

the WSP, a consequence of stronger nutrient supply in winter and enhanced iron supply. All three regions show a peak in 2008. The extraordinary event in the ESP and CSP is the chlorophyll spike in August 2008 (see also Section 4.1). This is a unique event in the satellite chlorophyll record and covered most of the ESP. The high nutrient-low chlorophyll waters of the ESP generally have stable chlorophyll levels of 0.3 to 0.5 $mg \cdot m^{-3}$ throughout the year. When offshore chlorophyll peaks have been observed, they were associated with iron transport by mesoscale eddies. Surface currents move waters from the Asian coast toward the ESP, but when they arrive iron levels are extremely low. Spring and summer growth in the ESP is strongly controlled by the availability of iron, relying mainly on winter mixing to infuse small amounts that support slightly enhanced primary productivity in spring. Occasionally, an old eddy stimulates growth as was seen near Station Papa in 2000 (Whitney et al. 2005). Others have theorized that dust is a potentially significant iron source (Boyd et al. 1998), although no strong evidence has yet been shown of stimulated phytoplankton growth from volcanic eruptions or dust storms. At the moment, the definitive cause of the 2008 bloom in the ESP and CSP is not known. Leading candidates are volcanic ash* and vertical transport enhanced by the deepened mixing of the previous winter. Oddities in nutrient dynamics and phytoplankton in 2008 are summarized as follows:

- A very cold winter resulted in deeper winter mixing and a delay in spring stratification;
- Little nitrate or silicate was drawn down between February and June;
- A bloom event in August, perhaps affiliated with a volcanic eruption in the Aleutian Islands, drew down Si and N at a high ratio which is typical of the response seen during an artificial iron enrichment study at Station Papa (Boyd et al. 2004).

---

*Hamme, R. et al. 2010. Natural Volcanic Iron Fertiization of the Subartic North Pacific, EOS Transactions. AGU 91(26), Ocean Sciences Meeting Supplement, Abstract IT23C-01

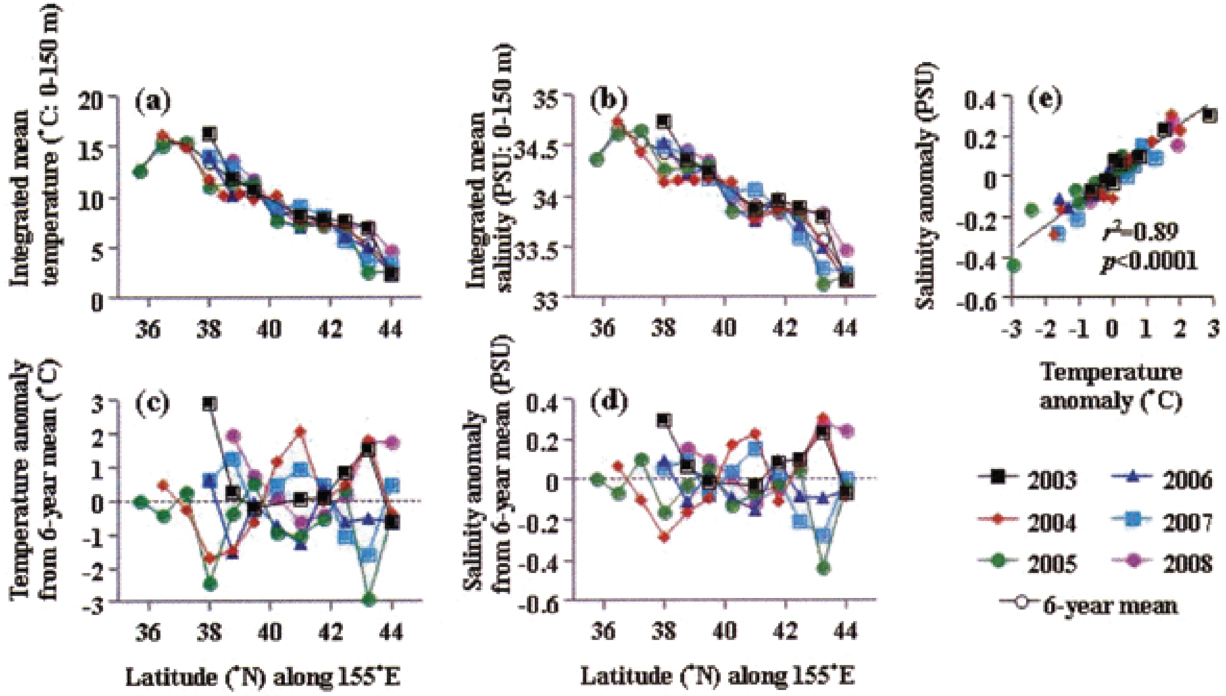

[Figure OC-29] Integrated mean temperature (a) and salinity (b) at 35° 45'N-44° 00'N along 155°E in the western North Pacific between 10-20 May, 2003-2008. Temperature (c) and salinity (d) anomalies from a 6-year mean are also calculated. Anomalies in salinity and temperature are highly correlated (e).

5.0 Zooplankton

5.1 Western North Pacific

5.1.1 Oshoro Maru *(Yamaguchi)*

Zooplankton sampling was conducted using vertical tows of NORPAC nets (0.33 mm mesh) from 0-150 m at twelve stations every 83.3 km, between 35°45'N and 44°00'N along the 155°E line in the western North Pacific between 10-20 May, 2003-2008. Each study region was classified according to latitude as: Subarctic Front (SF: >42°N), Transition Domain (TR: 40-42°N), Subarctic Boundary (SB: 38-40°N) or Subtropic Current System (ST: <38°N). Temperature and salinity anomalies from 6-year means were correlated with each other, and were higher at SF in 2008 (Fig. OC-29). Zooplankton biomass was greater in the TR (ca. 100 mgDM·m^{-3}), followed by the SF (60 mgDM·m^{-3}) and the SB (45 mgDM·m^{-3}) (Fig. OC-30). High zooplankton biomass at the SF in 2008 (100 mgDM·m^{-3}) may be related to the high temperature during that period (a northward shift of the transition domain). Taxonomic composition of zooplankton biomass showed latitudinal variation and was dominated by small and large copepods in regions >40°N (SF and TR), while regions <40°N (SB and ST) were dominated by amphipods, euphausiids and chaetognaths as well as copepods. There was similar taxonomic composition at the TR and SF, while the high biomass in the TR might be a reflection of faster copepod development caused by high temperatures in the region. Prominent high values (130-260 mgDM·m^{-3}) were noted in the TR in 2003, caused by a dominance of salps (*Salpa fusiformis*). Temperature and salinity anomalies could not explain the dominance of salps.

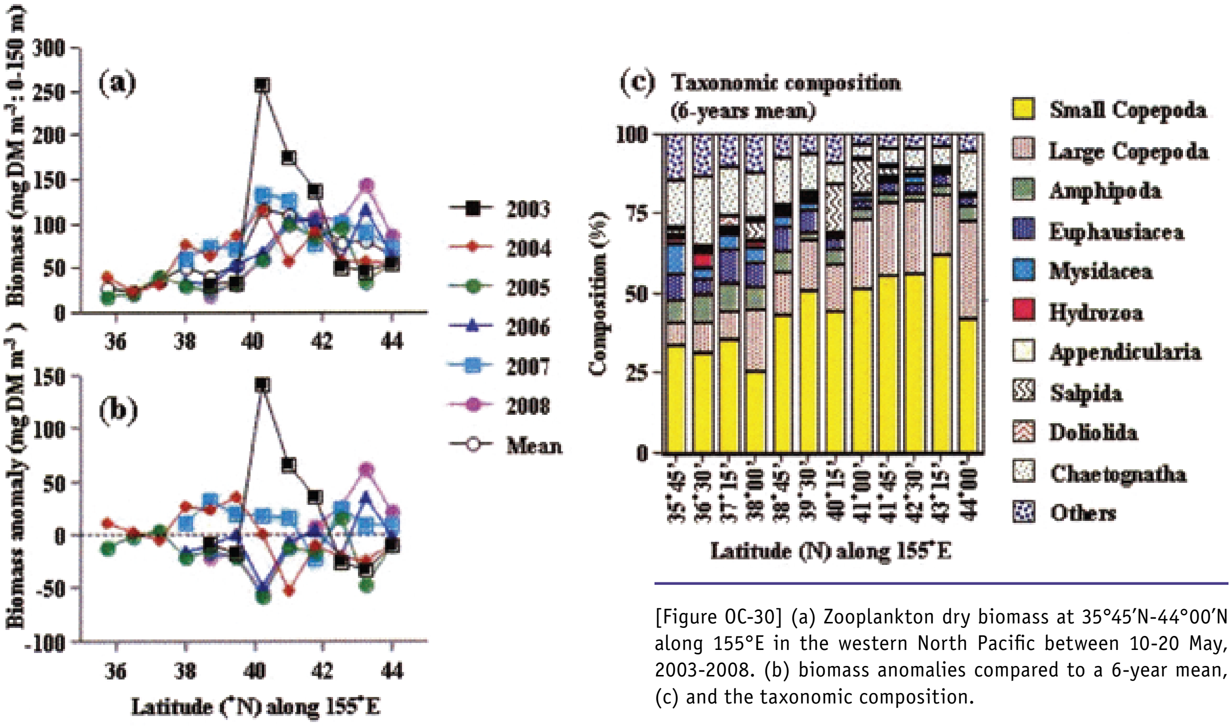

[Figure OC-30] (a) Zooplankton dry biomass at 35°45′N-44°00′N along 155°E in the western North Pacific between 10-20 May, 2003-2008. (b) biomass anomalies compared to a 6-year mean, (c) and the taxonomic composition.

5.1.2 Continuous Plankton Recorder *(Batten)*

The Continuous Plankton Recorder (CPR) was towed behind a merchant ship on a transect crossing the open western Pacific at a latitude of ~50°N so that it is further north and east than the *Oshoro Maru* data described above and can be considered as fully Subarctic waters. Taxonomic abundance data were converted to biomass using taxon specific dry weights and summed to give total biomass per sample (~3 m³). Samples collected between 160° and 168°W from the surface ~10 m in the late spring/early summer of each year were averaged to give mean values for the region (Fig. OC-31). Sampling usually took place in June but occasionally in May and July in which case both values are shown for that year (2006 and 2008). There was considerable variability, a factor of 10 between the lowest and highest years. There is some agreement with the most northerly *Oshoro Maru* data in that the most recent 3 years (2006, 2007 and 2008) had higher biomass than the prior 3 years (2003, 2004 and 2005), but the sampling locations and methodologies were very different so not too much emphasis should be placed on this result.

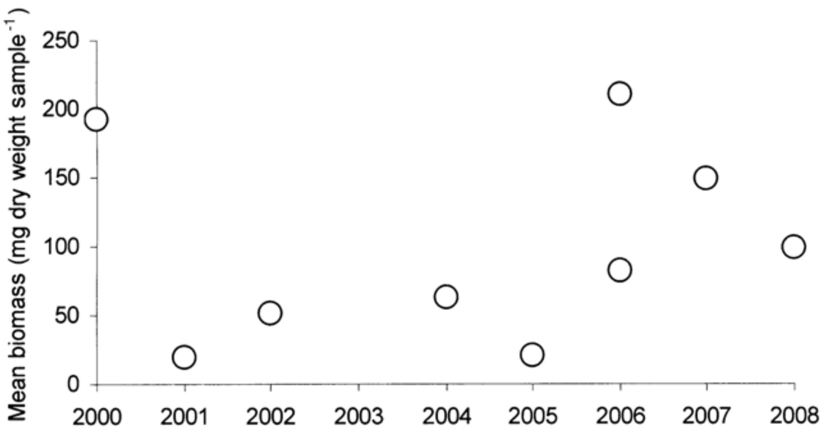

[Figure OC-31] Mean zooplankton biomass from CPR sampling, 160-168°W in late spring/early summer of each year. May and July values in 2008 are superimposed.

5.2 Eastern North Pacific *(Mackas, Batten)*

Frequent zooplankton sampling was conducted at Station Papa from 1956-1980 as part of the "Weathership" time series (Fulton 1983; Waddell and McKinnell 1995; McKinnell and Mackas 2003) but it ended with the retirement of weatherships. From 1980 to the late 1990s, most of the zooplankton sampling in the oceanic Alaska Gyre was either during two intensive but brief research projects; Project SUPER, 1983, 1987, and 1988 (e.g., Mackas et al. 1993, Miller 1993), Canadian JGOFS, 1996-1997 (e.g. ,Goldblatt et al. 1999) or the once-per-year sampling along 145°W that was done as part of the large scale Japanese *Oshoro Maru* surveys of the entire Subarctic Pacific (e.g., Sugimoto and Tadokoro 1997). More regular net tow sampling resumed along Line P in 1997, stimulated in part by the 1997-1998 El Niño (Mackas and Galbraith 2002). The present effort consists of three surveys per year: February, late May or June, and August or early September. For analysis purposes Line P was divided into two segments: outer Line P (stations P16, P20, and P26=Station Papa) ; this segment contains the HNLC stations that are usually iron limited from spring through autumn, and inner Line P (stations P4, P8, and P12). This segment has more exchange with the continental margin and often shows nitrate depletion in summer.

Monitoring zooplankton in the Alaska Gyre by the CPR began in 1997 with a pilot study in July-August (Fig. OC-32). Since 2000 sampling continued as a series of 6-8 survey lines per year. Both the "modern" Line P and the CPR time series are now about a decade in length, allowing relatively stable average seasonal cycles of zooplankton biomass and community composition to be computed. From these it is possible to examine interannual differences in seasonal timing of growth and dormancy of the dominant copepod *Neocalanus plumchrus* and to produce time series of taxon-specific deviations from the average seasonal abundance and biomass. Calculations used to convert raw net tow data to annual amount and composition anomalies are identical in sequence to those previously described for the longer continental margin time series (e.g., Mackas et al. 2001). Abundance, biomass and stage composition ratios can be used to measure changes in zooplankton seasonal timing (Mackas et al. 1998, 2007; Batten et al. 2003; Batten and Mackas 2009).

5.2.1 Seasonal cycles of amount and species composition

Based on presence-absence, the zooplankton taxa in the Line P time series samples are the same as those found in samples from the Vancouver Island continental margin. However, the dominance hierarchies differ between continental margin (Mackas et al. 2001) and oceanic regions (Mackas and Galbraith 2002). Seaward of the continental margin, the largest component of the annual total and spring-summer seasonal biomass (Fig. OC-33) consists of a small number of copepod species that can be characterized zoogeographically as "subarctic oceanic" (primarily *Neocalanus plumchrus*, *N. cristatus*, *N. flemingeri*, *Eucalanus bungii*, and *Metridia pacifica*, plus much smaller contributions from *Paraeuchaeta elongata* and *Racovitzanus antarcticus*). All have distributions that span the Pacific basin, north of the Subarctic Front. *Neocalanus*, *Eucalanus* and *Euchaeta* are large in individual size (~0.5-1 cm total length as late juveniles and adults), and both *Neocalanus* and *Eucalanus* have very distinctive life history strategies involving deep ontogenetic vertical migration, and 1-3 year life cycles (depending on location) including one or more prolonged seasonal dormancy periods (Fulton 1973; Miller et al. 1984; Miller and Clemons 1988; Miller and Terazaki 1989; Tsuda et al. 1999). The migration and dormancy strategies result in a distinct spring-early summer maximum of biomass, earliest and most pronounced for *N. plumchrus* and *N. flemingeri*; more prolonged for *Eucalanus* and *N. cristatus*.

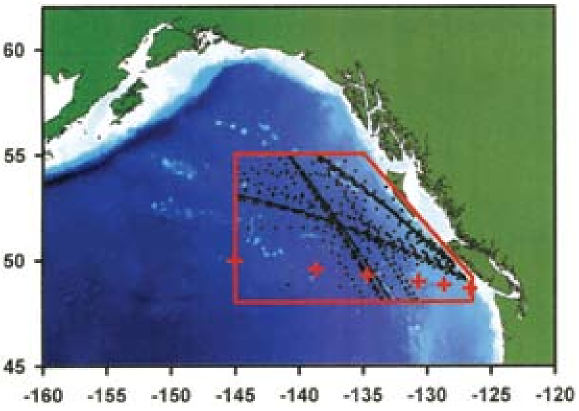

[Figure OC-32] Sampling locations for the recent Line P zooplankton monitoring program (red + are the Line P stations P26, P20, P16, P12, P8, P4 from west to east) and for the North Pacific CPR program (black dots are samples along north-south and east-west shipping routes, red box indicates the 48-55°N 'box' within which temporal coverage is best.

The second largest component of biomass is the chaetognaths, primarily two cool water species *Parasagitta elegans* and *Eukrohnia hamata*. These also peak in spring and summer, but slightly later than the copepods on which they feed. Other major contributors to total biomass are the pteropods (*Limacina helicina*, *Clione limacina*, and occasionally *Clio pyramidata*), gelatinous predators (siphonophores and medusae), and a "remainder" category dominated by large diel-migratory taxa such as shrimps, small squids, and small midwater fishes. Categories present but at lower average abundance/biomass than along the continental margin include euphausiids (with *Thysanoessa inspinata* replacing *Euphausia pacifica* and *T. spinifera* as the most common species), hyperiid amphipods, and "Boreal Shelf" and "California Current" copepod groups (see Mackas et al. 2001 or Mackas et al. 2007 for the species included in each group).

5.2.2 Anomalies of amount and species composition

Large interannual changes are seen in the "success" of various species and species groups (Fig. OC-34). The most striking results have been upward trends (equivalent to 3-5 fold increases) in the biomass of the large interzonal migrant "Subarctic oceanic" copepods (*Neocalanus cristatus, N. plumchrus, N. flemingeri, Eucalanus bungii*) and the cool-water chaetognaths (*Parasagitta elegans, Eukrohnia hamata*). These changes are correlated with the recent upper ocean cooling (r^2 = 0.3-0.4) but are even more strongly associated (r^2 = 0.5-0.65) with the recent strengthening of the eastward North Pacific Current that has been revealed by the Argo network of profiling drifters (H. Freeland pers. comm.).

Within the Subarctic Oceanic copepod group, which includes the overall dominant members of the zooplankton community (Fig. OC-33), the strongest increases have been by the two largest-bodied species, *N. cristatus* and *E. bungii*. These species also have longer growing seasons and later entry into seasonal dormancy. Note also that anomaly magnitudes are greater for the more oceanic outer Line P subregion. This suggests that we are observing oceanic processes, rather than seaward propagation of changes originating at the eastern margin.

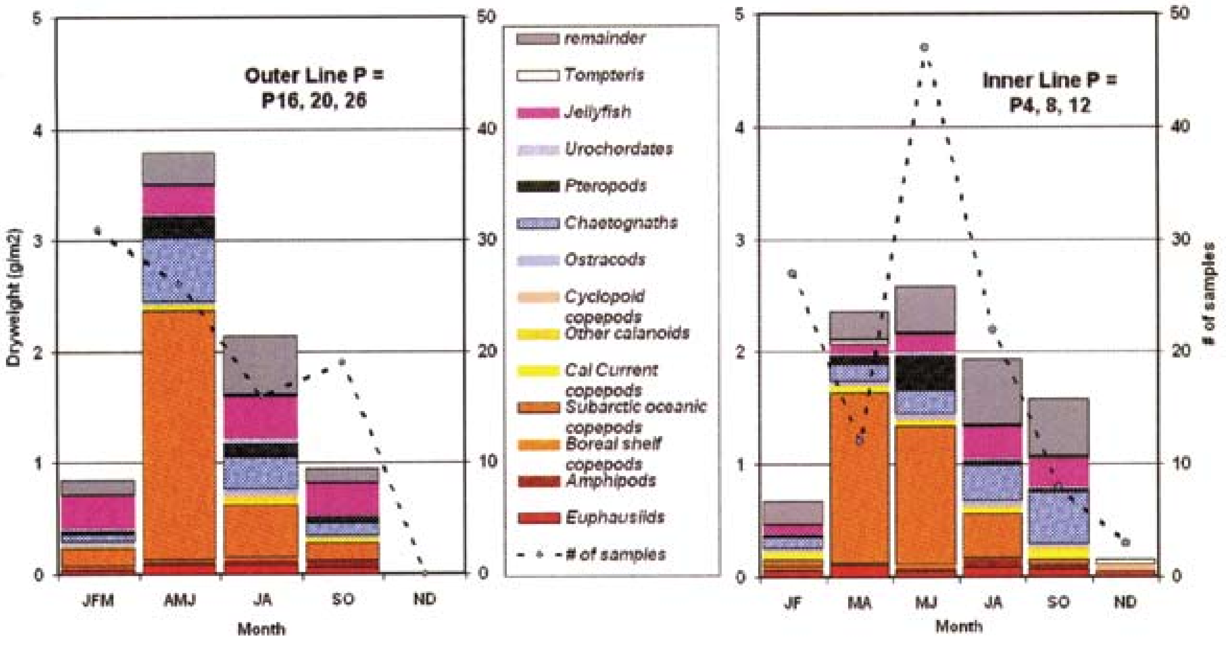

[Figure OC-33] Average seasonal cycles of mesozooplankton biomass (geometric mean dry weight m^{-2}) within various composite taxonomic groups, for "outer" and "inner" Line P. These are used as climatologies against which individual years are compared, to produce anomaly time series.

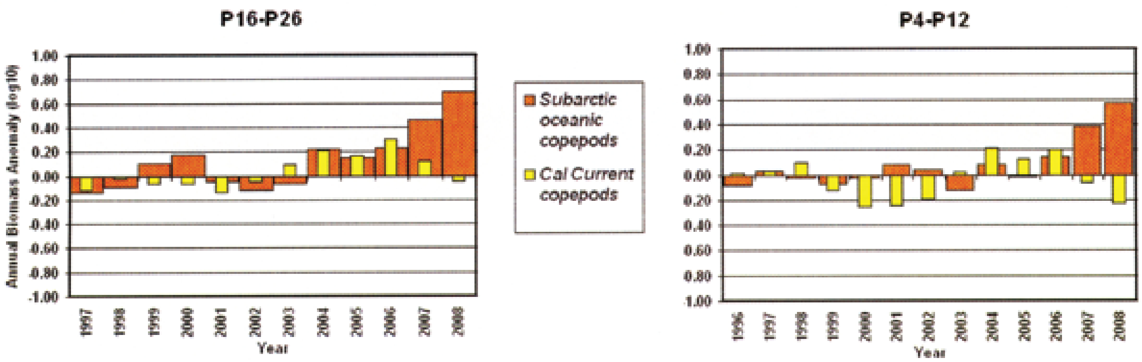

[Figure OC-34] Time series of annual anomalies of zooplankton biomass averaged within important species groups. The Subarctic oceanic copepods have increased considerably during the past decade, and are associated with increased transport by the North Pacific Current. Subtropical California Current copepods have fluctuated, and are most strongly associated with temperature variability.

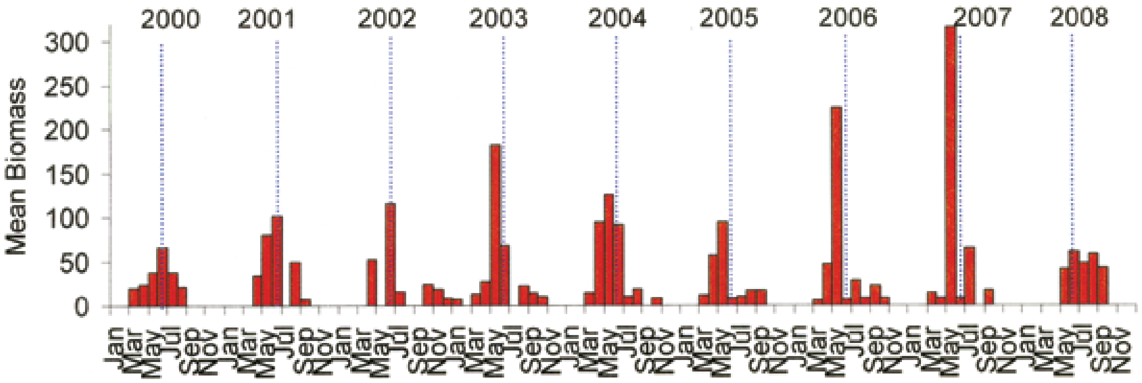

[Figure OC-35] Mean monthly mesozooplankton biomass for the Northeast Pacific from CPR sampling. The dashed lines indicate June of each year to emphasize the shift in peak timing and magnitude.

Biomass per sample was also calculated for the CPR samples according to procedure described in Section 5.1.2. Average monthly biomass (Fig. OC-35) was calculated for the region defined in Figure OC-31. In cool years the peak was late and protracted (2000, 2001 and 2008). In warm years the peak was early and narrow (2005, 2006). Variation within the focus period was considerable with the monthly profile of the adjacent years 2007 and 2008 very different from each other. The highest late summer biomass (August and September) in the CPR time series occurred in 2008.

5.2.3 *Neocalanus* seasonal timing

Upper-ocean temperature during spring (March-May) has a large effect on the seasonal timing of growth and dormancy for the dominant copepod *Neocalanus plumchrus* (Mackas et al. 1998, 2007). The fluctuations of zooplankton seasonal timing continue to be large (up to 3-4 months variation in the timing of a peak that is only about 1.5 month wide) and continue to be strongly associated with temperature (early in warm years, later in cool years). The timing fluctuations also appear to be spatially coherent throughout the Subarctic NE Pacific (separations up to ~1500 km). The focus period was especially variable with 2003-2005 seeing the earliest peaks in the 50 year Line-P record, while 2008 was much later reflecting the switch back to cool conditions (Fig. OC-36).

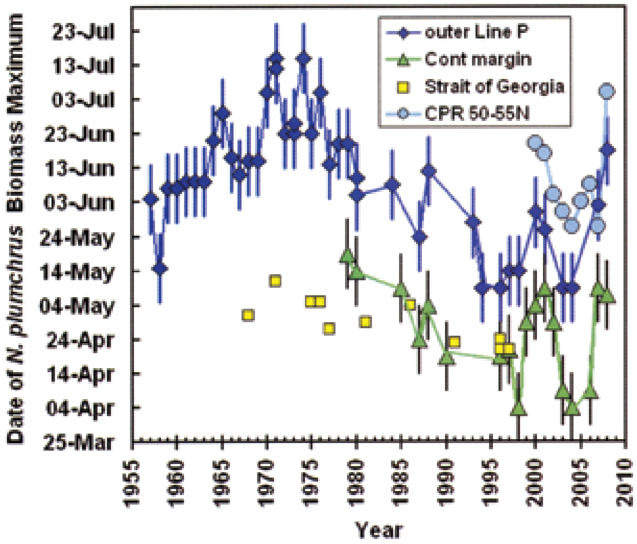

[Figure OC-36] Phenology time series for *Neocalanus plumchrus* populations in various subregions of the Northeast Pacific.

5.3 Central Subtropical zooplankton

(Landry)

Size fractionated zooplankton biomass has been measured at station ALOHA since 1994 as part of the Hawaii Ocean Time series (HOT) program. Cruises are conducted approximately once per month to the oligotrophic deep-water station ALOHA (22° 45'N, 158° 00'W) located 100 km north of Oahu, Hawaii. Three midnight (2200 - 0200) and 3 midday (1000 - 1400) oblique tows are collected through the euphotic zone on each cruise, and the catch is size-fractionated to give biomass for the 0.2-0.5 mm, 0.5-1 mm, 1-2 mm, 2-5 mm and >5 mm fractions. The mesh size of the net has been consistent at 202-µm, but the type of gear changed in 2005. The new gear may be easier to avoid by larger animals with fast escape responses and so some caution should be used in comparing the largest (>5 mm) size fraction before and after November 2005. The time series of total daytime (0530-1830) and nighttime zooplankton biomass extends from 1994 to June 2008 (Fig. OC-37). There is a clear seasonal cycle with the annual peak usually occurring June-August (Fig. OC-38). From 1994 to 2004, there was an increasing trend in biomass, which leveled, or even decreased after 2005. Although this coincides with the gear change, the pattern is the same if the largest size fraction is removed, with an increase in biomass through 2004 in size classes <5 mm, which subsequently reached a plateau. For the remainder of the focus period, biomass has remained relatively high (Fig. OC-37), with most months having values higher than the monthly mean for 1994-2002, although there is a suggestion that values were declining towards the end of the focus period. Among recent years, 2006 is notable in having a markedly depressed seasonal cycle, which typically shows a biomass peak in late summer or fall, as seen for example in 2005 and 2007. Within the full data set, only the period 1997 El Niño to 1998 La Niña conditions shows a sharper difference between nocturnal summer biomass values from one year to the next. Within the focus period, only two months had biomass values less than one standard deviation of the 1994-2002 monthly means; night samples in October 2006 and May 2008.

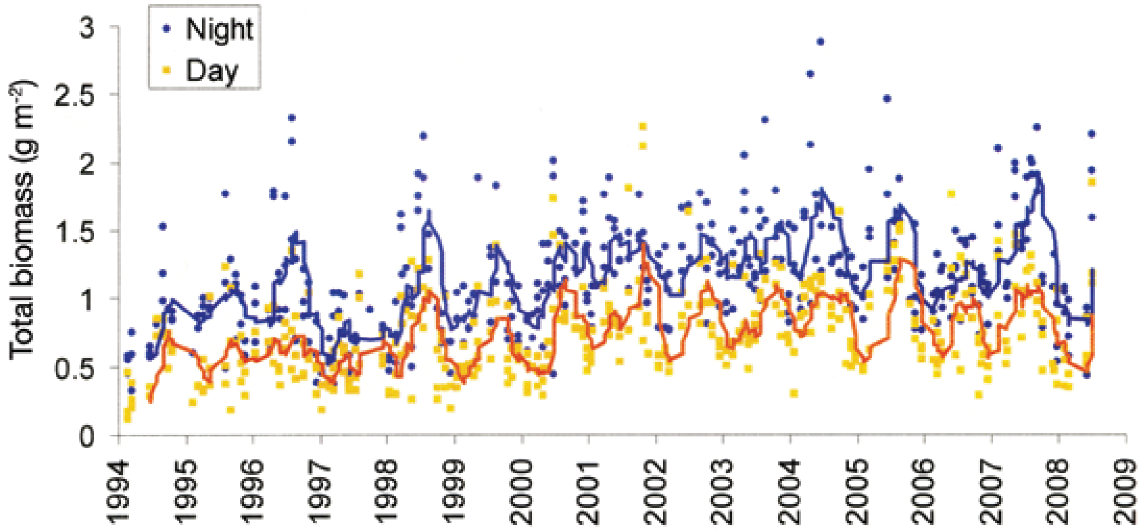

[Figure OC-37] Total zooplankton biomass with an 8-point running mean superimposed. Day (0530) and night (1830) are shown by red and blue lines, respectively.

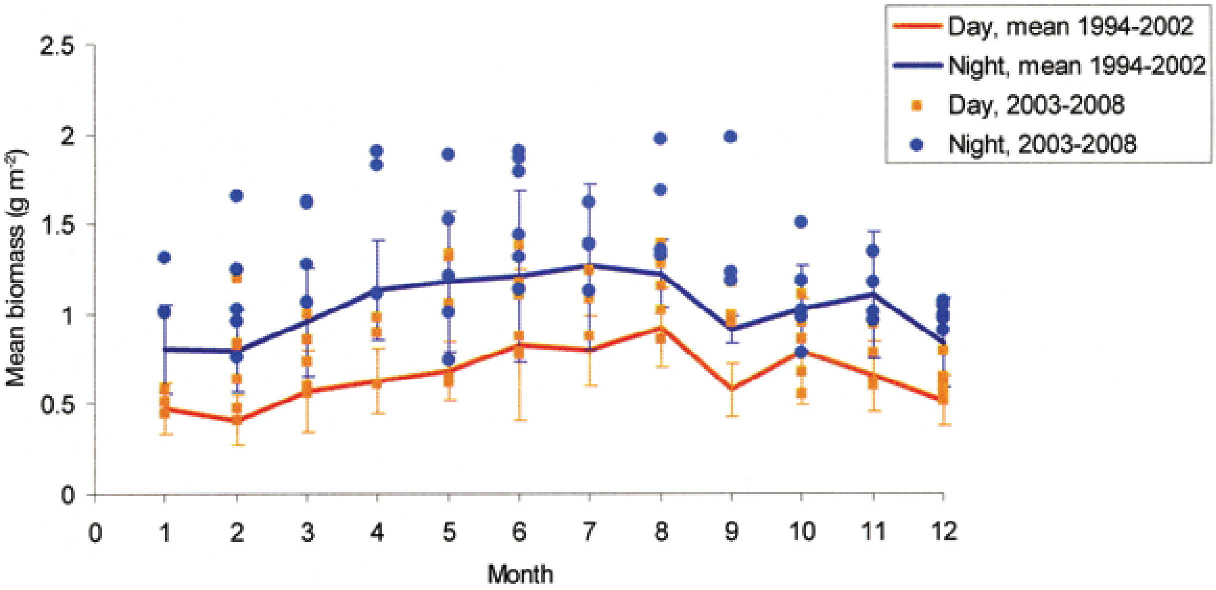

[Figure OC-38] Monthly mean and standard deviations for the period of 1994 to 2002, with monthly means for the focus period superimposed as symbols (blue = night, orange = day, as above).

6.0 Fishes and Invertebrates

6.1 Northeast Pacific

The fish fauna of the oceanic northeastern Pacific consists of a mix of temperate and subarctic species, resulting in a gradient in species composition along the shelf from the east to the west (Mueter and Norcross 2002). At least 383 species belonging to 84 families of marine and anadromous fishes have been reported from the Alaska continental shelf, slope, and offshore areas (Mecklenburg et al. 2002). The majority of fish biomass and commercial exploitation occurs on the continental shelf and slope in relatively nearshore areas. Few studies have been conducted to investigate long-term temporal patterns in fish abundance in the northeastern Oceanic Region. The central part of the Alaska Gyre provides the principal feeding habitat for many species, particularly salmon, throughout the year (Brodeur et al. 1999). South of the Alaska Gyre, the NPTZ once supported large-scale squid (*Ommastrephes bartrami*) driftnet fisheries until a moratorium prohibiting use of this gear was established by the United Nations General Assembly in 1992 (PICES 2004). Midwater trawling over seamounts in 1981 found low quantities of non-commercially valuable species of squid, bathypelagic fishes, and immature salmon (Hughes 1981).

Little is known about demersal species that inhabit the deeper parts of the continental slope and oceanic region. Due to the extreme depths in this region, there are few commercial fisheries and limited opportunities for fisheries research. Seamounts in the Gulf of Alaska represent one of the few areas in the oceanic region where exploitation of demersal fish species has occurred. Hughes (1981) first conducted exploratory fishing on Gulf of Alaska seamounts in 1979 using trawls and pots. Sablefish, (*Anaplopoma fimbria*) was the most common finfish found but rattails (family Macrouridae) were also caught. Other commercially important species encountered were several species of king crab (family Lithodidae) and tanner crab (*Chionoecetes tanneri*). Subsequent longline surveys conducted by Maloney (2004) on eight seamounts in the Gulf of Alaska from 1999-2002 produced high numbers of sablefish, giant grenadier (*Albatrossia pectoralis*), and Pacific grenadier (*Coryphaenoides acrolepis*). Tagging studies have verified that sablefish migrate among the continental shelf, slope region and seamounts but the route is unknown (Maloney 2004).

In 2005, the U.S. North Pacific Fisheries Management Council named 16 seamounts within the U.S. Exclusive Economic Zone off Alaska to be Alaska Seamount Habitat Protection Areas. These marine protected areas are now closed to all bottom contact fishing gear. Since the cessation of high seas driftnet fisheries and closure of seamounts to bottom contact fishing gear very little commercial exploitation has occurred. No time series information of abundance exists for fish species in this area. The best information likely comes from giant grenadier abundance estimates.

6.1.1 Grenadiers *(Lunsford)*

Grenadiers (family Macrouridae) are deep-sea fishes related to hakes and cods that occur world-wide in all oceans (Eschmeyer et al. 1983). Also known as "rattails", they are especially abundant in waters of the continental slope, but some species are found at abyssal depths. Of the seven species of grenadiers known to occur in Alaska, giant grenadier appear to be the most abundant and most common grenadier caught in the commercial fishery and in fish surveys (Clausen 2008). Survey information on giant grenadier in Alaska comes from comprehensive bottom trawl and longline surveys of the continental slope. Trawl surveys are too intermittent in time and depths sampled to show trends in abundance, but longline surveys provide estimates of relative biomass since 1990 up to depths of 1000 m (Clausen and Rodgveller 2008). Definitive trends in the relative abundance are difficult to discern, but generally there was an increasing trend from 1992-1997 and then somewhat of a decrease in subsequent years followed by a sharp increase in 2007 (Fig. OC-39). Both survey types show relatively high catch rates of giant grenadier in the deepest strata sampled, which indicates an unknown and possibly significant portion of the population may reside in deeper waters that have not been sampled (Clausen and Rodgveller 2008). A longline survey conducted in 2008 sampled depths up to 1600 m and found relatively high catch rates of giant grenadier at the deeper depths which supports the idea that an unknown portion of population resides in depths not sampled by traditional survey methods (D. Clausen, pers. comm.)

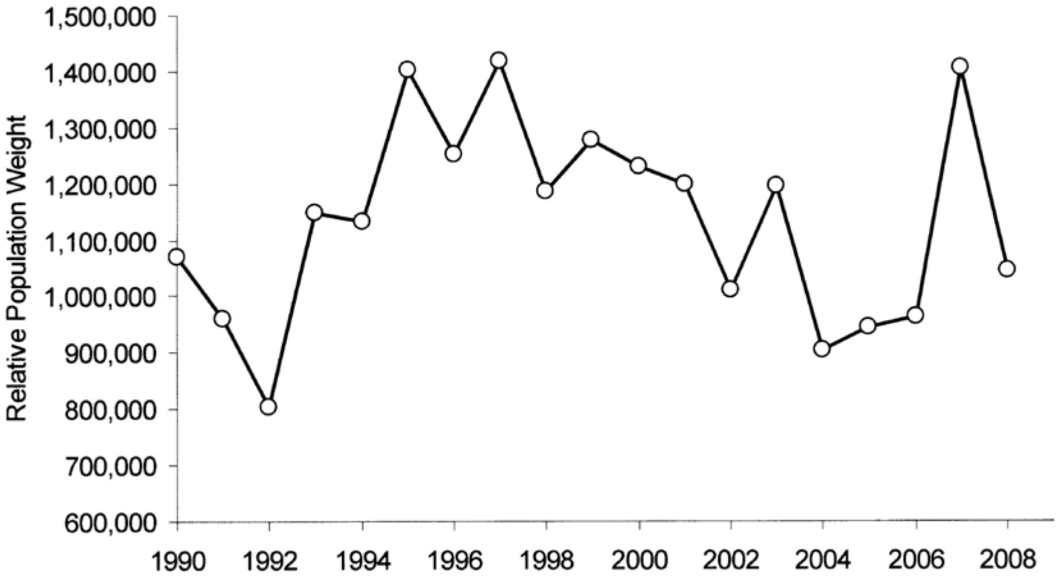

[Figure OC-39] Giant grenadier relative population weight in NMFS longline surveys in the Gulf of Alaska, 1990-2008. Values include data only for the upper continental slope at depths 201-1,000 m and do not include continental shelf gullies sampled in the surveys. Note: relative population weight, although an index of biomass (weight), is a unit-less value (from Clausen and Rodgveller 2008).

6.2 Central North Pacific

The primary fishery in the central North Pacific region is the pelagic longline fishery which includes fleets from the U.S. (based in Hawaii) as well as Japan and Taiwan. Several commercial fisheries currently operate in Transition Zone waters, including Japanese and U.S. vessels targeting tunas and billfishes, Japanese and U.S. troll vessels targeting tunas (notably albacore tuna), and a distant water Japanese (and to a much lesser extent U.S.) squid jigging fishery. The now defunct Asian high-seas driftnet fishing fleets targeting squid, tunas, and billfish also operated in Transition Zone waters. Information obtained by the multi-national observer program that monitored these fisheries provided the basis for much of our current understanding of the region's nektonic faunal composition (e.g., Yatsu et al. 1993).

6.2.1 Neon flying squid *(Chen, Ichii)*

The neon flying squid, *Ommastrephes bartrami*, is a large oceanic squid distributed in temperate and subtropical waters of the Pacific, Indian and Atlantic Oceans, and is especially abundant in the North Pacific. A large scale squid jigging fishery started in 1994, and a total of 23,000 t was landed. The maximum output in 1999 reached 132,000 t. The current fishing area is mainly located in the waters of 150°–165°E and 40°–46°N during August and November for the Chinese squid jigging boats, accounting for more than 65% of the total Chinese squid catch (Chen and Tian 2006). Data on catch per fishing boat and annual catch were obtained from the Chinese commercial jigging fleet operating in the area 150–165°E, 38–46°N during August and November from 1995 to 2007 (Fig. OC-40). Catch and CPUE remained relatively high and stable through the period 2003-2007 with the lowest CPUE in 2006 and the highest in 2004. However, the 2006 CPUE was similar to the previous highest CPUE in 1998.

A modified depletion model was fitted to the fisheries data to estimate the squid stock abundance during 2000–2005 (Chen et al. 2008). The proportional escapement ranged from 15.3% (in 2000) to 69.9% (in 2001), with an average of 37.2%, which was close to the management target of 40%. Thus, the current fishing mortality of the squid jigging fishery was considered to be sustainable and the annual maximum allowable catch was inferred to range from 80,000 to 100,000 t. The squid have been under-

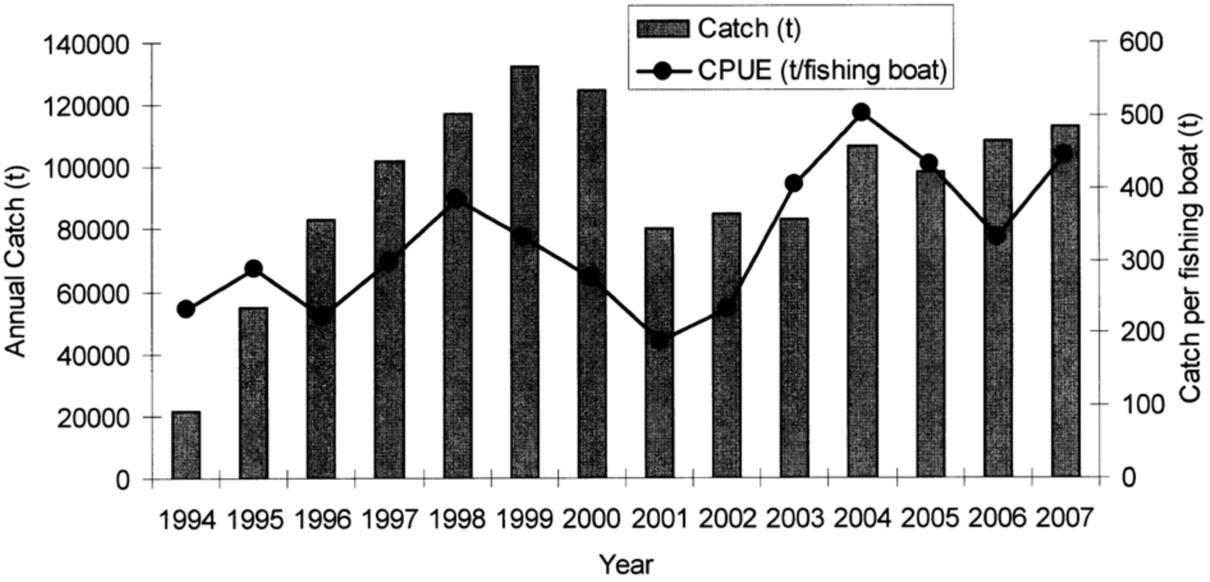

[Figure OC-40] Total annual catch of neon flying squid (*Ommastrephes bartrami*) caught by the Chinese squid-jigging fleet in the North Pacific, 1995–2007, and average CPUE in the area 150–165°E, 38–46°N for the same period.

exploited in the waters east of 170°E since 1993, and are exploited fully in the waters between 150°E and 170°E.

Chen et al. (2007) concluded that a La Niña event would result in a decrease in squid recruitment through variability in environmental conditions on the spawning grounds, whereas an El Niño event would lead to environmental conditions favourable to squid recruitment. ENSO events also influenced squid distribution on the feeding grounds, resulting in a northward shift of the fishing grounds in La Niña years and a southward shift in El Niño years. A relationship between CPUE and the monthly proportion of favourable SST areas at the spawning and feeding grounds was quantified for the years 1995-2004 (Cao et al. 2009) and used to predict CPUE for 2005 and 2006, where it performed well. February was the most important month to influence recruitment during the spawning season. The proportion of favourable SST areas on the feeding grounds could influence CPUE during the fishing season because of squid aggregations.

In the Subtropical Transition Zone, catch and catch per vessel-day for neon flying squid from Japanese jig boats show a decline over the period 1998–2002 but apparently this decline is a result of a change in the Japanese squid fleet rather than a change in the abundance of flying squid (Fig. OC-41). There is some agreement between the Chinese and Japanese squid catch data in that the late 1990s saw relatively high catches while the early 2000s saw lower catches but the correlation was not significant.

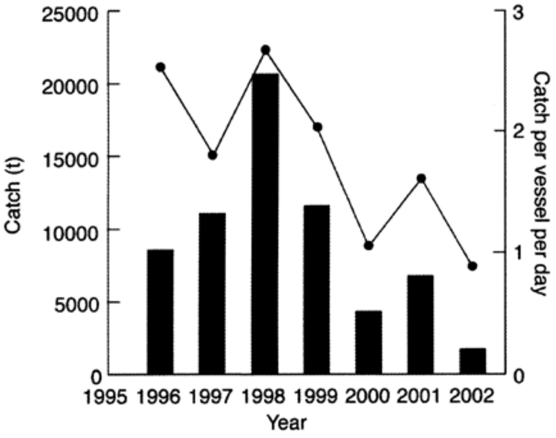

[Figure OC-41] Catch (bars) and catch per vessel per day (line) of flying squid (*Ommastrephes bartrami*) by the Japanese jig fishery.

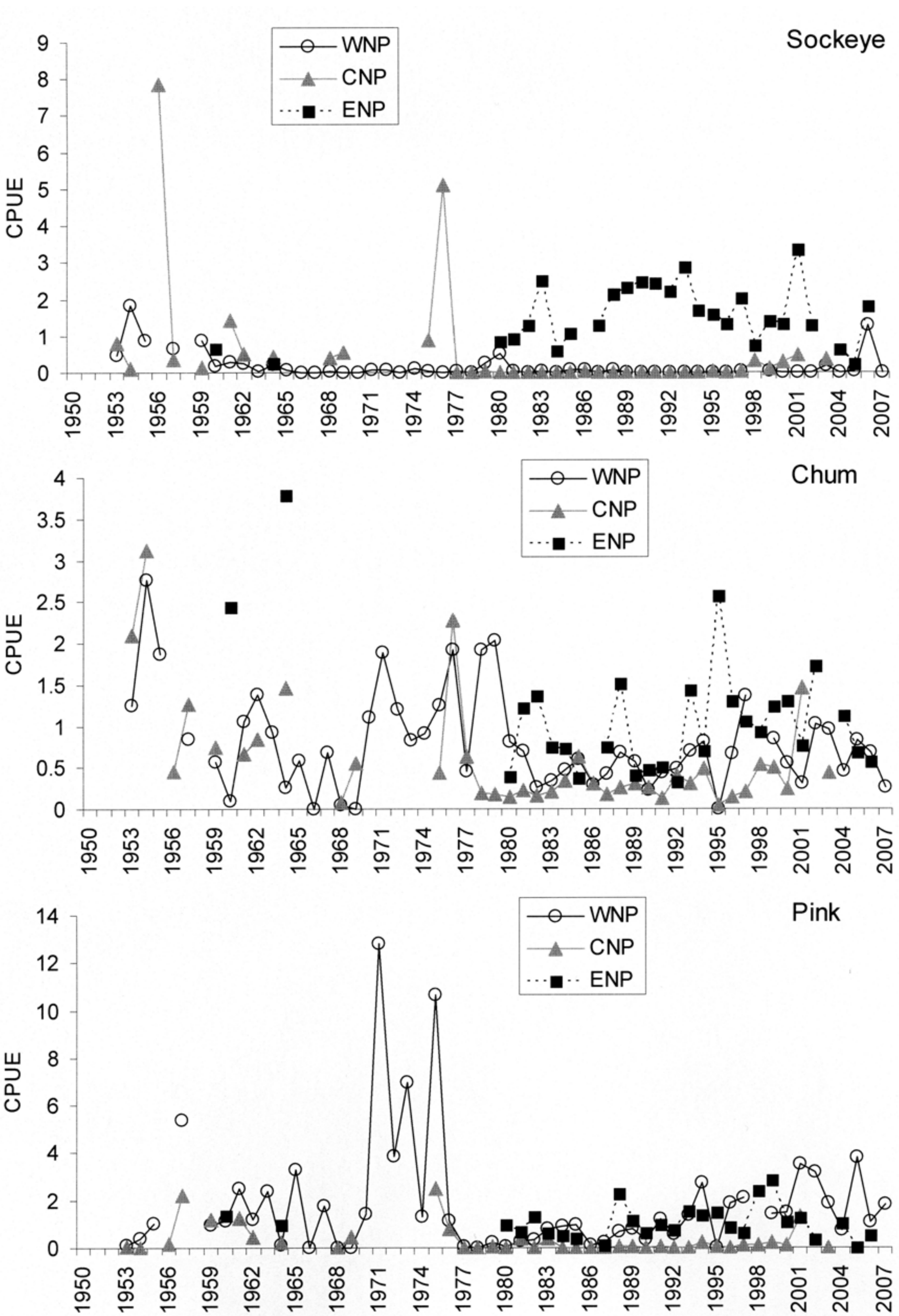

[Figure OC-42] Total catch (research, commercial, and other nets) as CPUE (individuals per net) of sockeye, chum and pink salmon in three regions of the oceanic North Pacific. WNP= western North Pacific, CNP= central North Pacific, and ENP= eastern North Pacific.

6.3 Pacific salmon

6.3.1 Oceanic surveys *(Kaeriyama, Matsuda)*

Hokkaido University has carried out continuous oceanographic and fishery surveys since 1957. Long-term changes have been measured in fork length of sockeye (*Oncorhynchus nerka*), chum (*O. keta*), and pink salmon (*O. gorbuscha*) collected by research gill nets from the T/V *Oshoro-maru* and the T/V *Hokusei-maru* in the North Pacific. Each species is distributed across 6 areas: the western Bering Sea (WBS), the eastern Bering Sea (EBS), the western North Pacific (WNP), the central North Pacific (CNP), the eastern North Pacific (ENP), and the Okhotsk Sea (OS). Only the WNP, CNP and ENP data will be considered here.

The age of a Pacific salmon is often identified as x.y where x is the number of years spent in freshwater and y is the number of years spent at sea. The fork length of chum salmon showed a significant declining trend since 1970 in 6 of 48 age-classes (age-0.3 and 0.4 female in WNP, age-0.3 female and age-0.2-0.4 male in CNP). The fork lengths of sockeye salmon and pink salmon did not show temporal changes (Table OC-1) although the mean length of odd-year pink salmon was larger than that of even-year broods. In 10 of 48 age-classes, significant correlations were observed between CPUE and fork length (8 were negative and 2 were positive, Table OC-2). Caution must be used to interpret these results as it is not clear that these measures of CPUE reflect the abundance of salmon. Sockeye salmon showed negative correlations ($r < -0.64$, $P < 0.05$) for four age-classes in the ENP and the EBS. Chum salmon indicated negative correlation ($r = -0.75$, $P < 0.05$) for a population in the CNP, and positive correlations ($r > 0.64$, $P < 0.05$) for two age-classes in the ENP and EBS. Pink salmon showed negative correlations ($r < -0.37$, $P < 0.05$) for two age-classes in the WNP and ENP (Table OC-2).

[Table OC-1] Correlations between year and fork length of sockeye, chum, and pink salmon in the North Pacific during 1970 to 2005 (*P<0.05, **P<0.01). WNP= western North Pacific, CNP= central North Pacific, ENP= eastern North Pacific.

Species	Sex	Ocean age	WNP	CNP	ENP
Sockeye	Female	1	0.70	0.29	0.24
		2	0.16	-0.10	0.16
		3	-0.48	0.16	-0.16
	Male	1	-0.70	0.48	0.03
		2	-0.10	-0.25	0.20
		3	-0.94	-0.56	-0.07
Chum	Female	1	0.27	0.43	0.21
		2	-0.45	-0.19	-0.06
		3	-0.48*	-0.69**	0.16
		4	-0.72**	-0.24	-0.11
	Male	1	0.31	0.09	0.41
		2	-0.32	-0.65**	-0.11
		3	-0.09	-0.59**	-0.03
		4	-0.40	-0.51*	-0.32
Pink	Female	1	-0.37	-0.21	-0.13
	Male	1	-0.30	-0.07	-0.26

[Table OC-2] Correlations between CPUE and fork length of sockeye, chum, and pink salmon in the North Pacific during 1970 to 2005 (*P<0.05, **P<0.01). WNP: Western North Pacific, CNP: Central North Pacific, ENP: Eastern North Pacific.

Species	Sex	Ocean age	WNP	CNP	ENP
Sockeye	Female	1	-0.85	-0.49	-0.17
		2	-0.06	0.49	-0.64**
		3	-0.08	0.40	-0.53*
	Male	1	-0.16	0.40	-0.21
		2	-0.17	0.61	-0.69**
		3	-0.89	0.60	-0.19
Chum	Female	1	0.22	0.18	0.71**
		2	-0.29	-0.35	0.32
		3	0.30	-0.32	-0.35
		4	0.15	-0.19	0.24
	Male	1	0.04	0.07	0.64**
		2	-0.24	-0.75**	0.24
		3	-0.04	-0.37	0.04
		4	0.27	-0.20	-0.22
Pink	Female	1	-0.30*	-0.28	-0.70**
	Male	1	-0.37*	-0.30	-0.69**

During the focus period, sockeye salmon CPUE was higher only in 2006 than the long-term mean (1950 to 2002) in the WNP and ENP (Fig. OC-42). Other years of the focus period were near average. CPUE of chum salmon during 2003-2007 was close to the long-term mean in the WNP and ENP. Pink salmon catches were relatively high in the WNP and relatively low in the ENP, compared to the 1990s, with the 2005 value in the WNP being the highest since 1975. Data for the CNP were only available for 2003 for all species.

6.3.2 Catch, hatchery production, and survival

(NPAFC; Irvine et al. 2009)

Aggregate commercial catches of Pacific salmon in the North Pacific are at or exceed all time highs (Fig. OC-43a) but the trends vary by species and region. Pink (*O. gorbuscha*), chum salmon (*O. keta*), and sockeye salmon (*O. nerka*) are generally the most abundant species in the North Pacific and their abundances remain high. Coho (*O. kisutch*), and chinook (*O. tshawytscha*) salmon are either decreasing or stable, depending on the region. Chum and pink salmon are most abundant in Asia (Fig. OC-43b) where significant increases were evident following the 1989 regime shift. In Russia, pink salmon catches have consistently been higher than catches of chum salmon, while the reverse has been true in Japan. Although Kaeriyama et al. (2009) suggested that the carrying capacity for Pacific salmon declined after 1998/99, the longer time series now available suggests that it has been reversed.

In North America, pink and sockeye salmon are generally the most abundant. Pink, sockeye, and chum salmon were more abundant following the 1989 regime shift than previously (Fig. OC-43c). Total catches in Alaska since the 1989 regime shift exceeded all previous periods (Fig. OC-43d). Catches of chum, pink, and sockeye salmon were highest during this period while chinook and coho salmon catches were similar to the previous period. Catches south of Alaska are small relative to those in Alaska. Canadian salmon abundances were relatively stable until 1989 when declines were experienced for all species (Fig. OC-43e). Abundances in Washington, Oregon, and California have declined throughout the time series (Fig. OC-43f). With the exception of chum salmon, catches along the U.S. west coast are at all time lows.

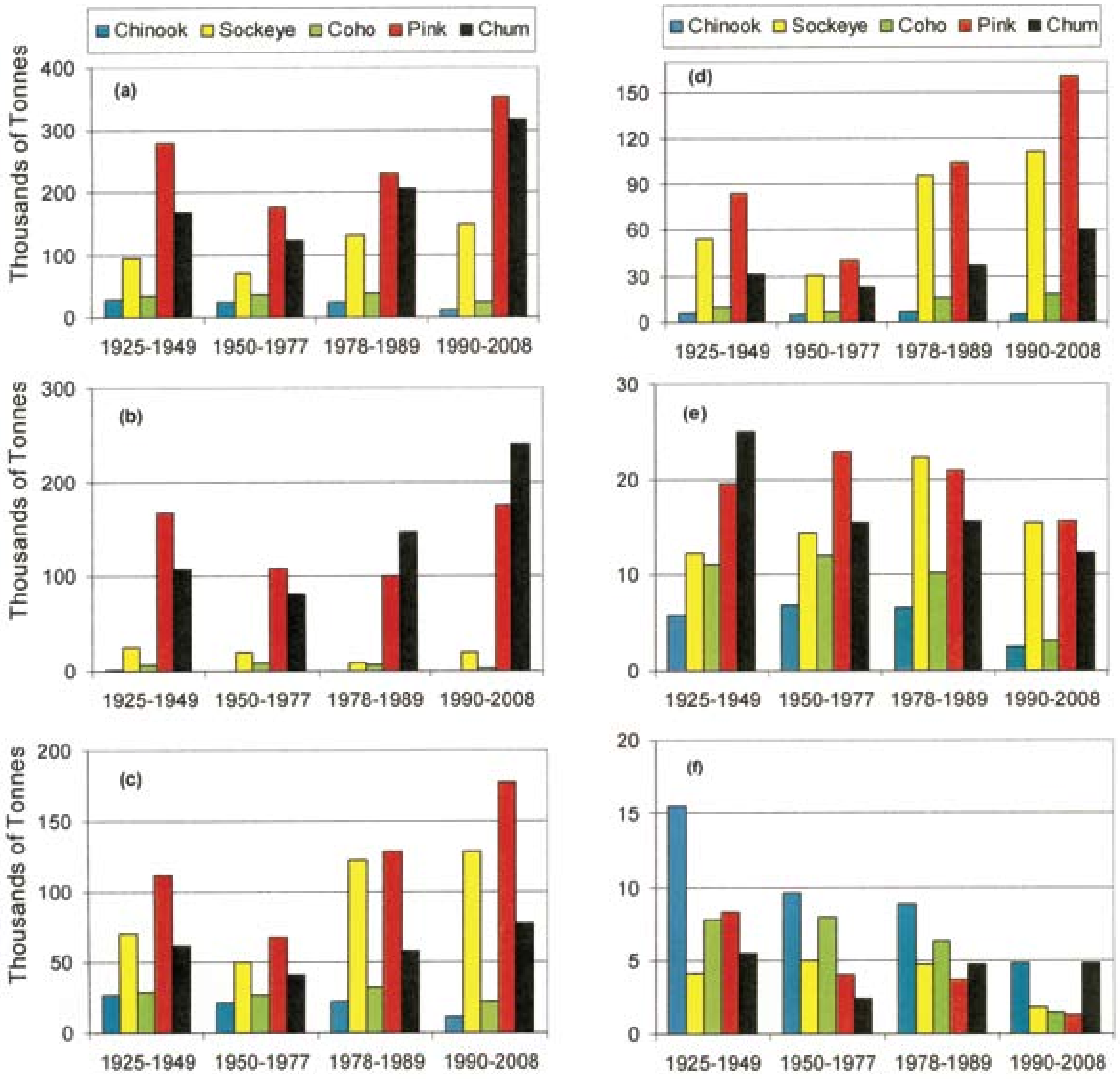

[Figure OC-43] Mean commercial catch (1000 t) of Pacific salmon by regime and species for (a) the North Pacific, (b) Asia, (c) North America, (d) Alaska, (e) Canada, and (f) U.S. west coast. (Data from Irvine et al. 2009).

To understand the latitudinal patterns of abundance within the North Pacific, the data were stratified by region (Fig. OC-44, note logarithmic axes). It was not possible to incorporate Russian catch data into this analysis, so regional patterns in the western North Pacific will not be considered. Chinook, coho, and sockeye salmon were caught in the three eastern regions (i.e. California Current, eastern Bering Sea, and Alaska Current). Catches since 1990 have declined for each species. Chinook salmon was the most abundant species in the California Current, coho salmon was the most abundant species in the Alaska Current region, and sockeye salmon was the most abundant in the eastern Bering Sea. The much less abundant and apparently declining masu salmon (*O. masou*) were reported only in western Pacific regions.

With the exception of even year pink salmon, temporal trends from 1990 are much less evident for the more abundant chum and pink salmon than for other species (Fig. OC-44). Chum salmon were generally more abundant during the recent focus period in the Alaska Current and western Pacific marginal seas where they are known to occur. All species are in decline in the California Current. Understanding reasons for changes in salmon catch and linking these to biological status is limited by a paucity of reliable information including estimates of fishing effort and the proportion of catch made up by hatchery-reared salmon.

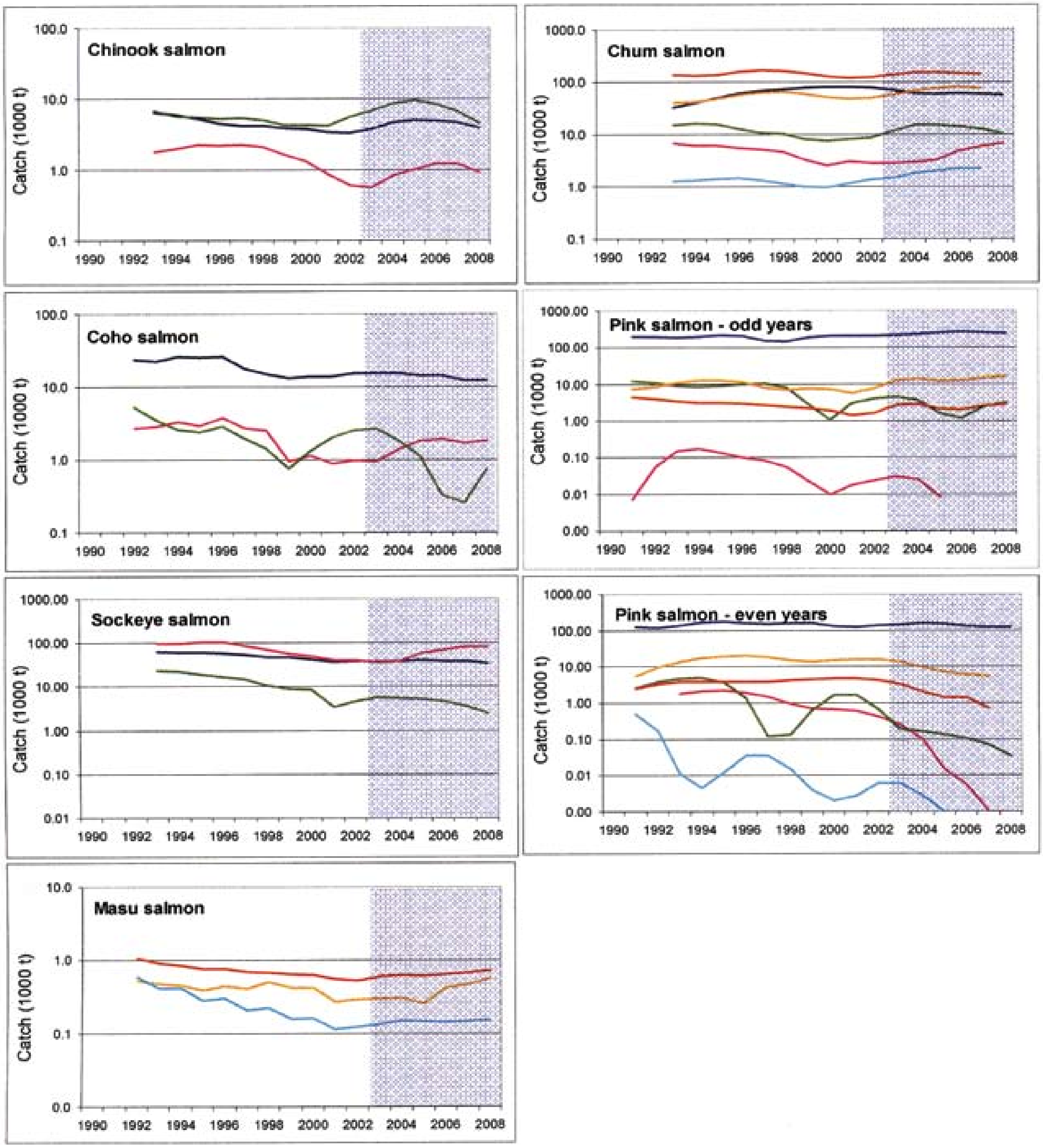

[Figure OC-44] Year-to-year variations in catch of Pacific salmon species by region (data from Irvine et al. 2009). Running averages are plotted (final year of 4-y moving window for sockeye, chinook, and chum salmon, 3-y for coho and masu salmon). The shaded region indicates the focus period.

Hatchery release numbers and survival time series have relatively short durations. Numbers of chum and pink salmon released from Russian hatcheries gradually increased during the last 15 years (Fig. OC-45a). Japanese hatcheries release greater numbers of chum salmon than other species. Their chum salmon fry releases increased rapidly in the late 1970s, but have been relatively stable for the last 25 years (Fig. OC-45b). Korean hatcheries tend to release chum salmon, but numbers released are relatively small (Fig. OC-45c). In Alaska, releases of pink and chum salmon in particular increased rapidly in the 1970s and 1980s but have been relatively constant since then (Fig. OC-46a). In Canada, release numbers declined after the 1990s but were reasonably constant thereafter (Fig. OC-46b). On the U.S. west coast, hatchery production has declined since the mid-1990s (Fig. OC-46c) where chinook salmon is the main species released.

Long-term time series of salmon marine survivals are not commonly available for Asia. Hiroi (1998) and Kaeriyama (1998) report increasing return rates (adult catches/juveniles released) for Japanese hatchery chum salmon from Hokkaido and Honshu respectively from the late 1970s through the early 1990s. A more recent review of Japanese hatchery chum survival (Saito and Nagasawa 2009) found that increased return rates for chum salmon from eastern Hokkaido were related, at least in part, to increases in the size of fry released. Chum salmon return rates from the Pacific side of Japan were influenced by interannual temperature variability during the late season of coastal residency after the release. Return rates for salmon released on the west side of Hokkaido decreased in recent years while those for chum salmon released on the west side of Honshu have been consistently low. Kaev and Ignatiev (2007) reviewed Sakhalin hatchery production information for pink and chum salmon. They attributed increasing chum salmon return rates to improvements in hatchery technology rather than more favourable natural marine conditions. Regardless of the mechanism responsible for improved survival, the benefits in terms of salmon catch have been significant. Chum caught near Sakhalin are now largely of hatchery origin, a major switch from the 1960s to 1980s (Kaev and Ignatiev 2007).

In Korea, chum salmon return rates were less than 0.4% during 1986-1988, increasing to 1.6% in 1990 (Lee et al. 2007). Declining return rates after 2000 were attributed to higher temperatures in the coastal area when young chum salmon are present. There is even less information on Asian pink salmon survivals. Since pink salmon recovery rate estimates are based on returns from a mixture of hatchery and wild fry, they are difficult to interpret. The data that are available do not indicate any significant temporal pattern, except for what appears to be a large increase for fish returning in 2007 (Irvine et al. 2009). Kaev and Geraschenko (2008) speculate that the unfavorable influence of a cold northern coastal current on juvenile feeding may be the reason pink salmon from southern Sakhalin Island appear to survive at higher rates than pink salmon from northeastern Sakhalin.

In the California Current region, lower catches of coho salmon are partly a consequence of reduced fishing effort, but low average marine survivals are contributing to the current situation. Temporal trends in the abundance of chinook salmon are positively associated with changes in survival. In some areas, changing exploitation patterns have affected spawner numbers. Sockeye salmon populations within Canada are generally better off in northern than in southern BC. Several major sockeye salmon populations in the Fraser River experienced very poor survival of the 2007 smolt year-class (returns in 2009). On the other hand, sockeye salmon returns to the Columbia River in 2008 and 2009 (2006 and 2007 smolt years) were extremely good and marine survival indices were high.

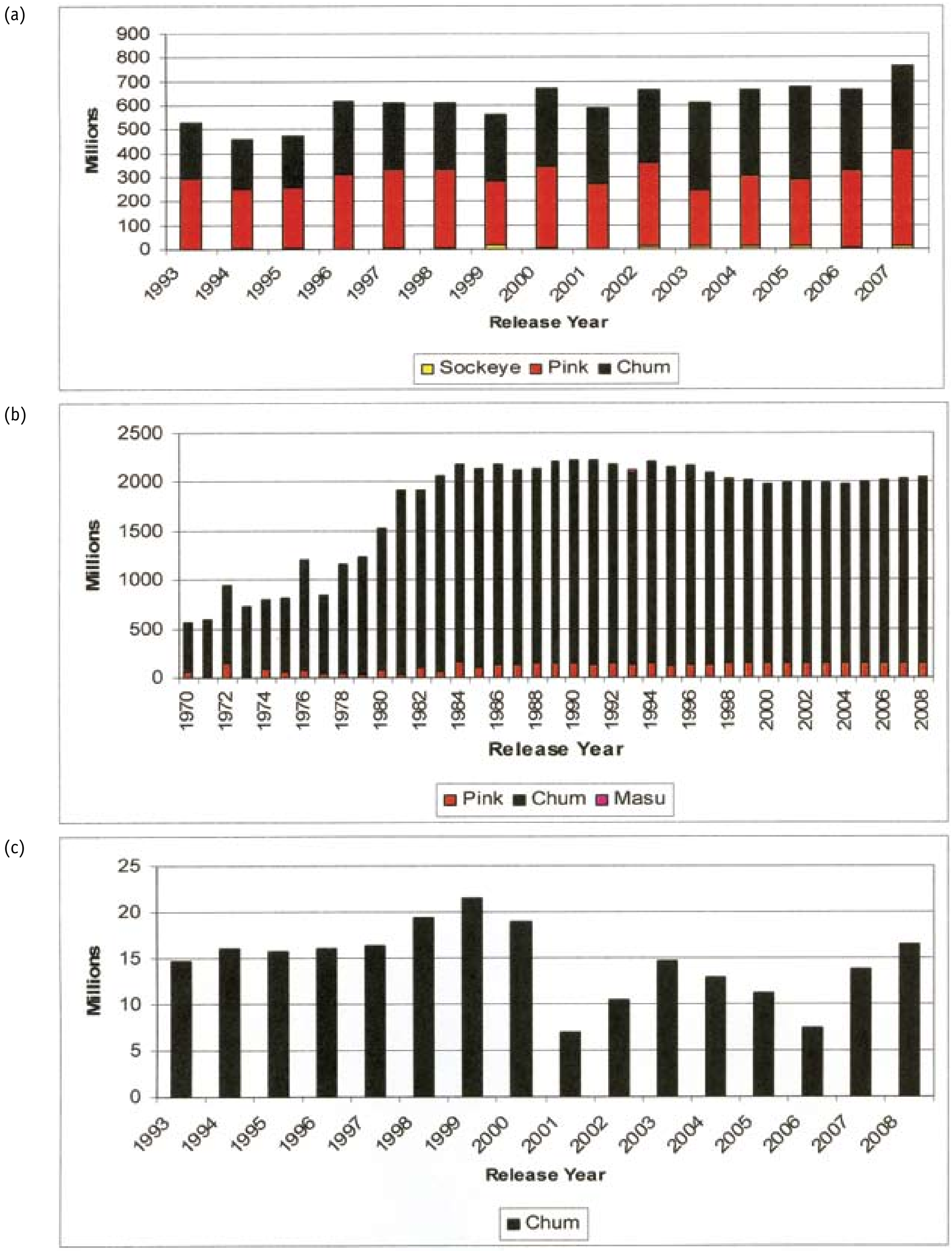

[Figure OC-45] Releases of hatchery salmon by (a) Russia, (b) Japan, and (c) Korea (Data from Irvine et al. 2009).

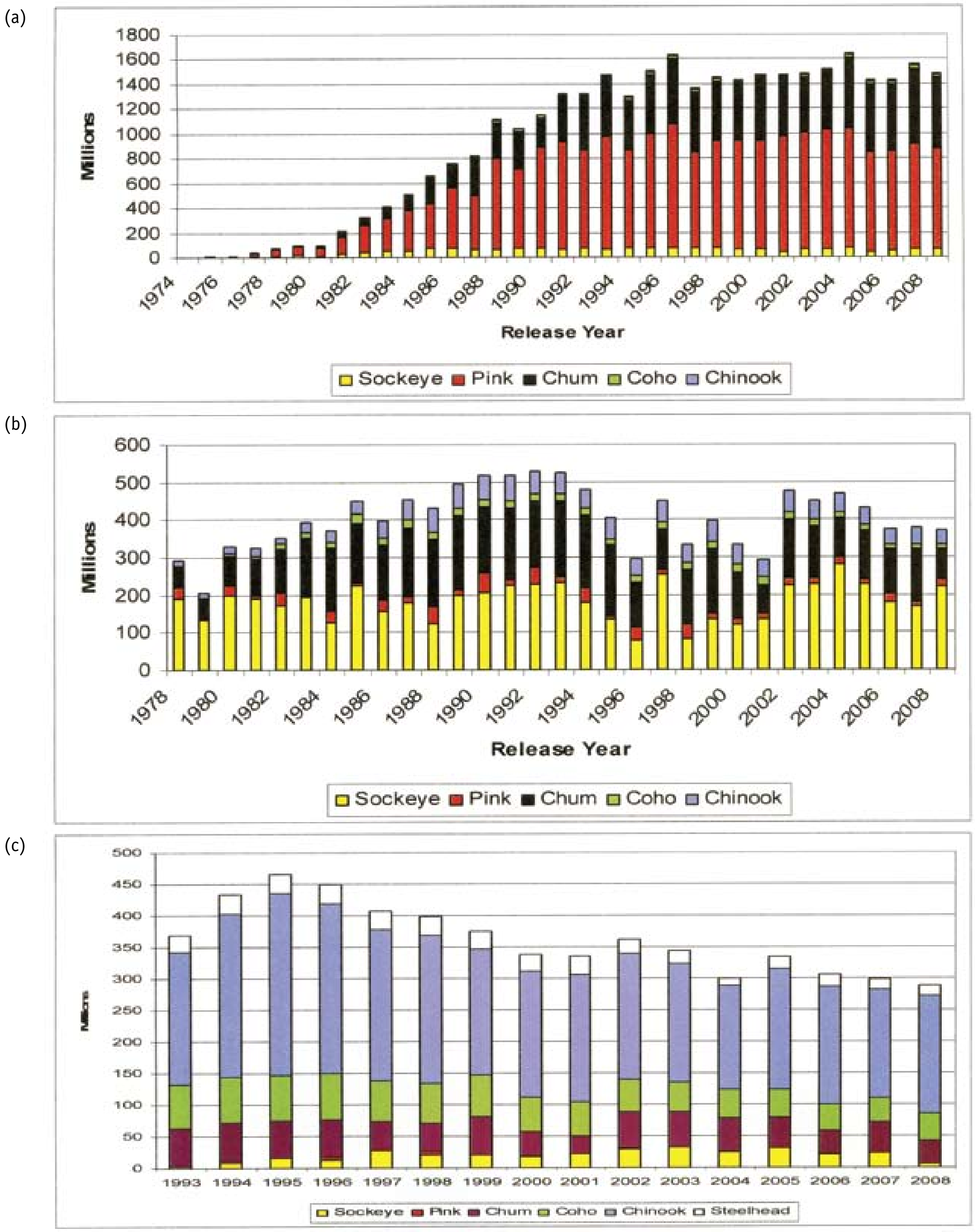

[Figure OC-46] Releases of hatchery salmon by (a) Alaska, (b) Canada, and (c) the U.S. west coast (Data from Irvine et al. 2009).

6.4 Tuna and billfish *(Holmes)*

Albacore tuna (*Thunnus alalunga*) is a widely distributed, economically important tuna species in the North Pacific Ocean. Of the large and highly migratory pelagic species (tunas, swordfish, marlins), the albacore has the most northerly distribution. The North Pacific stock is panmictic (a single population) without significant genetic structuring (Wu et al. 2009). Mature albacore spawn in tropical waters exceeding 24 °C between Japan and Hawaii, generally within 10 - 15° N of the Equator. Highest densities of larvae appear in the Kuroshio and its Countercurrent (10-25°N) from May through August (Ueyanagi 1969). Juvenile albacore (age 1+) are distributed across the North Pacific and are most abundant in the Kuroshio, the North Pacific Transition Zone, and the California Current. They undergo extensive seasonal migrations, including trans-Pacific movements by some individuals (Clemens 1961; Laurs and Lynn 1977). Albacore mature at 5-6 years of age and the adult fish are most abundant in the subtropical waters between Japan and Hawaii. Maximum life span is believed to be 11-12 years and maximum size is about 135 cm (Clemens 1961).

Albacore fisheries by Canada, the United States, Mexico, Japan, Korea, and China-Taipei (Taiwan) have caught up to 126,536 tonnes (t) in 1976 to a low of 37,320 t in 1991 (Fig. OC-47). The steep decline can be attributed to the development of high-seas driftnet fishing in the late 1970s and below average recruitment in the 1980s (Cox et al. 2002). In the early 1990s, catches increased again, peaking in 1999 at 125,576 t, and declining to 61,696 t by 2004. Modest increases in catches have occurred in recent years that may be related to strong recruitment from the 2001 and 2003 cohorts (ISC 2008) and catch has averaged 84,425 t since 2000.

The most recent (2006) stock assessment was carried out by scientists from Canada, Japan, China-Taipei, United States, Mexico, Korea and the Inter-American Tropical Tuna Commission (IATTC) using an age-structured model (ISC 2007). The results indicated that North Pacific albacore biomass is relatively high (~513,000 t), especially compared to the low values estimated for the late 1970s and 1980s. Spawning biomass (SSB) was estimated to be 153,000 t in 2006, which is 53% higher than the long-term average. The current estimate of fishing mortality (F2002-04 = 0.75 or F-17%) is high when compared with reference points commonly used in contemporary fisheries management. Although these high fishing levels have been sustained by good recruitment, total biomass and the SSB are expected to decline by 2015, even under optimistic recruitment assumptions. Fisheries for North Pacific albacore will have to be reduced (ISC 2007, 2008). However, since there is no formal guidance from managers on how these reductions will occur, the present scientific advice is that current fishing effort should not be increased and that all nations should adhere to precautionary fishing practices (ISC 2007, 2008).

Catch and effort data for the high trophic level fishes in the central North Pacific are obtained from mandated logbooks and observer reports from the Hawaii-based longline fishery. An analysis of these data for the deep-set portion of this fishery that targets bigeye tuna shows the catch rate for all species combined has declined from about 18 fishes per 1,000 hooks to 12 fishes per 1,000 hooks (Fig. OC-48). The declines occurred for the top trophic level species, billfishes, sharks, and tunas, while a group of lower trophic level species (called “others” in the figure) including mahi mahi (*Coryphaena hippurus*), sickle pomfret (*Taractichthys steindachneri*), snake mackerel (*Gempylus serpens*), and escolar (*Lepidocybium flavobrunneum*), showed statistically significant increases in catch rates (Fig. OC-48). The decline in catch rates of the top trophic level fishes is attributed to fishing. The increase in catch rates in the next lower trophic level has been attributed to reduced predation. (Polovina et al. 2009).

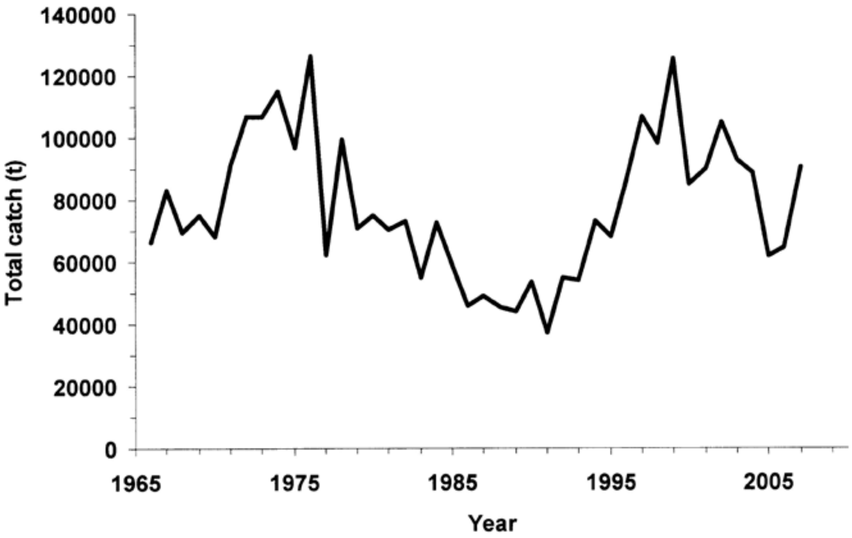

[Figure OC-47] Total annual catch (tonnes reported) of North Pacific albacore tuna by all nations, 1966-2007 (Data taken from ISC 2008). This excludes substantial catch and bycatch in large-scale pelagic driftnet fisheries that operated until 1992 (Waddell and McKinnell 1994).

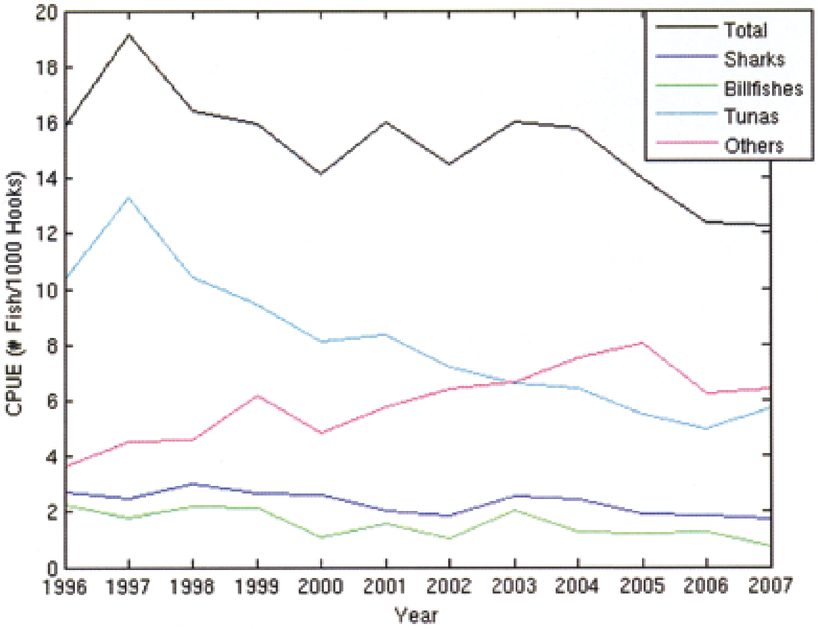

[Figure OC-48] Catch rates (number per 1,000 hooks) from Hawaii-based longline deep-set fishery logbook and observer logs 1996-2007. The "Others" group includes mahi mahi (*Coryphaena hippurus*), sickle pomfret (*Taractichthys steindachneri*), snake mackerel (*Gempylus serpens*), escolar (also called walu) (*Lepidocybium flavobrunneum*), and longnose lancetfish (*Alepisaurus ferox*); animals that feed at a lower level of the food web.

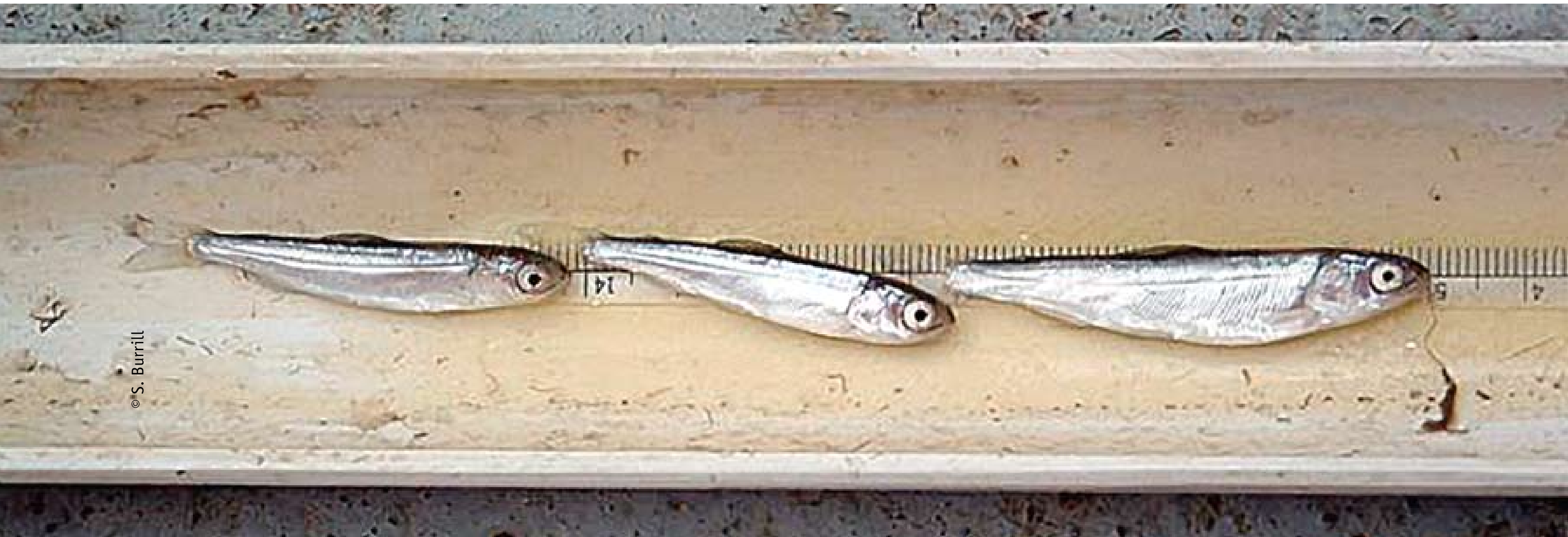
©S. Burrill

7.0 Marine Birds and Mammals

7.1 Seabirds *(Sydeman, Morgan, Thompson, Flint)*

7.1.1 Gulf of Alaska

Seabird distribution and abundance along Line P in the Gulf of Alaska has been surveyed since May 1996 as part of the Environment Canada pelagic seabird monitoring program. The Line P survey spans the transition between the California Current and the Gulf of Alaska ecosystems. Basic methods to survey and analyze seabird data on Line P may be found in O'Hara et al. (2006) and Yen et al. (2005). Relative abundance is expressed as density (number km^{-2}), with density estimated on a daily basis within each seasonal survey. Interannual changes in the overall seabird community (density, number of species observed, and relative abundance of the two most abundant seabird species in each season on Line P) were evaluated. For both summer (June-July) and fall (September-October) surveys, "dark" shearwaters (mostly sooty, *Puffinus griseus*) and Leach's storm-petrel (*Oceanodroma leucorhoa*) were the dominant species. Common murre (*Uria aalge*) and black-legged kittiwake (*Rissa tridactyla*) were dominant in winter.

The number of seabird species (richness) on Line P generally increased through time, especially from 2003-2006 (Table OC-3). Analysis of species richness revealed seasonal variability as well as a significant increase through time (Fig. OC-49a). Analysis of total seabird relative abundance also revealed seasonal variability and an increase though time (Fig. OC-49b). Changes in the relative abundance of the most abundant seabird species are summarized in Figures OC-50a-d. Leach's storm-petrel increased in summer (subdominant), dark shearwaters increased in fall (also subdominant after the storm-petrel), and there was no trend in common murre or black-legged kittiwake density through time in winter (Table OC-4). Dark shearwaters were most abundant during the relatively cool June of 2004 whereas storm-petrels were most abundant during the warm June of 2006. This reflects the water mass preferences of these species. Dark shearwaters prefer colder waters whereas the storm-petrel is most often found in warmer offshore habitats (Hyrenbach and Veit 2003).

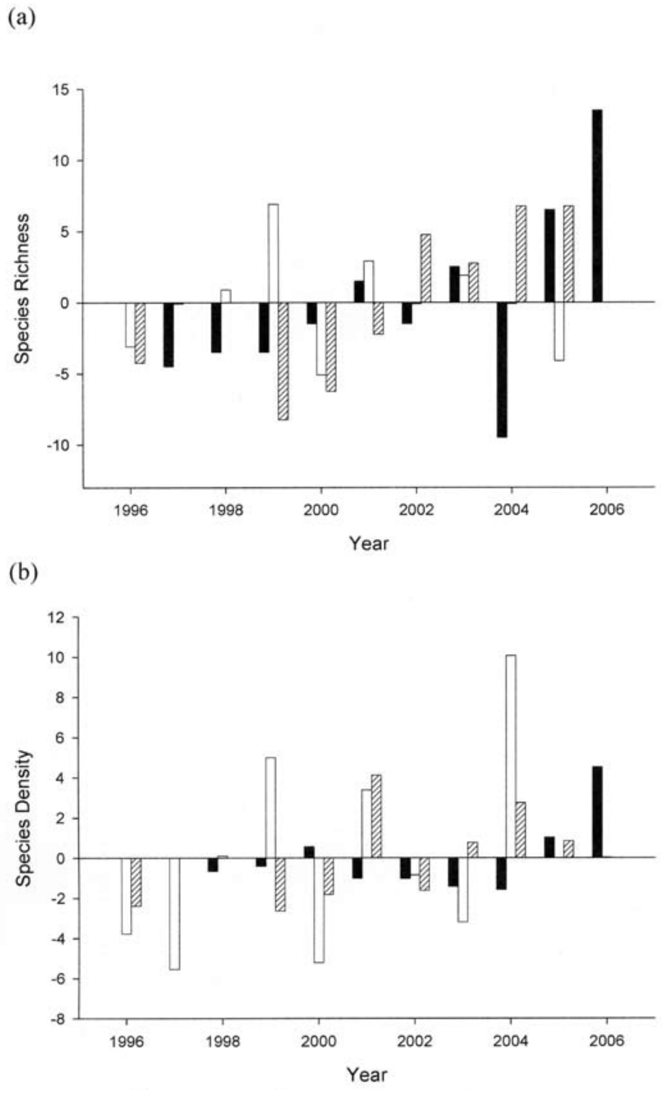

[Figure OC-49] (a) Seabird species richness seasonal anomalies and (b) seabird abundance anomalies (total numbers of birds km^{-2}) from winter (February), summer (June-July), fall (September-October) long-term Line P surveys in the GOA: Black bars= winter; open bars= summer, hatched bars= fall.

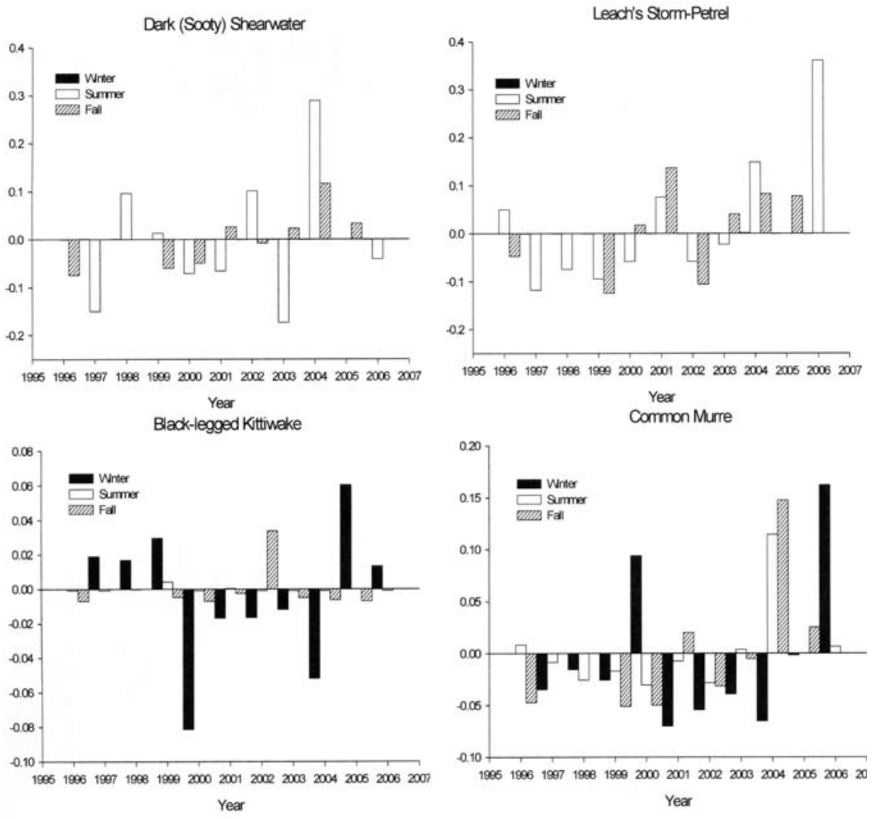

[Figure OC-50] Trends in the density (birds·km^{-2}) of the most abundant species in each season based on long-term Line P surveys in the GOA.

[Table OC-3] Trends in faunal diversity and relative abundance stratified by season for Line P surveys. Spearman rank correlations, sample size and P-values for the above datasets. Data are summarized by survey.

	Winter			**Summer**			**Fall**		
Dataset	N	Spearman rho	p<|t|	N	Spearman rho	p<|t|	N	Spearman rho	p<|t|
Line P Density	10	0.07	0.85	10	0.42	0.23	8	0.71	0.05
Line P Diversity	10	0.63	0.05	10	-0.07	0.85	8	0.90	0.00

[Table OC-4] Spearman rank correlations of trends in log(relative abundance) by day for the two dominant seabird species in each season on Line P, 1996-2006. Dark/sooty shearwaters and Leach's storm-petrel are dominant in summer and fall. Common murre and black-legged kittiwake are dominant in winter.

	Winter		**Summer**		**Fall**	
Species	Spearman Rho	p>|t|	Spearman Rho	p>|t|	Spearman Rho	p>|t|
Dark/sooty shearwater	-0.15	0.11	-0.05	0.50	0.23	0.02
Leach's storm-petrel	0.07	0.47	0.16	0.05	0.19	0.05
Black-legged kittiwake	0.02	0.82	-0.07	0.40	-0.02	0.82
Common murre	0.10	0.27	-0.01	0.91	0.14	0.15

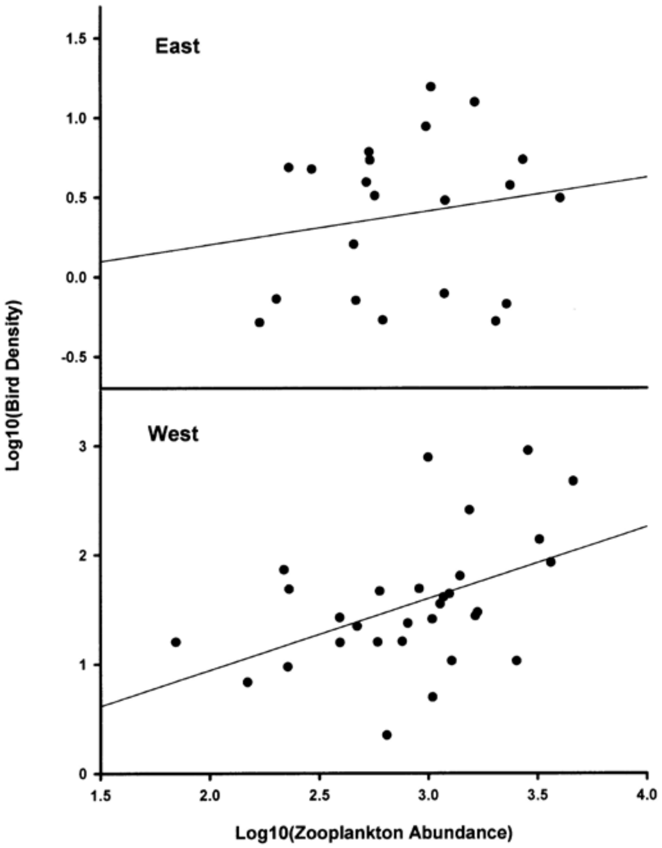

[Figure OC-51] The relationship between seabird density and zooplankton relative abundance as determined by the integrated CPR-MBM survey for June surveys in the eastern (Gulf of Alaska; not significant) and western (r^2=.21, P=0.01) North Pacific. Note the different scales on the ordinates between regions.

7.1.2 Pan-North Pacific

The Continuous Plankton Recorder Marine Bird and Mammal (CPR-MBM) survey was made three times per year and includes plankton and seabird observations on a 7,500 km transect along the "great circle route" from Vancouver, Canada to Tokyo, Japan (Batten et al. 2006). Methods used to survey and analyze seabird data from this vessel of opportunity program may be found in Hyrenbach et al. (2007). The CPR-MBM time series is, at present, too short to conduct trend analyses.

Seabirds are excellent sentinels of coupled climate-marine ecosystem change (Bertram et al. 2001; Piatt et al. 2007) in part because they may amplify variation in physical oceanographic attributes or biological productivity at lower trophic levels (Taylor et al. 2002). The relative abundance of seabirds at sea is thought to reflect water mass and prey base characteristics (Cairns 1987; Briggs et al. 1987; Hyrenbach and Veit 2003; Hedd et al. 2006). Trends in the Line P seabird community from 1996-2006 are consistent with interannual variability in water temperature, salinity, and overall ocean productivity (Fig. OC-51). Additionally, a significant increase in the abundance of Murphy's petrel (*Pterodroma ultima*), a predominantly southern hemisphere species, is evident in the eastern Gulf of Alaska over the past three decades (Morgan et al. unpubl.). An increase in shearwaters in fall may suggest that these migratory birds are staying longer in the Gulf of Alaska during the austral spring, instead of moving to the southern hemisphere where they reproduce. An increase in Leach's storm-petrel might indicate an increase in open ocean neuston production, as these birds take prey from the ocean surface. The increase in overall species richness and abundance may reflect a redistribution of seabird species from the south to the north. This may be a signal of marine climate change, or simply interannual variability over the study period.

Populations of Laysan albatross (*Phoebastria immutabilis*) and blackfooted albatross (*P. nigripes*) breed and nest at French Frigate Shoals in the Hawaiian Archipelago and forage in the North Pacific Transition Zone and beyond. A time series of reproductive success (proportion of chicks fledged per egg laid) for both these species show strong coherence and sharp declines in 1984 and 1999 (Fig. OC-52). Both years of low reproductive success occurred about one year after strong El Niños.

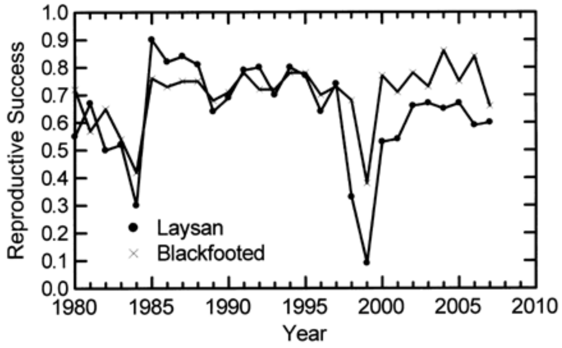

[Figure OC-52] Reproductive success of Laysan albatross and blackfooted albatross at French Frigate Shoals (Hawaiian Archipelago) from 1980-2007.

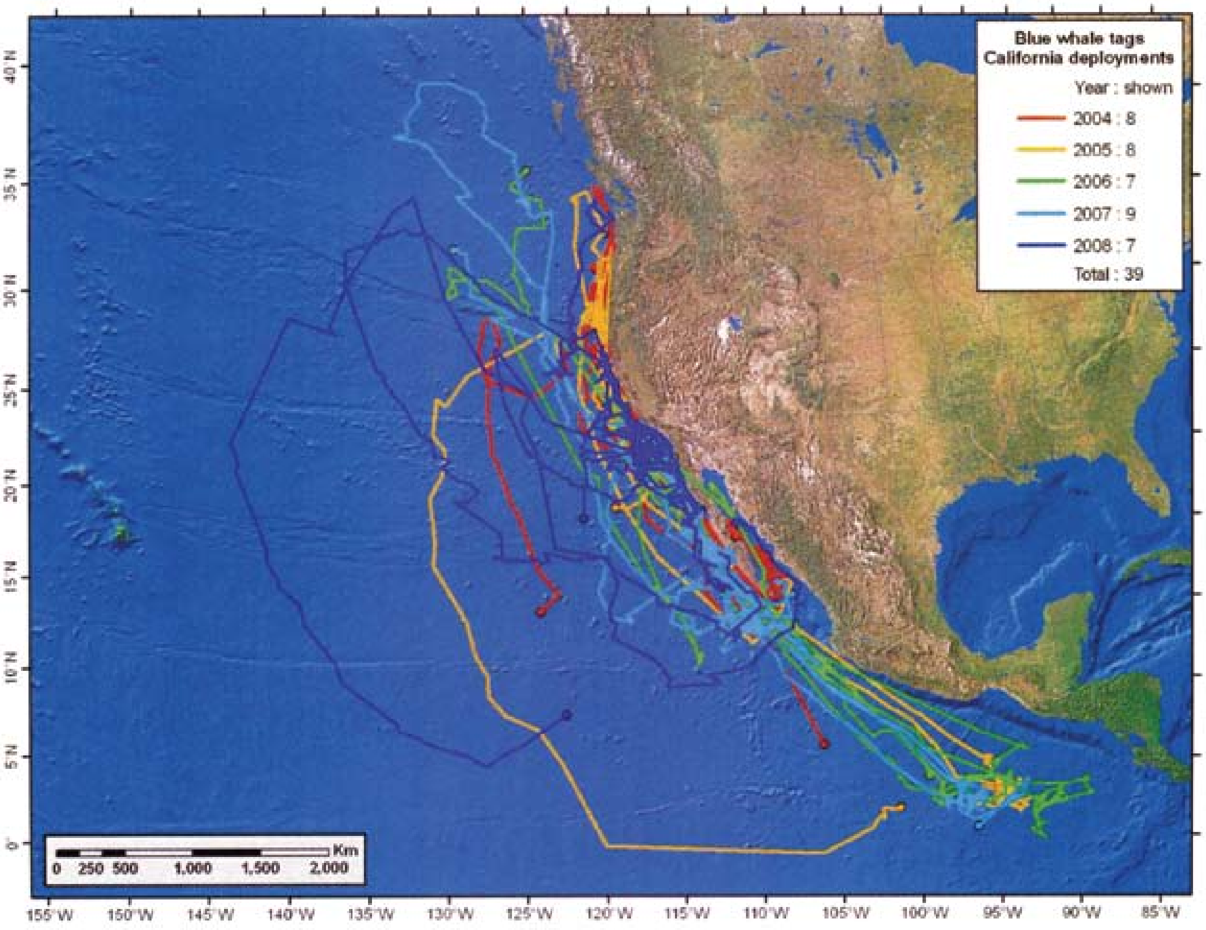

[Figure OC-53] Tracks of 39 blue whales tagged from 2003 to 2008 with satellite-monitored radio tags (www.argos-system.org) off the coast of central and southern California (Mate et al. 2007).

7.2 Blue whale *(Mate)*

The blue whale population feeding off California in the summer is estimated at 2,200-3,500 individuals (Barlow and Forney 2007). Unlike other large whale species, blue whales choose winter areas which are productive enough for them to forage throughout their reproductive season. Some of these areas, such as "down-stream" (west) from the Costa Rica Dome upwelling, are reasonably far off shore and their precise location may vary by hundreds of kilometres from year to year, due to changes in both currents and prevailing winds. Such remote and variable oceanographic structures probably contributed to the survival of this species during the intense whaling of the 20th century, when whalers probably could not find whales reliably in areas of previous hunting success. Satellite-monitored radio tags have revealed the movements and seasonal habitats of tagged whales, including feeding, reproduction, and migration areas (Fig. OC-53). The tagging technique is reviewed in Mate et al. (2007) and analyses of their area-restricted search and state space models have recently been completed (Bailey et al. 2009). The wide-ranging seasonal movements are generally south in the winter for reproduction and north in the summer for feeding. Numerous foraging "hot spots" coincide with seasonal krill concentrations over a 35° range in latitude (and pelagic red crabs off Baja California, Mexico in winter). Their large size allows them to survive through severe El Niño events, but can result in up to 50% of the population appearing emaciated, with lower reproduction evident for several years as whales recover their physiological "fitness". The relatively high sustained speed of blue whales allows them to move between foraging areas quickly (Irvine 2007). The E-W distribution of tagged whales (to within 800 km of Hawaii) suggests the ENP may be a single foraging area with most of the animals moving N-S between relatively near shore "hot spots", including areas off Vancouver Island, which have recently been described as re-populated (Calambokidis et al. 2009). Knowledge of the movements and habitat preferences of ENP blue whale is more extensive than for any other population in the world, yet the question of how many stocks may use the area is still unresolved.

The June to November feeding season is from 27-54°N (central Baja to Gulf of Alaska), followed by a diffuse migration south over a 4 month period to wintering areas east of southern Baja, in the Gulf of California, and at the Costa Rica Dome upwelling (~7-10°N). While krill is the dominant prey nearly everywhere, the color of blue whale feces off Magdalena Bay suggest feeding also on pelagic red crabs (Etnoyer et al. 2004, 2006). High productivity in wintering areas allows foraging for extended periods (Mate et al. 1999), allowing the world's largest newborn (8.5 m) to suckle sufficient quantities of its mother's rich milk to grow to 16 m in one year.

Acknowledgements

Argo data were collected and made freely available by the International Argo Project and the national programs that contribute to it (http://www.argo.ucsd.edu, http://argo.jcommops.org). Argo is a pilot program of the Global Ocean Observing System. A representative of the North Pacific Anadromous Fish Commission (Dr. James Irvine) helped to make the most recent results of the Commission's work available to the project.

References

Alverson, D.L. 1961. Ocean temperatures and their relation to albacore tuna (*Thunnus germo*) distribution in waters off the coast of Oregon, Washington, and British Columbia. Journal of the Fisheries Research Board of Canada 18: 1145-1152.

Bailey, D.M., Ruhl, H.A., Smith Jr., K.L. 2006. Long-term change in benthopelagic fish abundance in the abyssal N.E. Pacific Ocean. Ecology 87: 549-555.

Bailey, D.M., Collins, M.A., Gordon, F.D.M., Zuur, A.F., Priede, I.G. 2009. Long-term changes in deep-water fish populations in the northeast Atlantic: a deeper reaching effect of fisheries. Proceedings of Royal Society (B) 276: 1965-1969.

Bailey, H., Mate, B.R., Palacios, D.M., Irvine, L., Bograd S.J., Costa, D.P. 2009. Behavioural estimation of blue whale movements in the Northeast Pacific from state-space model analysis of satellite tracks. Endangered Species Research 10: 93-106.

Barlow, J. Forney, K.A. 2007. Abundance and population density of cetaceans in the California Current ecosystem. Fishery Bulletin 105:509-526.

Barwell-Clarke, J. Whitney, F.A. 1996. Institute of Ocean Sciences nutrient methods and analysis. Canadian Technical Report of Hydrography and Ocean Sciences 182, 43 p.

Batten, S.D., Hyrenbach, K.D., Sydeman, W.J., Morgan, K.H., Henry, M.F., Yen, P.Y., Welch, D.W. 2006. Characterising meso-marine ecosystems of the North Pacific. Deep Sea Research II 53: 270-290.

Batten, S.D., Mackas, D.L. 2009. Shortened duration of the annual *Neocalanus plumchrus* biomass peak in the Northeast Pacific. Marine Ecology Progress Series. 393, 189-198.

Batten, S.D., Welch, D.W., Jonas, T. 2003. Latitudinal differences in the duration of development of *Neocalanus plumchrus* copepodites. Fisheries Oceanography 12: 201-208.

Beamish, R.J., Leask, K.D., Ivanov, O.A., Balanov, A.A., Orlov, A.M., Sinclair, B. 1999. The ecology, distribution and abundance of midwater fishes in the subarctic Pacific gyres. Progress in Oceanography 43: 399-442.

Bertram, D.F., Mackas, D.L. McKinnell, S.M. 2001. The seasonal cycle revisited: Interannual variation and ecosystem consequences. Progress in Oceanography 49: 283-207.

Boyd, P.W., Berges, J.A., Harrison, P.J. 1998. In vitro iron enrichment experiments at iron-rich and iron-poor sites in the NE subarctic Pacific. Journal of Experimental Marine Biology and Ecology 227: 133-151.

Boyd, P.W., Law, C.S., Wong, C.S., Nojiri, Y., Tsuda, A., Levasseur, M., Takeda, S., Rivkin, R., Harrison, P.J., Strzepek, R., Gower, J., McKay, R.M., Abraham, E., Arychuk, M., Barwell-Clarke, J., Crawford, W.R., Crawford, D., Hale, M., Harada, K., Johnson, K., Kiyosawa, H., Kudo, I., Marchetti, A., Miller, W., Needoba, J., Nishioka, J., Ogawa, H., Page, J., Robert, M., Saito, H., Sastri, A., Sherry, N., Soutar, T., Sutherland, N., Taira, Y., Whitney, F.A., Wong, S.E., Yoshimura, T. 2004. The decline and fate of an iron-induced subarctic phytoplankton bloom. Nature 428: 549-553.

Boyd, P.W., Wong, C.S., Merrill, H., Whitney, F., Snow, J., Harrison, P.J., Gower, J. 1998. Atmospheric iron supply and enhanced vertical carbon flux in the NE subarctic Pacific: Is there a connection? Global Biogeochemical Cycles 12: 429-441.

Briggs, K.T., Breck Tyler, W.M., Lewis, D.B., Carlson, D.R. 1987. Bird communities at sea off California: 1975-1983. Studies in Avian Biology 11: 1-74.

Brodeur, R.D., McKinnell, S.M., Nagasawa, K., Pearcy, W.G., Radchenko, V., Takagi, S. 1999. Epipelagic nekton of the North Pacific Subarctic and Transition Zones. Progress in Oceanography 43: 365–397.

Cairns, D.K. 1987. Seabirds as indicators of marine food supplies. Biological Oceanography 5: 261-271.

Calambokidis, J. 2009. Abundance estimates of humpback and blue whales off the US West Coast based on mark-recapture of photo-identified individuals through 2008. Cascadia Research, 218½ W 4th Ave., Olympia, WA 98501. Document PSRG-2009-07.

Cao J., Chen X.J., Chen Y. 2009. Influence of surface oceanographic variability on abundance of the western winter-spring stock of neon flying squid (*Ommastrephes bartramii*) in the northwest Pacific Ocean. Marine Ecology Progress Series 381: 119-127.

Carpenter, J.H. 1965. The Chesapeake Bay Institute technique for the Winkler dissolved oxygen method. Limmnology and Oceanography 10: 141-143.

Chen, X.J., Tian, S.Q. 2006. Temp-spatial distribution on abundance index of neon flying squid *Ommastrephes bartramii* in the northwest Pacific using generalized additive models. Journal of Jimei University 11: 40-454.

Chen, X.J., Chen, Y., Tian, S., Liu B., Qian, W. 2008. An assessment of the western winter–spring cohort of neon flying squid (*Ommastrephes bartramii*) in the Northwest Pacific Ocean. Fisheries Research 92: 221-230.

Chen, X.J., Zhao, X.H., Chen,Y. 2007. El Niño/La Niña influence on the western winter–spring cohort of neon flying squid (*Ommastrephes bartarmii*) in the northwestern Pacific Ocean. ICES Journal of Marine Science 64: 1152-1160.

Clausen, D. M. 2008. The giant grenadier in Alaska. In A. M. Orlov and T. Iwamoto (Editors), Grenadiers of the world oceans: biology, stock assessment, and fisheries, p. 413-450. American Fisheries Society Symposium 63.

Clausen, D.M., Rodgveller, C.J. 2008. Grenadiers in the Gulf of Alaska, eastern Bering Sea, and Aleutian Islands. *In* Stock assessment and fishery evaluation report for the groundfish resources of the Gulf of Alaska and Bering Sea/Aleutian Islands regions, Appendix F, p. 613-656. North Pacific Fishery Management Council, 605 W 4th Ave., Suite 306, Anchorage AK 99501.

Clemens, H.B. 1961. The migration, age, and growth of Pacific albacore (*Thunnus germo*), 1951–1958. Bulletin of the California Department of Fish and Game 115: 128 p.

Cox, S.P., Martell, S.J.D., Walters, C.J., Essington, T.E., Kitchell, J.F., Boggs, C.H., Kaplan, I. 2002. Reconstructing ecosystem dynamics in the central Pacific Ocean, 1952-1998: I. Estimating population biomass and recruitment of tunas and billfishes. Canadian Journal of Fisheries and Aquatic Sciences 59: 1724-1735.

Eschmeyer, W.N., Herald, E.S., Hammann. H. 1983. A field guide to Pacific coast fishes of North America. Houghton Mifflin Co., Boston, 336 p.

Etnoyer, P., Canny, D., Mate, B., Morgan, L., Ortega-Otiz, J., Nichols, W. 2006. Sea-surface temperature gradients across blue whale and sea turtle foraging trajectories off the Baja California Peninsula, Mexico. Deep-Sea Research II 43: 340-358.

Etnoyer, P., Canny, D., Mate, B., Morgan, L. 2004. Persistent pelagic habitats in the Baja California to Bering Sea (B2B) ecoregion. Oceanography 17: 90-101.

Freeland, H. 2007. A short history of Ocean Station Papa and Line P. Progress in Oceanography 75: 120-125.

Freeland, H., Denman, K., Wong, C.S., Whitney, F., Jacques, R. 1997. Evidence of change in the winter mixed layer in the Northeast Pacific Ocean. Deep-Sea Research I 44: 2117-2129.

Fulton, J. 1973. Some aspects of the life history of *Calanus plumchrus* in the Strait of Georgia. Journal of the Fisheries Research Board of Canada 30: 811-815.

Fulton, J. 1983. Seasonal and annual variations of net zooplankton at Ocean Station "P", 1956-1980. Canadian Data Report of Fisheries and Aquatic Sciences 374. 65 p.

Gargett, A.E., Li, M., Brown, R. 2001. Testing the concept of an optimal stability window for salmonid marine survival, with application to southern British Columbia. Canadian Journal of Fisheries and Aquatic Sciences 58: 208-219.

Goldblatt, R.H., Mackas, D.L., Lewis, A.J. 1999. Mesozooplankton community characteristics in the NE subarctic Pacific. Deep-Sea Research II 46: 2619-2644.

Hart, J.L. 1973. Pacific Fishes of Canada. Bulletin of the Fisheries Research Board of Canada 180. 740 p.

Hedd, A., Bertrand, D.F., Ryder, J.L., Jones, I.L. 2006. Effects of interdecadal climate variability on marine trophic interactions: rhinoceros auklets and their fish prey. Marine Ecology Progress Series 309: 263-278.

Hiroi, O. 1998. Historical trends of salmon fisheries and stock conditions in Japan. North Pacific Anadromous Fish Commission Bulletin 1: 23-27.

Hughes, S.E. 1981. Initial U.S. exploration of nine Gulf of Alaska seamounts and their associated fish and shellfish resources. Marine Fisheries Review 42: 26-33.

Hyrenbach, K.D., Veit, R.R. 2003. Ocean warming and seabird assemblages of the California Current System (1987-1998): response at multiple temporal scales. Deep Sea Research II 50: 2537-2565.

Hyrenbach, K.D., Henry, M.F., Morgan, K.H., Welch, D.W., Sydeman, W.J. 2007. Optimizing the width of strip transects for seabird surveys from vessels of opportunity. Marine Ornithology 35: 29-37.

ISC (International Scientific Committee for Tuna and Tuna-like Species in the North Pacific Ocean). 2007. Annex 5. Report of the Albacore Working Group workshop (November 28-December 5, 2006, Shimizu, Japan). In Report of the Seventh Meeting of the International Scientific Committee for Tuna and Tuna-like Species in the North Pacific Ocean. Plenary Session, 25-30 July 2007, Busan, Korea.

ISC (International Scientific Committee for Tuna and Tuna-like Species in the North Pacific Ocean). 2008. Report of the Eighth Meeting of the International Scientific Committee for Tuna and Tuna-like Species in the North Pacific Ocean. Plenary Session, 22-27 July 2008, Takamatsu, Japan. 47p. Available at: http://isc.ac.affrc.go.jp/isc8/ISC8rep.html

Irvine, J.R., Fukuwaka, M., Kaga, T., Park, J.H., Seong, K.B., Kang, S., Karpenko, V., Klovach, N., Bartlett, H., Volk, E. 2009. Pacific salmon status and abundance trends. NPAFC Document 1199, Rev. 1, 153 pp.

Irvine, L. 2007. Characterizing the habitat and diving behavior of satellite-tagged blue whales (Balaenoptera musculus) off California. MS thesis, Oregon State University, Newport, OR

Kaeriyama, M. 1998. Dynamics of chum salmon, *Oncorhynchus keta*, populations released from Hokkaido, Japan. North Pacific Anadromous Fish Commission Bulletin 1: 90-102.

Kaeriyama, M., Nakamura, M., Edpalina, R., Bower, J.R., Yamaguchi, H., Walker, R.V., Myers, K.W. 2004. Change in feeding ecology and trophic dynamics of Pacific salmon (*Oncorhynchus* spp.) in the central Gulf of Alaska in relation to climate events. Fisheries Oceanography 13: 197-207.

Kaeriyama, M., Seo, H., Kudo, H. 2009. Trends in run size and carrying capacity of Pacific salmon in the North Pacific Ocean. NPAFC Bulletin 5: 293–302.

Kaev, A.M., Geraschenko, G.V. 2008. Reproduction indices of the north-eastern Sakhalin pink salmon. NPAFC Doc. 1124, Rev. 1, 11 pp.

Kaev, A.M., Ignatiev, Y.I. 2007. Hatchery production of salmon in Sakhalin. Rybnoye Khoziaystvo (Fisheries) 6: 57-60.

Laurs, R.M., Lynn, R.J. 1977. Seasonal migration of North Pacific albacore, *Thunnus alalunga*, into North American coastal waters: distribution, relative abundance, and association with transition zone waters. Fishery Bulletin 75: 795-822.

Laurs, R.M., Fieldler, P.C., Montgomery, D.R. 1984. Albacore tuna catch distributions relative to environmental features observed from satellites. Deep-Sea Research 31: 1085-1099.

Lee, C.S., Seong, K.B., Lee, C.H. 2007. History and status of the chum salmon enhancement program in Korea. Journal of the Korean Society of Oceanography 12: 73-80.

Lehodey, P., Chai, F., Hampton, J. 2003. Modelling climate-related variability of tuna populations from a coupled ocean-biogeochemical-populations dynamics model. Fisheries Oceanography 12: 483-494.

Mackas, D.L., Batten, S., Trudel, M. 2007. Effects on zooplankton of a warmer ocean: Recent evidence from the Northeast Pacific. Progress in Oceanography 75: 223-252.

Mackas, D.L., Galbraith, M. 2002. Zooplankton community composition along the inner portion of Line P during the 1997-98 El Niño event. Progress in Oceanography 54: 423-437.

Mackas, D.L., Goldblatt, R., Lewis, A.G. 1998. Interdecadal variation in developmental timing of *Neocalanus plumchrus* populations at OSP in the subarctic North Pacific. Canadian Journal of Fisheries and Aquatic Sciences 55: 1878-1893.

Mackas, D.L., Sefton, H.A., Miller, C.B., Raich, A. 1993. Vertical habitat partitioning by large calanoid copepods in the oceanic Subarctic Pacific during spring. Progress in Oceanography 32: 259-294.

Mackas, D.L., Thomson, R.E., Galbraith, M. 2001. Changes in the zooplankton community of the British Columbia continental margin, 1985-1999, and their covariation with oceanographic conditions. Canadian Journal of Fisheries and Aquatic Sciences 58: 685-702.

Mackey, M.D., Mackey, D.J., Higgins, H.W., Wright, S.W. 1996. CHEMTAX – A program for estimating class abundances from chemical markers: Application to HPLC measurements of phytoplankton. Marine Ecology Progress Series 144: 265-283.

Maloney, N.E. 2004. Sablefish, *Anoplopoma fimbria*, populations on Gulf of Alaska seamounts. Marine Fisheries Review 66: 1-12.

Mantua, N.J., Hare, S.R., Zhang, Y., Wallace, J.M., Francis, R.C. 1997. A Pacific decadal climate oscillation with impacts on salmon. Bulletin of the American Meteorological Society 78: 1069-1079.

Mate, B., Mesecar, R, Lagerquist, B. 2007. The evolution of satellite-monitored radio tags for large whales: One laboratory's experience. Deep-Sea Research II 54: 224-247.

Mate, B.R., Lagerquist, B.A., Calambokidis, J. 1999. The movements of North Pacific blue whales off Southern California and their southern fall migration. Marine Mammal Science. 15: 333-344.

McKinnell, S.M., Mackas, D.L. 2003. Intercalibrating SCOR, NORPAC and bongo nets and the consequences for interpreting decadal-scale variation in zooplankton biomass in the Gulf of Alaska. Fisheries Oceanography 12: 126-133.

Mecklenburg, C.W., Mecklenburg, T.A., Thorsteinson, L.K. 2002. Fishes of Alaska. American Fisheries Society, Bethesda, Maryland.

Miller, C.B., Frost, B.W., Batchelder, H.P., Clemons, M.J., Conway, R.E. 1984. Life histories of large, grazing copepods in a subarctic ocean gyre: *Neocalanus plumchrus*, *Neocalanus cristatus*, and *Eucalanus bungii* in the Northeast Pacific. Progress in Oceanography 13: 201-243.

Miller, C.B., Clemons, M. 1988. Revised life history analysis for large grazing copepods in the subarctic Pacific Ocean. Progress in Oceanography 20: 293-313.

Miller, C.B. (ed.). 1993. Pelagic ecodynamics in the Gulf of Alaska. Results from the SUPER program. Progress in Oceanography 32: 1-353.

Miller, C.B., Terazaki, M. 1989. The life histories of *Neocalanus flemingeri* and *Neocalanus plumchrus* in the Sea of Japan. Bulletin of the Plankton Society of Japan 36: 27-41.

Morgan, K., Hyrenbach, D., Bentley, M., Henry, M., Kenyon, J., O'Hara, P., Rintoul, C., Sydeman, W. Warm-water gadfly petrels (*Pterodroma* spp.) off Canada's west coast, observed from vessels of opportunity (1996–2005) – Sentinels of changing ocean climate? Poster presented at the 2007 Pacific Seabird Group Meeting, Pacific Grove, CA, February 7–11, 2007.

Mueter, F.J., Norcross, B.L. 2002. Spatial and temporal patterns in the demersal fish community on the shelf and upper slope regions of the Gulf of Alaska. Fishery Bulletin 100: 559-581.

O'Hara, P.D., Morgan, K.H., Sydeman, W.J. 2006. Primary producer and seabird associations with AVHRR-derived sea surface temperatures and gradients in the southeastern Gulf of Alaska. Deep-Sea Research II 53: 359-369.

Piatt, J.F., Harding, A.M.A., Shultz, M., Speckman, S.G., van Pelt, T.I., Drew, G.S., Kettle, A.B. 2007. Seabirds as an indicator of marine food supplies: Cairns revisited. Marine Ecology Progress Series 352: 221-234.

PICES. 2004. Marine Ecosystems of the North Pacific. PICES Special Publication 1, 280 p.

Polovina, J.J., Howell, E., Kobayashi, D.R., Seki, M.P. 2001. The transition zone chlorophyll front, a dynamic global feature defining migration and forage habitat for marine resources. Progress in Oceanography 49: 469-483.

Polovina J.J., Howell, E.A, Abecassis, M. 2008. The ocean's least productive waters are expanding. Geophysical Research Letters 35, L03618, doi:10.1029/2007GL031745.

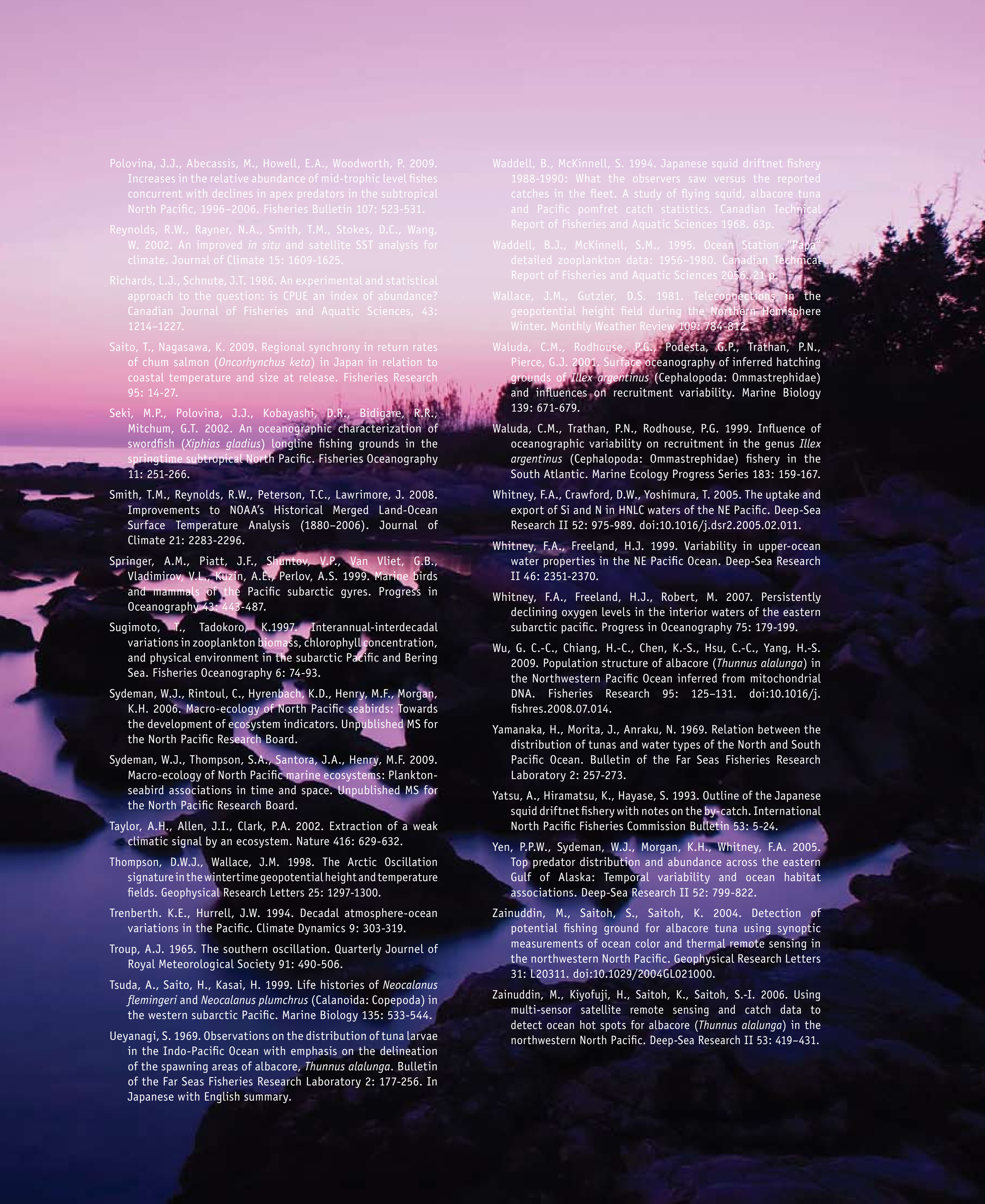

Polovina, J.J., Abecassis, M., Howell, E.A., Woodworth, P. 2009. Increases in the relative abundance of mid-trophic level fishes concurrent with declines in apex predators in the subtropical North Pacific, 1996–2006. Fisheries Bulletin 107: 523-531.

Reynolds, R.W., Rayner, N.A., Smith, T.M., Stokes, D.C., Wang, W. 2002. An improved *in situ* and satellite SST analysis for climate. Journal of Climate 15: 1609-1625.

Richards, L.J., Schnute, J.T. 1986. An experimental and statistical approach to the question: is CPUE an index of abundance? Canadian Journal of Fisheries and Aquatic Sciences, 43: 1214–1227.

Saito, T., Nagasawa, K. 2009. Regional synchrony in return rates of chum salmon (*Oncorhynchus keta*) in Japan in relation to coastal temperature and size at release. Fisheries Research 95: 14-27.

Seki, M.P., Polovina, J.J., Kobayashi, D.R., Bidigare, R.R., Mitchum, G.T. 2002. An oceanographic characterization of swordfish (*Xiphias gladius*) longline fishing grounds in the springtime subtropical North Pacific. Fisheries Oceanography 11: 251-266.

Smith, T.M., Reynolds, R.W., Peterson, T.C., Lawrimore, J. 2008. Improvements to NOAA's Historical Merged Land-Ocean Surface Temperature Analysis (1880–2006). Journal of Climate 21: 2283-2296.

Springer, A.M., Piatt, J.F., Shuntov, V.P., Van Vliet, G.B., Vladimirov, V.L., Kuzin, A.E., Perlov, A.S. 1999. Marine birds and mammals of the Pacific subarctic gyres. Progress in Oceanography 43: 443-487.

Sugimoto, T., Tadokoro, K.1997. Interannual-interdecadal variations in zooplankton biomass, chlorophyll concentration, and physical environment in the subarctic Pacific and Bering Sea. Fisheries Oceanography 6: 74-93.

Sydeman, W.J., Rintoul, C., Hyrenbach, K.D., Henry, M.F., Morgan, K.H. 2006. Macro-ecology of North Pacific seabirds: Towards the development of ecosystem indicators. Unpublished MS for the North Pacific Research Board.

Sydeman, W.J., Thompson, S.A., Santora, J.A., Henry, M.F. 2009. Macro-ecology of North Pacific marine ecosystems: Plankton-seabird associations in time and space. Unpublished MS for the North Pacific Research Board.

Taylor, A.H., Allen, J.I., Clark, P.A. 2002. Extraction of a weak climatic signal by an ecosystem. Nature 416: 629-632.

Thompson, D.W.J., Wallace, J.M. 1998. The Arctic Oscillation signature in the wintertime geopotential height and temperature fields. Geophysical Research Letters 25: 1297-1300.

Trenberth. K.E., Hurrell, J.W. 1994. Decadal atmosphere-ocean variations in the Pacific. Climate Dynamics 9: 303-319.

Troup, A.J. 1965. The southern oscillation. Quarterly Journal of Royal Meteorological Society 91: 490-506.

Tsuda, A., Saito, H., Kasai, H. 1999. Life histories of *Neocalanus flemingeri* and *Neocalanus plumchrus* (Calanoida: Copepoda) in the western subarctic Pacific. Marine Biology 135: 533-544.

Ueyanagi, S. 1969. Observations on the distribution of tuna larvae in the Indo-Pacific Ocean with emphasis on the delineation of the spawning areas of albacore, *Thunnus alalunga*. Bulletin of the Far Seas Fisheries Research Laboratory 2: 177-256. In Japanese with English summary.

Waddell, B., McKinnell, S. 1994. Japanese squid driftnet fishery 1988-1990: What the observers saw versus the reported catches in the fleet. A study of flying squid, albacore tuna and Pacific pomfret catch statistics. Canadian Technical Report of Fisheries and Aquatic Sciences 1968. 63p.

Waddell, B.J., McKinnell, S.M., 1995. Ocean Station "Papa" detailed zooplankton data: 1956–1980. Canadian Technical Report of Fisheries and Aquatic Sciences 2056. 21 p.

Wallace, J.M., Gutzler, D.S. 1981. Teleconnections in the geopotential height field during the Northern Hemisphere Winter. Monthly Weather Review 109: 784-812.

Waluda, C.M., Rodhouse, P.G., Podesta, G.P., Trathan, P.N., Pierce, G.J. 2001. Surface oceanography of inferred hatching grounds of *Illex argentinus* (Cephalopoda: Ommastrephidae) and influences on recruitment variability. Marine Biology 139: 671-679.

Waluda, C.M., Trathan, P.N., Rodhouse, P.G. 1999. Influence of oceanographic variability on recruitment in the genus *Illex argentinus* (Cephalopoda: Ommastrephidae) fishery in the South Atlantic. Marine Ecology Progress Series 183: 159-167.

Whitney, F.A., Crawford, D.W., Yoshimura, T. 2005. The uptake and export of Si and N in HNLC waters of the NE Pacific. Deep-Sea Research II 52: 975-989. doi:10.1016/j.dsr2.2005.02.011.

Whitney, F.A., Freeland, H.J. 1999. Variability in upper-ocean water properties in the NE Pacific Ocean. Deep-Sea Research II 46: 2351-2370.

Whitney, F.A., Freeland, H.J., Robert, M. 2007. Persistently declining oxygen levels in the interior waters of the eastern subarctic pacific. Progress in Oceanography 75: 179-199.

Wu, G. C.-C., Chiang, H.-C., Chen, K.-S., Hsu, C.-C., Yang, H.-S. 2009. Population structure of albacore (*Thunnus alalunga*) in the Northwestern Pacific Ocean inferred from mitochondrial DNA. Fisheries Research 95: 125–131. doi:10.1016/j.fishres.2008.07.014.

Yamanaka, H., Morita, J., Anraku, N. 1969. Relation between the distribution of tunas and water types of the North and South Pacific Ocean. Bulletin of the Far Seas Fisheries Research Laboratory 2: 257-273.

Yatsu, A., Hiramatsu, K., Hayase, S. 1993. Outline of the Japanese squid driftnet fishery with notes on the by-catch. International North Pacific Fisheries Commission Bulletin 53: 5-24.

Yen, P.P.W., Sydeman, W.J., Morgan, K.H., Whitney, F.A. 2005. Top predator distribution and abundance across the eastern Gulf of Alaska: Temporal variability and ocean habitat associations. Deep-Sea Research II 52: 799-822.

Zainuddin, M., Saitoh, S., Saitoh, K. 2004. Detection of potential fishing ground for albacore tuna using synoptic measurements of ocean color and thermal remote sensing in the northwestern North Pacific. Geophysical Research Letters 31: L20311. doi:10.1029/2004GL021000.

Zainuddin, M., Kiyofuji, H., Saitoh, K., Saitoh, S.-I. 2006. Using multi-sensor satellite remote sensing and catch data to detect ocean hot spots for albacore (*Thunnus alalunga*) in the northwestern North Pacific. Deep-Sea Research II 53: 419–431.